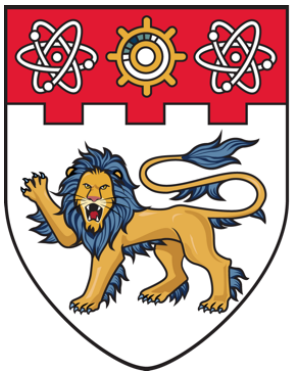

NANYANG TECHNOLOGICAL UNIVERSITY
SINGAPORE

Carbene-Catalyzed Asymmetric Modification of Carboxylic Acids and Sulfonamides

LIU YINGGUO

SCHOOL OF PHYSICAL AND MATHEMATICAL SCIENCES

2019

Carbene-Catalyzed Asymmetric Modification of Carboxylic Acids and Sulfonamides

LIU YINGGUO

SCHOOL OF PHYSICAL AND MATHEMATICAL SCIENCES

A thesis submitted to the Nanyang Technological University in partial fulfilment of the requirement for the degree of Doctor of Philosophy

2019

Statement of Originality

I hereby certify that the work embodied in this thesis is the result of original research done by me except where otherwise stated in this thesis. The thesis work has not been submitted for a degree or professional qualification to any other university or institution. I declare that this thesis is written by myself and is free of plagiarism and of sufficient grammatical clarity to be examined. I confirm that the investigations were conducted in accord with the ethics policies and integrity standards of Nanyang Technological University and that the research data are presented honestly and without prejudice.

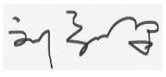

Aug. 1st 2019

. . . . . .

. . . . . .

Date LIU YINGGUO

Supervisor Declaration Statement

I have reviewed the content and presentation style of this thesis and declare it of sufficient grammatical clarity to be examined. To the best of my knowledge, the thesis is free of plagiarism and the research and writing are those of the candidate's except as acknowledged in the Author Attribution Statement. I confirm that the investigations were conducted in accord with the ethics policies and integrity standards of Nanyang Technological University and that the research data are presented honestly and without prejudice.

Aug. 1st 2019

. . . . . .

. . . . . .

Date Yonggui Robin Chi

Authorship Attribution Statement

This thesis contains material from 1 paper(s) published in the following peer-reviewed journal(s) / from papers accepted at conferences in which I am listed as an author.

Chapter 2 is published as Liu, Y.; Chen, Q.; Mou, C.; Pan, L.; Duan, X.; Chen, X.; Chen, H.; Zhao, Y.; Lu, Y.; Jin, Z.; Chi, Y. R., Catalytic asymmetric acetalization of carboxylic acids for access to chiral phthalidyl ester prodrugs. *Nat. Commun.* **2019**, *10* (1), 1675 DOI:10.1038/s41467-019-09445-x.

The contributions of the co-authors are as follows:

Prof. Chi conceptualized the project and revised the manuscript drafts.
I prepared the manuscript drafts and conducted most of the experiments
Dr. Chen Q. worked on synthesis of products from the alkyl acids.
Dr. Mou, Dr. Duan, Dr. Chen X., Dr. Jin conducted some experiments regarding condition optimizations and substrate scope studies.
Prof. Zhao, Prof. Pan, Dr. Chen H. contributed in discussion, design, and experiments regarding bio-evaluation.
Dr. Lu discussed about the reaction mechanism
All authors contributed to discussions and manuscript preparation.

Aug. 1st, 2019

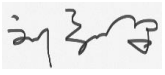

. . . . . .

Date

. . . . . .

LIU YINGGUO

Abstract

In this thesis, we demonstrated the new reaction mode enabled by NHC in the enantioselective synthesis of 3-substituted phthalides, which could be used for structural modification on heteroatoms within the medicinally significant molecules. Our method shall expand the synthetic toolbox and bring significant values for the discovery and manufacturing of better chiral prodrugs in enantiomerically enriched forms.

In this thesis chapter 1 delivers the brief introduction on the chemical modification, molecular modification as prodrugs, and phthalidyl prodrugs. We also introduced briefly reaction modes enabled by NHCs and key intermediates within them.

Chapter 2 demonstrates that synthetic challenges in enantioselective modification of carboxylic acids into enantiopure phthalidyl esters were addressed. Such reaction involves a chiral carbene-catalyzed asymmetric addition of a carboxylic acid to a catalyst-bound intermediate generated from a phthalaldehyde substrate. A broad range of carboxylic acids worked effectively under mild and transition metal-free conditions. Selected modified drugs demonstrated improved bioactivities against tumor cell growth.

Chapter 3 describes that the methodology was extended to the compounds with modifiable nitrogen atoms. With benzenesulfonamides as substrates, the 3-(*N*-substituted) aminophthalides were synthesized in excellent yield and excellent enantiomeric ratios (up to 99% and 99:1). This is the first enantioselective synthesis of chiral aminophthalides. More application is under investigation.

Acknowledgements

Firstly, I would like to express my sincere gratitude and respect to my supervisor, Professor Yonggui Robin Chi, for his continuous guidance and support during my entire PhD study. The research attitude and philosophy that I learned from professor Chi would be great gift and treasure for my future life.

Secondly, I would like to extend my acknowledgement to my Thesis Advisory Committee (TAC) members, Prof. Shuzhou Li and Prof. Yanli Zhao, for their timely advices, crucial guidance and greater collaborations.

I also give my thanks to all my labmates in professor Chi's group for the valuable assistance and advice in the lab: Dr. Zhu Tingshun, Dr. Chen Xingkuan, Dr. Huang Xuan, Dr. Duan Xiaoyong, Dr. Chen Qiao, Dr. Hao Lin, Dr. Zhou Leijin, Dr Li Yongjia, Dr. Wu Xingxing, Dr. Wang Yuhuang, Dr. Wang Fangxin Wang Hongling, Majhi Pankai Kumar, Bivas Mondal, Liu Bin, Mou Chengli, Maiti Rakesh, and Song Runjiang

Furthermore, I would like to thank the CBC staff for their service with laboratory instruments: Ms Goh Ee Ling and Mr Keith Leung for NMR; Dr. Li Yongxin and Dr. Ganguly Rakesh for X-ray analysis and Ms Zhu Wenwei for mass spectroscopy analysis.

I gratefully acknowledge the scholarship from School of Physical and Mathematical Sciences, Nanyang Technological University, which made my PhD work possible.

Last but not the least, I would like to thank my family for their love and support throughout my Ph.D study.

Table of Contents

PUBLICATIONS

1. **Liu Yingguo**, Chen Qiao, Mou Chenli, Pan Lutai, Duan Xiaoyong, Chen Xingkuan, Chen Hongzhong, Zhao Yanli, Lu Yunpeng, Jin Zhichao, Chi Yinggui Robin. Catalytic asymmetric acetalization of carboxylic acids for access to chiral phthalidyl ester prodrugs. *Nat. Commun.* **2019,** *10*, 1675. (*Highlighted* by Benjamin List, *Synfacts* **2019**, *15*, 0793)

2. Tingshun Zhu, **Yingguo Liu (Equal contribution)**, Marie Smetankova, Shitian Zhuo, Chengli Mou, Huifang Chai, Zhichao Jin, and Yonggui Robin Chi, Carbene-Catalyzed Desymmetrization and Direct Construction of Arenes with All-Carbon Quaternary Chiral Center. *Angew. Chem. Int. Ed.* **2019**, *131*, 15925.

3. **Yingguo Liu**, Pankaj Kuamr Majhi, Chenli Mou, Lin Hao, Huifang Chai, Zhichao Jin, Yonggui Robin Chi. Carbene-Catalyzed Dynamic Kinetic Resolution of Hydroxyphthalides with Applications in Natural Product Synthesis of Modifications. DOI: 10.1002/anie.201912926 and 10.1002/ange.201912926.

4. Chen Xingkuan, Song Runjiang, **Liu Yingguo**, Ooi Chong Yih, Jin Zhichao, Zhu, Tingshun, Wang, Hongling, Hao, Lin, Chi Yonggui. Carbene and Acid Cooperative Catalytic Reactions of Aldehydes and o-Hydroxybenzhydryl Amines for Highly Enantioselective Access to Dihydrocoumarins. *Org Lett* **2017,** *19*, 5892. (*Highlighted* by Philip Kocienski, *Synfacts* **2018**, *14*, 0004).

5. Carbene Catalyzed Enantioselective Synthesis of 3-(*N*-Substituted) Amino Phthalides Pankaj Kumar Majhi, **Yingguo Liu (Equal contribution)**, Ng Pei Rou, Bivas Mondal, Lin Hao, Xingkuan Chen, Yonggui Robin Chi (to be submitted).

6. Carbene Catalyzed Enantioselective Synthesis of Phthalidyl acetals

Yingguo Liu, Runjiang Song, Tingshun Zhu, Yonggui Robin Chi (In preparation).

Abbreviations

Ac	acetyl
Ar	aryl
Boc	*tert*−butyloxycarbonyl
Bu	butyl
Bn	benzyl
DABCO	1,4−diazabicyclo[2.2.2]octane
DBU	1,8−diazabicyclo[5.4.0]undec−7−ene
TEA	Triethylamine
DIPEA	N,N-Diisopropylethylamine
THF	tetrahydrofuran
e.r.	enantiomeric ratio
equiv.	equivalent
ESI	electrospray ionization
^{i}Pr	isopropyl
Mes	mesityl
TBS	tert-butyldimethylsilyl
SET	single electron transfer
TLC	thin layer chromatography
NHC	*N*-heterocyclic carbene
α	alpha
β	beta

Chapter I

Introduction

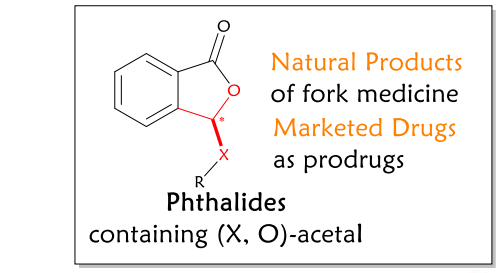

Fungus

Apium

L. chuanxiong

1.1 Introduction on heteroatoms in medicine

Heteroatoms are ubiquitous in nearly all functional organic molecules and materials. In particular, oxygen, nitrogen, and sulfur atoms are key elements in medicines and numerous bioactive molecules. For example, the Njardarson groups at Arizona, who produces the posters of "Top 200 Drugs"[1], analyzed 1035 small-moecule drugs which have been approved by FDA(**Scheme 1.1**).[2] It was discovered that 84% of the analyzed small-molecule drugs have more than one nitrogen atom in them, and 59% of these molecules are heterocyclic compounds with some sort of nitrogen ring. Another popular element in drugs is sulfur. It was disclosed recently that about 26% of these small-molecules have sulfur as the heteroatom. These ratios are incredibly high percentages. These sulfur and nitrogen-containing heterocyclic compounds also contains other heteroatoms such as oxygen and phosphorus, which are not demonstrated in numbers here.

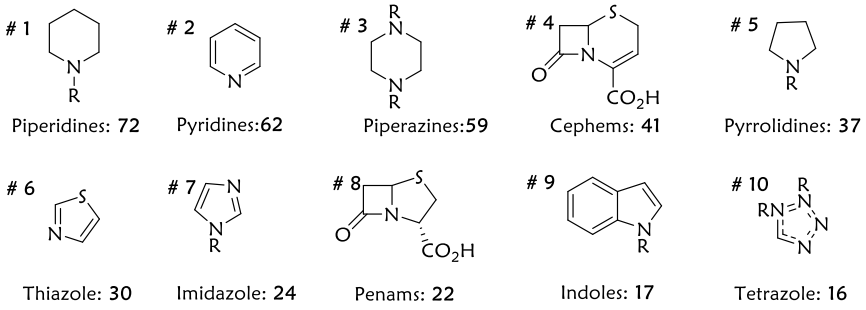

Scheme 1.1 Top 10 popular nitrogen heterocycles in U.S. FDA approved drugs.

As a matter of fact, heteroatoms are indispensable for drugs in almost all cases. The major function of heteroatoms in drugs is to provide specificity by participating in ligand-receptor binding via hydrogen bonding.[3] According to Lipinski's rule[4], the acceptor numbers is defined as the number of nitrogen and oxygen, whereas the number of donors is expressed as the sum of NHs and OHs. Another function of heteroatoms

within drugs is to determine the polarity, which is involved in pharmacodynamic and pharmacokinetic effects. Lipinski described it by defining the octanol-water partition coefficient (log P < 5). Lipinski's rule of five is not the golden rule but clearly demonstrates the importance of the heteroatoms in medicines.

1.2 Introduction on chemical modification for drug discovery

Chemical modification is a process of the alteration of the structure, scaffold, functional groups, configuration, biosynthetic ability or form of a compound. Modification is involved with structural changes, including variations in the bioactivity of the corresponding lead compounds. By chemical modification, many lead compounds may be developed into the pharmacological market.[5]

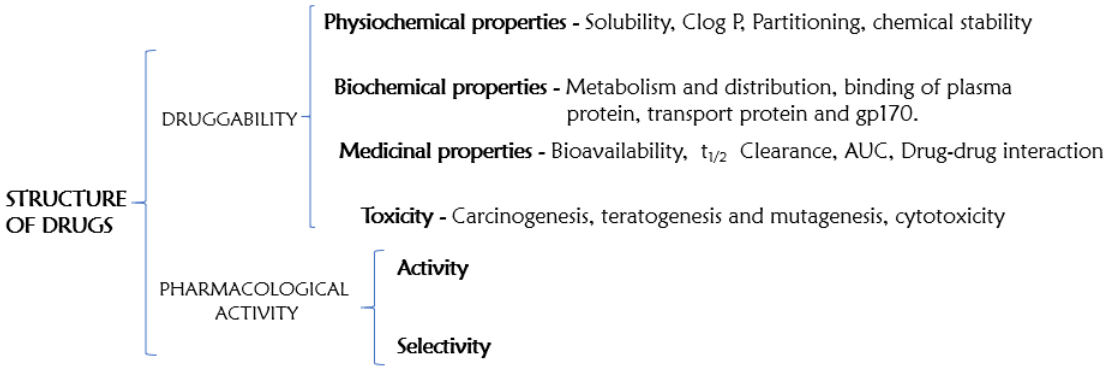

Figure 1.1 The relationship of druggability and pharmacological activity

Two essential factors for drug discovery are pharmacological activity and druggability (**Figure 1.1**).[6] The former one is indispensable. The druggability is defined by physico-chemical, biochemical, biopharmaceutical (pharmacodynamic and pharmacokinetic) and safety properties of drugs. The predominant reasons for failure and/or slowdown in drug development are the inappropriate druggability sush as poor chemical stability, poor solubility (dissolution rate), insufficient permeability

(absorption process), and inadequate metabolic and / or elimination profile (**Table 1.1**).[7] Even the lead compound with the best pharmacological effects may unlikely meet these demands for druggability. The well-known examples are taxol (poor solubility)[8], and doxorubicin (poor solubility). Therefore, it is necessary to modify and optimize these structural phenotypes into more suitable therapeutic reagents.

Table 1.1 Reasons for failure and / or slow-down of drug candidates

Reasons for failure	**Reasons for slow down**
Poor biopharmaceutical profiles 39%	Sophisticated structures
insufficient efficacy 29%	Finding inappropriate toxicities
Safety problems 21%	Poor biopharmaceutical profiles
Marketing 6%	Low potency

Note: This is not an exhaustive list.

The molecular modification is to enhance the usefulness of a previously discovered lead compound as a drug via chemical alteration of its structure.[5, 9-10] This is to provide the desired features by enhancing its specificity for the particular receptors or targets in the human body, increasing its potency, optimizing the AMDE process, modifying to advantage the pharmacodynamic/pharmacokinetic effects *in vivo*, reducing its toxicity, and changing its physicochemical properties (e.g. solubility). Structural modification is intended to

1) Make logical and systematic changes to increase their potency and activity spectrum and therefore counter resistance mechanisms.

2) Provide structurally simpler compounds that retain bioactivities.
3) Increase metabolic stability by reducing compound binding affinity or reactivity at the labile site.
4) Improve the solubility according to the previously characterized pharmacokinetic data.
5) Improve other biopharmaceutical profiles.
6) Eliminate or reduce side effects, while attaining intellectual properties.
7) Explore the structure-activity relationship for the next round modification.

To date, structural modification of lead compounds and natural products for new chemical entities is still a sound and practical tool of research in medicinal chemistry. Many synthetically modified molecules have been successfully developed into therapeutic reagents in almost all therapeutic areas. The efforts involved the famous drugs such as penicillin, and paclitaxel. These endeavors demonstrate that the structural modification could overcome the limitations of the existing drug candidates and lead to the discovery of a novel drug.

1.3 Introduction on prodrugs

Prodrug design is one of the most common chemical modification strategies that aim to optimizing the physicochemical properties and biopharmaceutical properties of parent drugs to enhance the potency and reduce the undesired side effects.[11] This concept could date back to the recognition by Adrian Albert in 1958.[12] However, in fact, medicinal chemists have started to use the concept decades earlier. The famous and successful cases include methenamine, phenacetin and prontosil.[13]

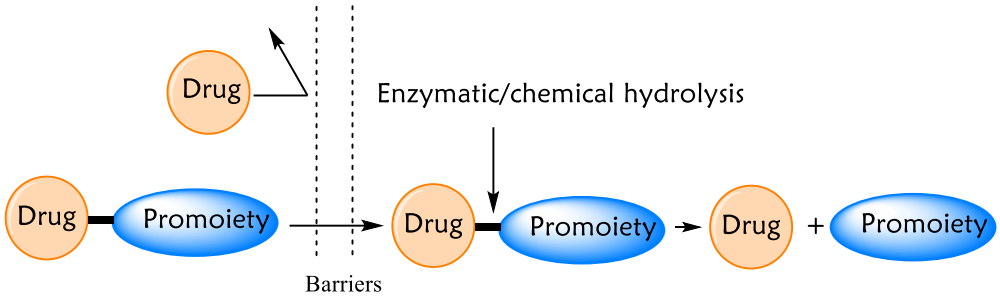

Figure 1.2 Simplified prodrug concept

Prodrugs are bioreversible molecules, which could release the active parent drug in vivo under enzymatic or chemical transformation (**Figure 1.2**).[14] Prodrugs have been used as the salvage efforts for drugs with undesired physicochemical properties or adverse effects. But nowadays it is utilized to medicinally design the prodrugs, intentionally to avoid drug development challenges that constrain formulation design or lead to unacceptable biopharmaceutical profiles, or poor targeting.[15] Over the past 10 years, more than 30 prodrugs have been approved by the US FDA (Food and Drug Administration), which takes up more than 12% of all approved small-molecule new synthetic drugs.[16] To date, prodrug strategies are still the established and applicable tool for development of new chemical entities.

1.3.1 Benefits of prodrug development

Prodrugs bring substantial benefits for the drug candidates. Through modification of physicochemical properties and key biopharmaceutical properties such as electro-steric factors (including ionization constants), polarizability, topological factors, hydro/lipophobicity, hydrogen bonds and chemical reactivity, key biopharmaceutical profiles such as solubility, dissolution, partitioning coefficient factor, permeability, chemical/enzymatic stability and affinities to transporter and receptor can be

intentionally altered.[14, 16] Examples of biopharmaceutical profiles improved by prodrug development are shown below (**Figure 1.3**):

Prodrug name (therapeutic area)	Structure	Prodrug strategy
Pivampicillin (β-lactam antibiotic)	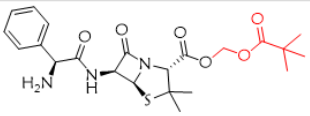	Oral bioavailability: 32–55% to **87–94%**
Adefovir dipivoxil (antiviral)	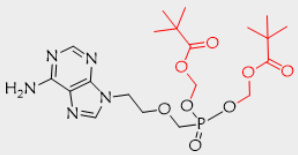	Oral bioavailability: ~10% to **30–45%**
Gabapentin enacarbil (Restless leg syndrome or postherpetic neuralgia)	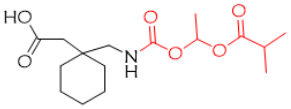	**Increased permeation** via gastrointestinal transporters

Figure 1.3 Prodrugs with improved biopharmaceutical profiles

Typical advantages related to the modification are listed here:

1. Improving aqueous solubility for drug absorption.[17] Formulation strategies for drugs with insufficient solubility, for example, pH adjustment and co-solvents, surfactants, and solubilizers, could cause irritation or toxicity and have proved inadequate. Prodrug strategies can employ ionizable promoieties to increase aqueous solubility then promote the parenteral/oral delivery.
2. Passive permeability.[18-19] Passive permeability is the important way for drugs across biological membrane, which usually become the main barriers for polar and charged drugs. To date, ameliorating the diffusion ability of drugs has been one of the most fertile areas of prodrug development. Medicinal chemists usually improve the lipophilicity of the drugs by modifying the polar group (including ionized functionalities) into hydrocarbon promoieties. For instance, amine and carboxyl

groups have been modified into more lipophilic N-acyl derivatives or aryl or alkyl esters. These ester or amide type prodrug could be easily subject to the ubiquitous esterases or peptidase in the biological process and then hydrolyzed into parent drugs.

3. Improving metabolic stability. The first pass effect exists widely during the metabolism. To avoid the rapid deactivation of drugs by liver, prodrugs protect the active drugs by modifying the metabolically labile but indispensable pharmacophore. This is supported by the long-standing drug-bambuterol.[20] The phenol functional group (metabolically susceptible) on terbutaline is modified into dimethylcarbamate promoieties, which is to avoid extensive and rapid first-pass effect.
4. As drug delivery carrier.[21-22] The promoieties of prodrugs could sometimes play a role as carriers to mediate the transportation of the parent drugs. They facilitate the absorption of drugs by target tissue. The famous example was dopamine and its prodrug-levodopa. Both are hydrophilic but levodopa could make full use of carrier-mediated transport mechanisms, recognized by L-type amino acid transporter 1 and go across the brain blood barrier (BBB).[23] Dopamine could not be absorbed by brain effectively, although it is the active form for levodopa.
5. Develop targeted drugs. Better targeting, less side effect. Development of targeted prodrugs includes: (1) Site directed drugs. Prodrugs with promoieties recognizing specific receptor or transporter could be directed into target sites. (2) Site specific bioactivation drug. This kind of prodrugs could be designed to target the physiological conditions, site specific enzyme or receptor.[24] For instance, the microenvironment in the tumor issue is acidic, and differs from physiological conditions from the rest of body. Some enzymes usually expressed predominantly

in specific sites. [25] These characteristics could be used for designing targeted drugs so that the prodrugs can be mostly hydrolyzed into parent drug and take effects in the tumor.

6. Prolonged duration of action.[26] The duration of drug effect relies on the plasma concentration. Controlled release of drugs could provide therapeutic plasma concentration for long time and reduce the medical cost and time. Prodrugs can be used to achieve this goal by modifying its physicochemical properties that affects ADME process.

1.3.2 Common functional groups for prodrugs

Suitable functional groups for prodrug design include carboxylic, hydroxyl, amine, and carbonyl groups (**Figure 1.4**). They could be typically converted into prodrug by modifying them via[26]:

1) Esters as prodrugs of carboxyl, hydroxyl and thiol functionalities including phosphate esters, phthalidyl esters (the synthesis will be described in this thesis), and thioesters
2) Carbonates and carbamates for hydroxyl, carboxyl or amine functional groups.
3) Oximes for ketones, amidines, and guanidines.
4) Other derivatives, such as ethers.

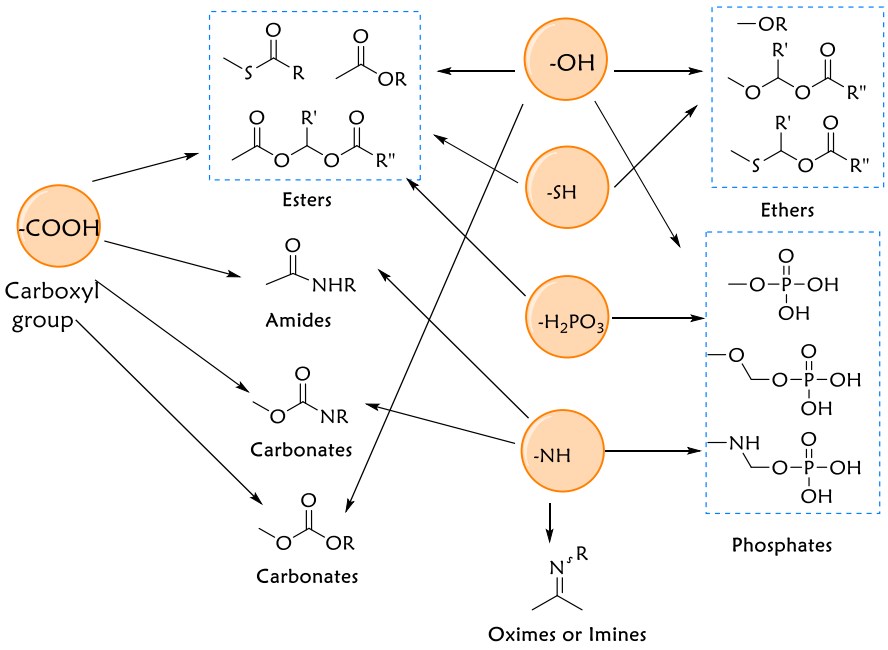

Figure 1.4 Most popular functional groups suitable to prodrug design

1.3.3 Existing problems for prodrug design

The ideal prodrugs should enhance the usefulness of the drug with excellent physicochemical and biopharmaceutical properties as mentioned above. A safe promoiety should have no undesirable pharmacological effects and could be excreted from body rapidly. However, it is still challenging to make prodrugs that meet all these characteristics.[14] The challenges involving the discovery and development of prodrugs still exist: (1) The synthesis can be challenging and costly. (2) Difficulties in controlling bioconversion rate and metabolism site. (3) Preclinical results are unpredictable and complicated (4) Complex analytical profiling requiring analysis of the parent drug, the prodrug and each of their respective metabolites. (5) Challenges in pharmacokinetic modelling. (6) toxicity of the promoiety and its by-product. (7) Regulatory environment may be not friendly, particularly for prodrug of patented drugs.

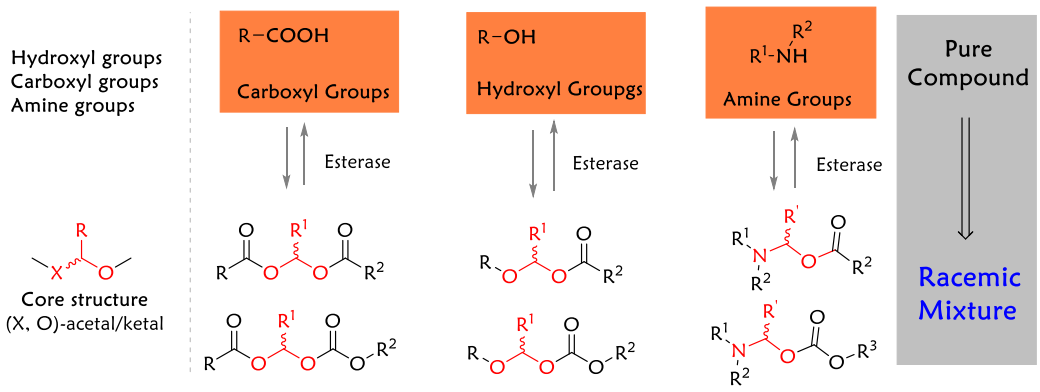

Figure 1.5 Racemic acetal/ketal linkage used in promoieties

In view of these challenges, the synthesis of prodrugs usually involves readily available reactions such as esterification, amidation and acetalization. The bonds generated by these methods could be easily hydrolyzed *in vivo* by chemical/enzymatic transformation, releasing the parent drugs. However, there lies a configuration problem for the prodrugs bearing core structure of acetal/ketal. They are all used in racemic form (**Figure 1.5**). No enantioselective approach has been utilized for synthesis of prodrugs of this kind yet. The existing prodrugs are generally synthesized in the racemic form and then sold on market as a mixture (**Scheme 1.2**).

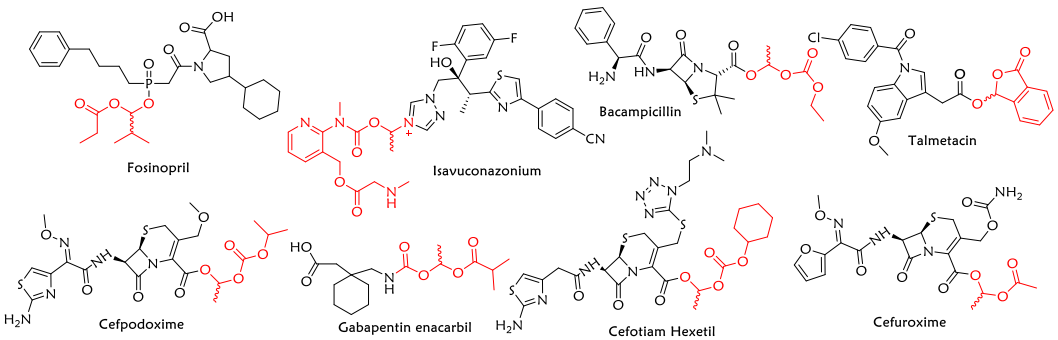

Scheme 1.2 Marketed prodrugs in racemic form

A typical example is the phthalide. It has been developed as prodrug in racemic form for decades. It is also prevalent in naturally occurring substances. In this thesis,

enantioselective synthesis of phthalides as prodrugs will be introduced for medicinally significant molecules bearing carboxylic acids and sulfonamides.

1.4 Introduction on phthalides

The phthalide identified as a promoiety of the prodrug dates back to the 1970s. It was employed to improve the oral availability of ampicillin in the form of the lactonyl ester. [27] After that, several impressive prodrugs were developed for the pharmaceutical market (**Scheme 1.3**). Since then, phthalides have been widely studied as prodrugs by medicinal chemists and most of these studies have been extensively patented. However, the most well-known phthalides were extracted from the natural products.

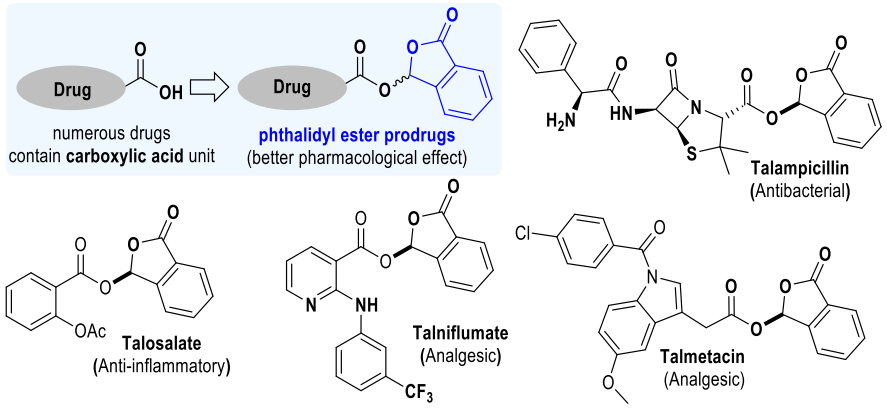

Scheme 1.3 Examples of phthalide prodrugs.

1.4.1 The origin and application of phthalides

The phthalides have been known more than 100 years and used as herbal remedies in traditional and folk medicines early in the 18th century.[28-29] They usually exhibit a broad spectrum of biological activities[30] such as bioactivities on central nervous system, antiplatelet aggregation, anti-thrombosis, modulating cardiac function, and protecting cerebral ischemia. Some of them have proven useful in the treatment of circulatory and

heart diseases. To date, more than 180 naturally occurring phthalides have been isolated (**Scheme 1.4**).

In practice of traditional Chinese medicine (TCM), herbs containing phthalides are recognized as the most commonly used natural medicines. One of these outstanding stories is 3-*n*-butylphthalide (NBP)[31], which is now on the market as an antiplatelet drug. It was approved by China Food and Drug Administration in 2002 against ischemic stroke. It is worthy to note that the phthalides are also be used as the promoiety for some drugs and some drugs have been on the market for over 30 years (e.g. talosalate in Argentina)[32]. These successes have also inspired interest of researchers in development of phthalides as a class of medicinally important synthetic/natural occurring products.

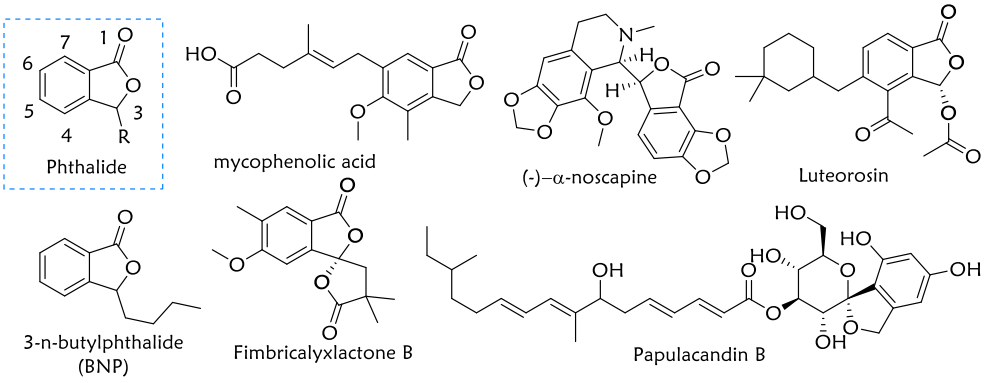

Scheme 1.4 Selected examples of naturally occurring phthalides.

Another application of phthalides is the use as building blocks for organic synthesis. The famous name reaction Hauser Kraus annulation is to construct naphthalene hydroquinone frameworks with 3-substituted phthalides (**Scheme 1.5**).[33] It is used mostly to synthesize polyketide compounds.

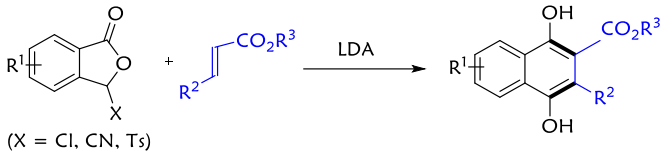

Scheme 1.5 3-substituted phthalides used in the Hauser Kraus reaction

1.4.2 Progress on chemical synthesis of phthalides.

Since 1980, chemists have studied the phthalides in detail due to the wide spectrum of biological activities and usefulness as synthetic intermediates. The methods for the synthesis of phthalides was pioneered by Wislicenus.[34] Then the total synthesis of phthalidyl compounds bloomed. The development of new methodologies mostly focused on synthesis of more sophisticated phthalides and 3-substituted enantiopure phthalides. In the view of synthetic technology, these emerging methods could be categorized into 2 groups. The first group is intramolecular reactions including substitution, lactonization, and addition; the second group involves aromatic hydrogen/halogen activation via organometallic catalysis.[35]

The intermolecular reaction for phthalides usually construct the acid scaffolds firstly, then the oxygen within the acid group attacked the electrophilic site at the *ortho*-position to form the lactone ring moiety of the phthalides. Selected examples are shown in **Scheme 1.6**.[36-38]

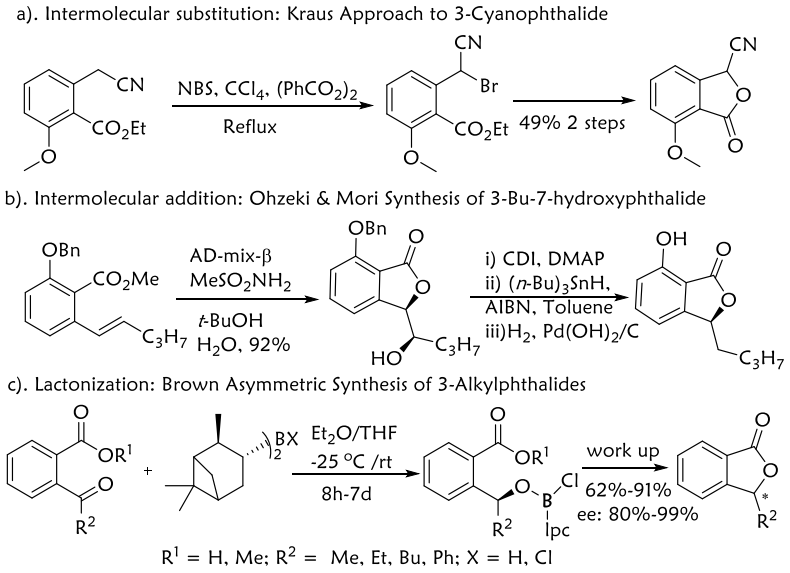

Scheme 1.6 Synthesis of phthalides via intramolecular reactions

The organometallic strategy is to activate the hydrogen/halogen with the carbonyl group at the corresponding *ortho* position (within acid, aldehyde or ester) (as the directing group), then one carbon unit is incorporated into the lactone ring of the phthalides. Representative synthesis approaches[39-40] are illustrated below (**Scheme 1.7**):

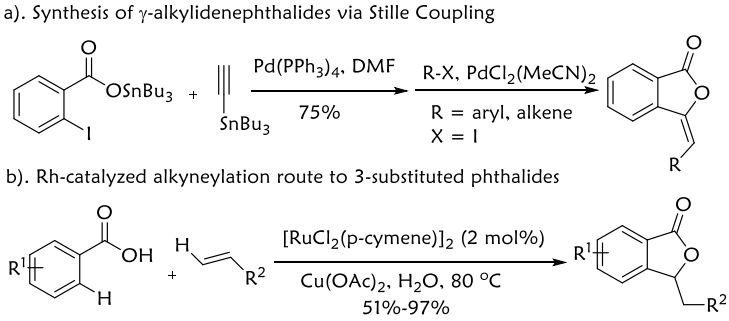

Scheme 1.7 Synthesis of phthalides via organometallic strategy.

Although many methods have been developed for the synthesis of phthalides, most of them focused on the 3-alkylphthlalides. The enantioselective installation of phthalide onto heteroatoms as prodrug design is not yet well developed. The industrial production of 3-substituted phthalides still relies on the racemic synthesis (**Scheme 1.8**).

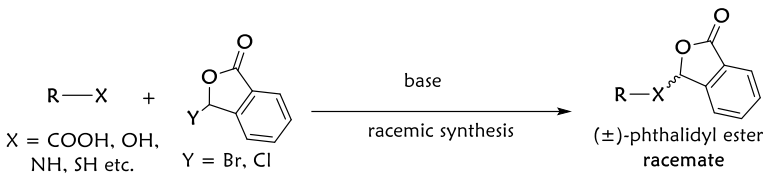

Scheme 1.8 Racemic synthesis of phthalide derivatives.

1.5 Introduction on NHCs

N-Heterocyclic carbenes (NHC) has been defined as heterocyclic scaffolds containing a carbene carbon and at least one nitrogen atom within the ring structure. The first stable NHC was demonstrated by Bertrand[41] and Arduengo[42] and their co-workers. Since then, the property of NHC as neutral two-electron-donor has stimulated extensive interest in the scientific community (**Scheme 1.9**).[43] As a kind of persistent carbene, the ever-increasing number of NHCs demonstrate its current state of the art trends and continue to develop new and scientifically significant applications across the chemical sciences.

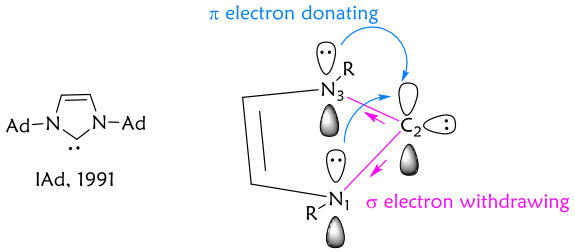

Scheme 1.9 First stable NHC and its ground-state electronic structure.

1.5.1 Diversity of NHCs

As the more and more interests have been attracted to the nucleophilic carbenes, a plethora of diverse carbenes have been developed for the transition-metal catalysis and organocatalysis. The advent of NHC as organocatalysis was dominated by thiazolium salts. With the advance in this field, imidazolium and triazolium scaffold popularized because they could be easily derivatized.

Based on their intrinsic chemical structures, commonly used NHCs could be categorized into eight groups:[44] (1) Acyclic triazoliums, (2) Thiazole-based heterazoliums, (3) Imidazoline-based heterazoliums, (4) Imidazole-based heterazoliums, (5) Pyrroline-based triazoliums, (6) Morpholine-based trizaoliums, (7) Oxazolidine-based heterazoliums and (8) Aminoindane-based triazoliums. These various carbenes enrich the organocatalysis library and benefit the development of new reaction modes enabled by NHC (**Scheme 1.10**).

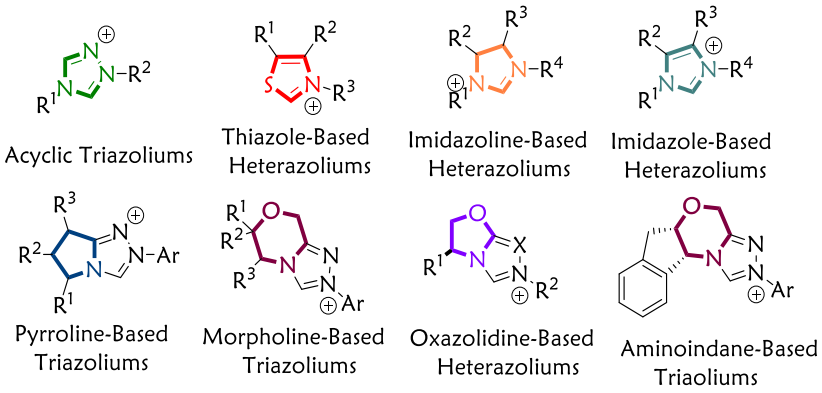

Scheme 1.10 The diverse NHC catalysts

1.5.2 Reaction modes enabled by NHCs

The first employment of *N*-heterocyclic carbene (NHC) in the reaction should give credit to Kai et al.'s work utilizing thiazolium salts in the benzoin reaction. Subsequently, Breslow's group determined the mechanism of this reaction and proposed the famous Breslow intermediate, which was extensively accepted and supported in carbene catalyzed chemistry. Since then, continuous efforts are made to develop new reaction mode enabled by carbene catalyzed reactions. In 1966, Hunneman and Sheehan presented enantioselective benzoin reaction via a chiral thiazolium salts. Since then, more and more interests have been attracted to the N-

heterocyclic carbene catalyzed reactions. Numerous reaction modes have been developed.[45-48]

In fact, the reaction modes enabled by NHC are much more than the above-mentioned examples. β-Functionalization and single electron transfer have been also be developed in the presence of NHC. However, we summarized the common NHC intermediates during the carbene catalyzed reactions below (**Scheme 1.11**). To the best of our knowledge, all the reactions catalyzed by NHC involve at least one of these intermediates[44]:

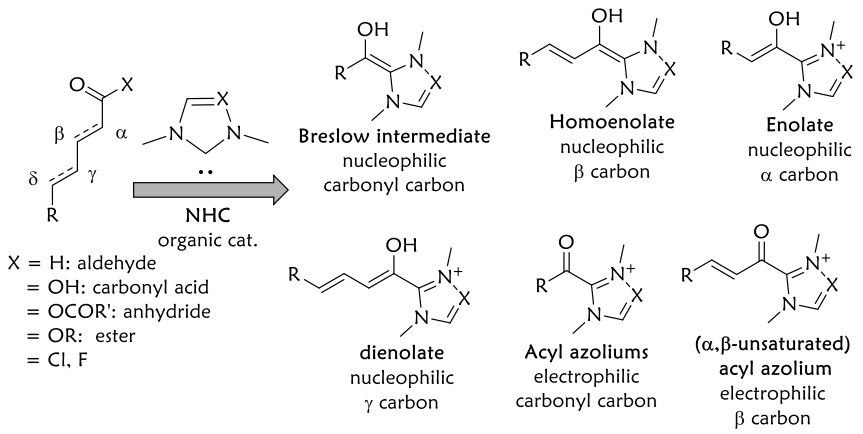

Scheme 1.11 The diverse activation modes enabled by NHC catalysts

Breslow Intermediate is considered as a general intermediate in the NHC-catalyzed reactions with an aldehyde as the substrate (**Scheme 1.12a)**. This intermediate has a nucleophilic carbonyl carbon and attacks another electrophile (e.g. aldehyde or Michael acceptor) to afford the benzoin product or Stetter product.

In 2010, Enders and co-workers overcame the low chemoselectivity between homobenzoin and the desired cross-product. They accomplished the enantioselective cross-benzoin reaction with trifluoromethyl ketones with a chiral triazolium A (**Scheme 1.12b**).[49] In 2005, Rovis group developed a highly enantioselective and

diastereoselective intramolecular Stetter reaction for the synthesis of chromanones (**Scheme 1.12c**).[50]

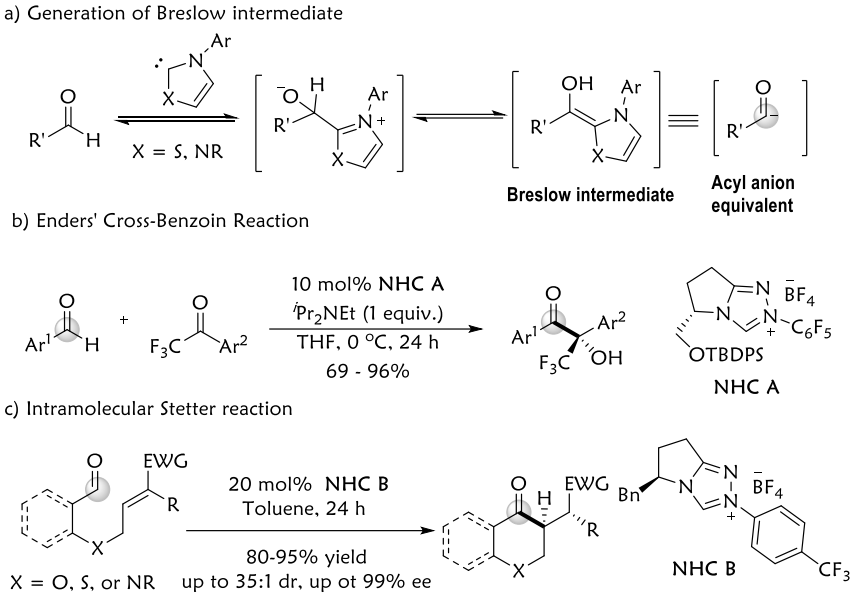

Scheme 1.12 Typical reactions via Breslow intermediates

Homoenolate referred here is an analogous Breslow intermediate with extended conjugation generated from the interaction between an NHC and an α,β-unsaturated aldehyde (**Scheme 1.13a**). By virtue of the conjugation, the NHC-bound homoenolate has a nucleophilic carbon at the β position to the original carbonyl group. This intermediate is mainly developed for β-functionalization/annulation.

In 2015, Our group developed an NHC-catalyzed oxidative SET of enals that introduces a hydroxyl group to the β-carbon of enals via homoenolate intermediate (**Scheme 1.13b**).[51] Bode and coworker disclosed that the chiral NHC-bound homoenolate can react with N-sulfonyl ketimines to afford bicyclic β-lactams (**Scheme 1.13c**).[52]

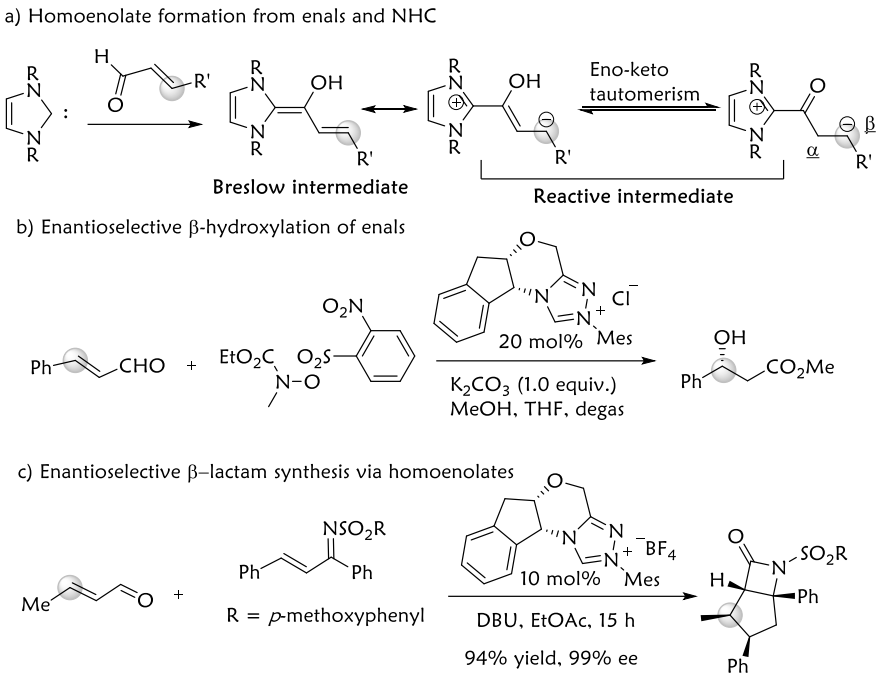

Scheme 1.13 Typical reactions via homoenolates

Azolium enolate and dienolate (conjugated enolate) have been well developed from ketenes, carboxylic derivatives and α-functionalized aldehydes, including α-chloroaldehydes, α-epoxyaldehydes, and enals, via NHC-catalyzed transformation (**Scheme 1.14**). Azolium enolate has a nucleophilic α carbon and can undergo enantio-transformation and a range of [2+n] annulation reactions. Azolium dienolate has a nucleophilic γ carbon and is usually used in the formal [4+2] reactions. They are developed to synthesize a wide of heterocyclic compounds.

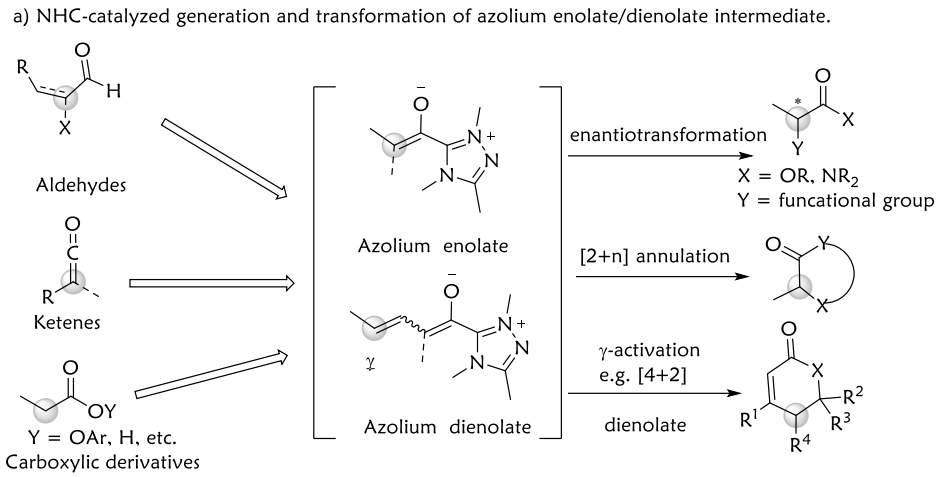

Scheme 1.14 Generation and transformation of azolium enolate/dienolate intermediate

Our groups demonstrated that the generation of enolate from the activated ester and achieve the dynamic kinetic resolution of α,α-disubstituted carboxylic esters with up to 99:1 er and 99% yield in 2016 (**Scheme 1.15a**).[53] In the same year, Bode and co-workers disclosed a [2+4] cycloaddition via azolium enolate generated from α-chloroaldehydes, providing the corresponding dihydropyran-2-ones in excellent yield and high enantioselectivity (**Scheme 1.15b**).[54]

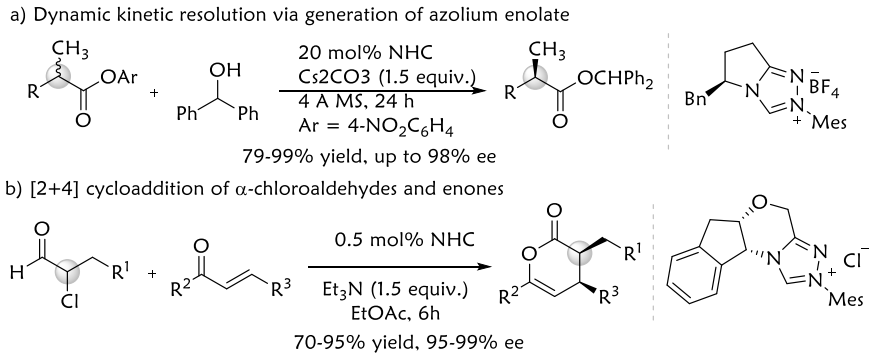

Scheme 1.15 Typical reactions via azolium enolates

Dienolate can facilitate γ-activation of the substrate and served as four-carbon building blocks in various cycloadditions. For example, α,β-unsaturated activated esters have been used as the dienolate precursor for the synthesis of δ-lactam.

Unsaturated γ-amino acid derivatives were realized in excellent yield and enantiomeric excess (**Scheme 1.16**).[55]

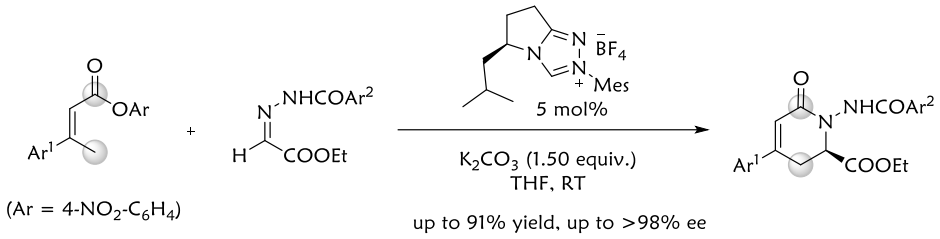

Scheme 1.16 Typical reaction via azolium dienolate

Acyl azolium is the tautomer (or precursor) of the corresponding azolium enolate. It could be developed by the same method as the azolium enolate. Compared with azolium enolates, acyl azoliums have an electrophilic carbonyl carbon with chiral azolium as the leaving group. They are widely used in the (dynamic) kinetic resolution and desymmetrization strategies**.** They are important reactive intermediates for carbene-promoted transesterification and amidation reactions.

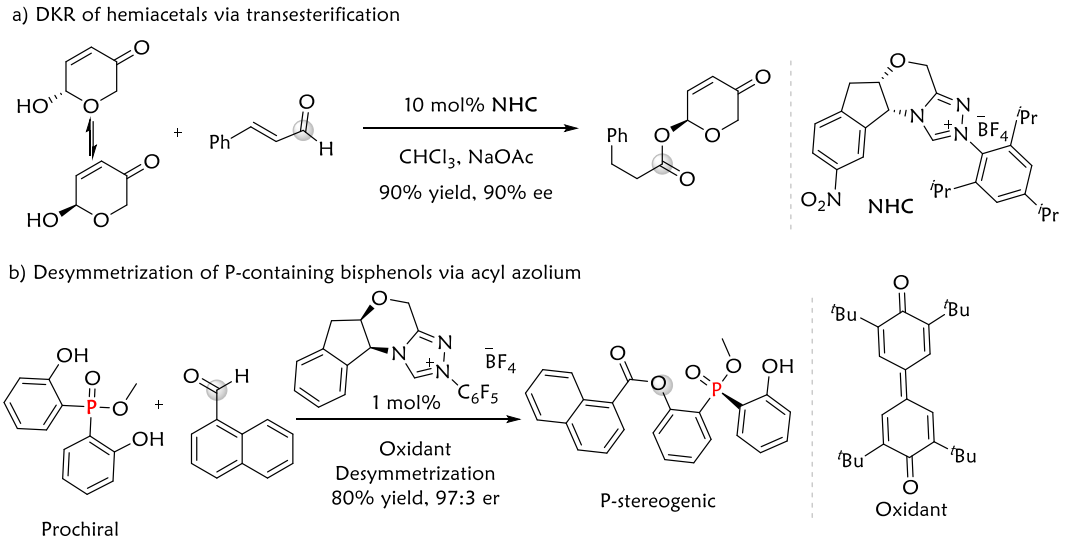

Scheme 1.17 Typical reactions via acyl azoliums

Carbene catalyzed dynamic kinetic resolution of sex membered lactols through a redox esterification was disclosed by Wang's group in 2016 (**Scheme 1.17a**).[56] Our

group developed desymmetriczation of prochiral phosphorus compound with P-stereogenic center via acyl azolium, delivering access to optically enriched P-stereogenic phosphinates (**Scheme 1.17b**).[57]

Acyl azolium can be extended to α,β-unsaturated acyl azolium, which allows bond formation at the α-, β-, γ- and carbonyl carbon. Compared with the homoenolate, it has a nucleophilic α carbon and an electrophilic β carbon, providing the different reactivity patterns. One of the typical reactions involved with the α,β-unsaturated acyl azolium was reported by our group. bicyclic δ-lactones were synthesized through carbene-catalyzed activation of α,β-unsaturated ester in a single step cascade process (**Scheme 1.18**).[58]

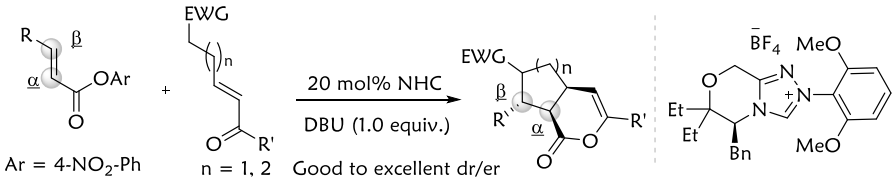

Scheme 1.18 Typical reaction via unsaturated acyl azolium

In summary, the typical intermediates involved with the carbene catalyzed reactions were illustrated above according to the reactivity sites. In this thesis, acyl azolium is going to be investigated in the asymmetric (O/N, O)-acetalization of carboxylic acids and sulfonamides for access to phthalidyl derivatives.

1.5.3 Related NHC-catalyzed reactions of phthalaldehydes

In order to synthesize the phthalidyl prodrugs, phthalaldehyde is chosen as the substrate, which is not the common building block in the carbene catalyzed reactions.

It is usually utilized in construction of indane/hydroxytetralone derivatives by carbene catalyzed domino formal [4+1]/[4+2] annulation reactions.

Phthalaldehyde can undergo cross-dimerization with *o*-formyl chalcones in a Stetter-aldol-aldol reaction in presence of *N*-benzyl thiazolium salt. The spiro bis-indanes was achieved with modest to good yield albeit with poor the diastereomeric ratios (**Scheme 1.19**).[59]

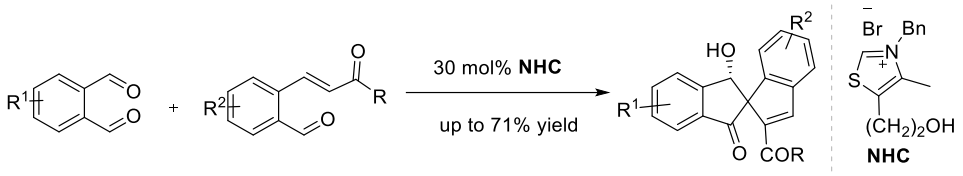

Scheme 1.19 domino Stetter-aldol-aldol reactions for [4+1] annulation

In 2011, Cheng's group disclosed dimerization of phthalaldehyde for stereoselective access to polyhydroxylated spiro- and fused indenones dominated by different NHC catalysts. An imidazole carbene catalyzed reaction of phthalaldehydes produced spiro indenones with good to excellent yields, whereas fused indenones were obtained by a triazole carbene in high yields (**Scheme 1.20**).[60]

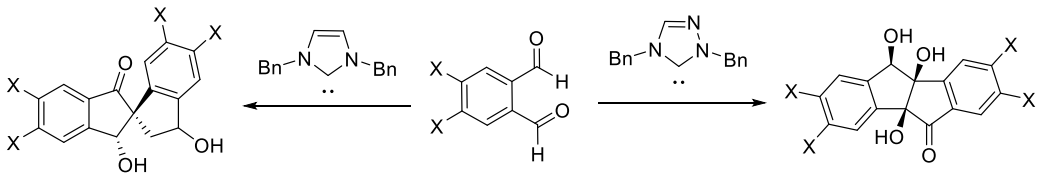

Scheme 1.20 Switchable dimerization of phthalaldehyde via different NHCs

Early in 2010, Ye et al. reported that good yield and diastereomeric ratios of 4-hydrotetralone were obtained when phthalaldehydes and mono-substituted olefins were employed in a carbene catalyzed domino Stetter-adol reaction with a [4+2] annulation

(**Scheme 1.21a**).[61] Later in 2011, Ye et al. extended this strategy with a [4+1] annulation that delivered the hydroindanones. Instead of mono-substituted olefins, they carried out reactions using 1,2-diactivated Michael receptor or imines. The reaction proceeded with excellent yield and diastereoselectivity (**Scheme 1.21b**).[62, 63]

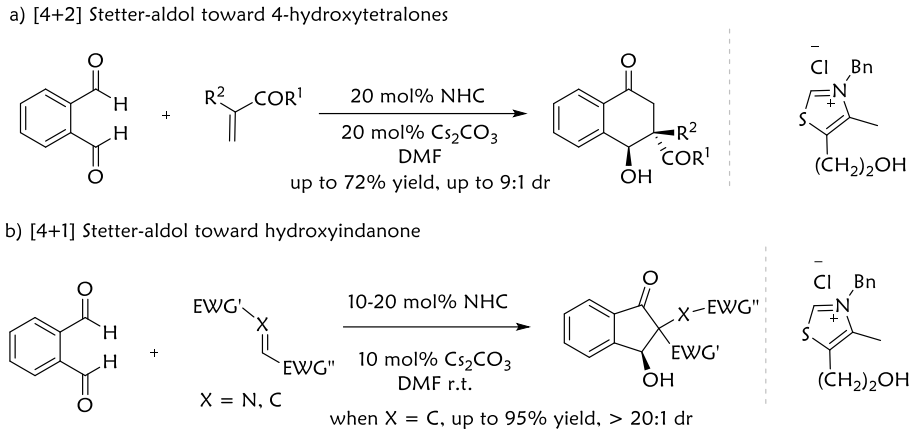

Scheme 1.21 [4+2]/[4+1] Stetter-aldol reactions using phthalaldehyde.

In 2019, Our group developed a ca4+rbene and thiourea cocatalytic dissymmetric domino Stetter-aldol reaction of phthalaldehyde and 1,3-cyclopentanedione derivatives. This reaction constitutes the first success in the carbene-catalyzed enantioselective synthesis of all-carbon spirocycles (**Scheme 1.22**).[64]

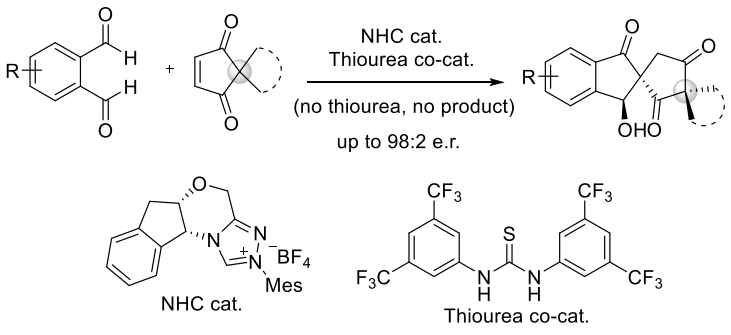

Scheme 1.22 Carbene and thiourea catalyzed access to all carbon spirocycles

1.6 Research Design

The difficulty in the synthesis of phthalidyl prodrugs lies in chirality control over the acetal/ketal moieties. Each phthalide contain a lactone unit. Considering the excellent enantioselective chirality control of acyl azolium during the transesterification, chiral NHC is going to be introduced to construct the lactone unit.

Phthalaldehyde is chosen as the substrate. The chiral NHC can attack one aldehyde group of phthalaldehyde to generate the chiral acyl azolium I. The generated acyl azolium is attacked by a nucleophile at the *ortho*-position to give the diastereomeric acetal intermediate I and II. There lies a dynamic equilibrium between them through the acyl azolium intermediate. One of the two acetal intermediates preferentially undergoes the lactonization to afford the enantioselective product. The proposed reaction scheme is shown below (**Scheme 1.23**).

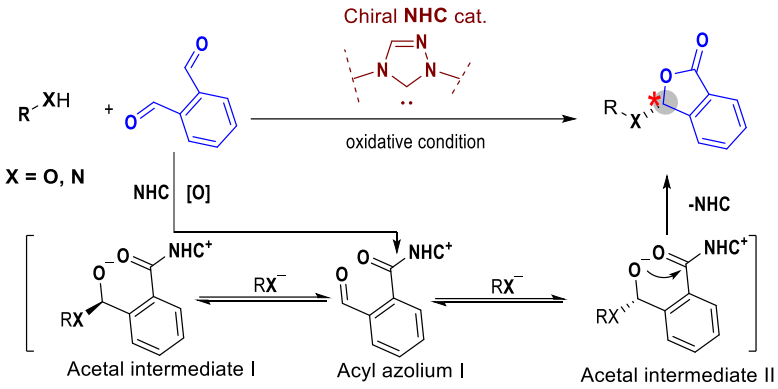

Scheme 1.23 Proposed carbene catalyzed chiral synthesis of phthalides

1.7 Summary

The development of new reaction modes could expand the synthetic toolbox for molecular modification in the medicinal chemistry area. N-heterocyclic carbene, as one

of the powerful tools in the toolbox, has led to wide application in chemical synthesis. In this thesis, we demonstrated the new reaction mode enabled by NHC in the enantioselective synthesis of 3-substituted phthalides, which could be used for structural modification on heteroatoms within the drugs. Our method shall expand the synthetic toolbox and bring significant values for the discovery and manufacturing of better chiral prodrugs in enantiomerically enriched forms.

In this thesis Chapter 2 will demonstrate our solution to the synthetic challenges in enantioselective modification of carboxylic acids for asymmetric access to optically enriched phthalidyl esters. Such solution involves a chiral carbene-catalyzed asymmetric addition of a carboxylic acid to a catalyst-bound intermediate generated from a phthalaldehyde substrate. A broad range of carboxylic acids could work effectively under mild and transition metal-free conditions. Selected modified drugs will be tested against tumor cell growth.

Chapter 3 will present that such methodology could be extended to the compounds with modifiable nitrogen atoms. With appropriate substrates bearing modifiable nitrogen atoms, the 3-(N-substituted) aminophthalides could be synthesized in excellent yield and excellent enantiomeric ratios. This will be the first enantioselective synthesis of chiral aminophthalides. More application will be investigated.

1.8 References

(1). David T. Smith, M. D. D., Haziq Qureshi, Jón T. Njarðarson *Njardarson Group* **2019**, URL: https://njardarson.lab.arizona.edu/content/top-pharmaceuticals-poster.

(2). Vitaku, E.; Smith, D. T.; Njardarson, J. T. *J. Med. Chem.* **2014,** *57*, 10257.

(3). Feher, M.; Schmidt, J. M. *J. Chem. Inf. Model.* **2003,** *43*, 218.

(4). Bemis, G. W.; Murcko, M. A. *J. Med. Chem.* **1996,** *39*, 2887.

(5). Yao, H.; Liu, J.; Xu, S.; Zhu, Z.; Xu, J. *Expert Opin. Drug. Discov.* **2017,** *12*, 121.

(6). Keller, T. H.; Pichota, A.; Yin, Z. *Curr. Opin. Chem. Biol.* **2006,** *10*, 357.

(7). Venkatesh, S.; Lipper, R. A. *J. Pharm. Sci.* **2000,** *89*, 145.

(8). Zhu, L.; Chen, L. *Cell. Mol. Biol. Lett.* **2019,** *24*, 40.

(9). Tishler, M. A. X. *J. Med. Chem.* **1964,** *45*, 1.

(10). Guo, Z. *Acta Pharm. Sin. B* **2017,** *7*, 119.

(11). Jornada, D. H.; dos Santos Fernandes, G. F.; Chiba, D. E.; de Melo, T. R.; dos Santos, J. L.; Chung, M. C. *Molecules* **2015,** *21*, 42.

(12). Albert, A. *Nature* **1958,** *182*, 421.

(13). Huttunen, K. M.; Raunio, H.; Rautio, J. *Pharmacol. Rev.* **2011,** *63*, 750.

(14). Rautio, J.; Kumpulainen, H.; Heimbach, T.; Oliyai, R.; Oh, D.; Jarvinen, T.; Savolainen, J. *Nat. Rev. Drug. Discov.* **2008,** *7*, 255.

(15). Takagi, T.; Ramachandran, C.; Bermejo, M.; Yamashita, S.; Yu, L. X.; Amidon, G. L. *Mol. Pharm.* **2006,** *3*, 631.

(16). Rautio, J.; Meanwell, N. A.; Di, L.; Hageman, M. J. *Nat. Rev. Drug. Discov.* **2018,** *17*, 559.

(17). Stella, V. J.; Nti-Addae, K. W. *Adv. Drug. Deliv. Rev.* **2007,** *59*, 677.

(18). Maag, H. *Drug Discov. Today Technol.* **2012,** *9*, e71.

(19). Beaumont, K.; Webster, R.; Gardner, I.; Dack, K. *Curr. Drug Metab.* **2003,** *4*, 461.

(20). Svensson, L. A.; Tunek, A. *Drug. Metab. Rev.* **1988,** *19*, 165.

(21). Dahan, A.; Khamis, M.; Agbaria, R.; Karaman, R. *Expert Opin. Drug. Discov.* **2012,** *9*, 1001.

(22). Sinkula, A. A. *Ann. N. Y. Acad. Sci.* **1987,** *507*, 281.

(23). Brogden, R. N.; Speight, T. M.; Avery, G. S. *Drugs* **1971,** *2*, 262.

(24). Rooseboom, M.; Commandeur, J. N.; Vermeulen, N. P. *Pharmacol. Rev.* **2004,** *56*, 53.

(25). Zhang, X.; Li, X.; You, Q.; Zhang, X. *Eur. J. Med. Chem.* **2017,** *139*, 542.

(26). Dhareshwar, S. S.; Stella, V. J. *Springer & AAPS Press,* **2007,** *2*, 31.

(27). Clayton, J. P.; Cole, M.; Elson, S. W.; Ferres, H.; Hanson, J. C.; Mizen, L. W.; Sutherland, R. *J. Med. Chem.* **1976,** *19*, 1385.

(28). Mitsuhashi, H.; Muramatsu, T.; Nagai, U.; Nakano, T.; Ueno, K. *Chem. Pharm. Bull. (Tokyo)* **1963,** *11*, 1317.

(29). Murakoshi, I.; Kubo, A.; Saito, J. I.; Haginiwa, J. *Chem. Pharm. Bull. (Tokyo)* **1964,** *12*, 747.

(30). Lin, G.; Chan, S. S.-K.; Chung, H.-S.; Li, S.-L. *Elsevier: Amsterdam* **2005,** *32*, 611.

(31). Diao, X.; Pang, X.; Xie, C.; Guo, Z.; Zhong, D.; Chen, X. *Drug Metab. Dispos.* **2014**, dmd.113.056218.

(32). Castaer, J.; Prous, J. *Drugs Fut.* **1986,** *11*, 394.

(33). Hauser, F. M.; Rhee, R. *J. Am. Chem. Soc.* **1977,** *99*, 4533.

(34). Wislicenus, J. *J. Ber.* **1893,** *26*, 2144.

(35). Karmakar, R.; Pahari, P.; Mal, D. *Chem. Rev.* **2014,** *114*, 6213.

(36). Ramachandran, P. V.; Chen, G.-M.; Brown, H. C. *Tetrahedron Lett.* **1996,** *37*, 2205.

(37). Ohzeki, T.; Mori, K. *Biosci. Biotechnol. Biochem.* **2003,** *67*, 2240.

(38). Kraus, G. A.; Cho, H.; Crowley, S.; Roth, B.; Sugimoto, H.; Prugh, S. *The Journal of Organic Chemistry* **1983,** *48*, 3439.

(39). Duchêne, A.; Thibonnet, J.; Parrain, J.-L.; Anselmi, E.; Abarbri, M. *Synthesis* **2007,** *2007*, 597.

(40). Ackermann, L.; Pospech, J. *Org. Lett.* **2011,** *13*, 4153.

(41). Igau, A.; Grutzmacher, H.; Baceiredo, A.; Bertrand, G. *J. Am. Chem. Soc.* **1988,** *110*, 6463.

(42). Siemeling, U.; Farber, C.; Bruhn, C. *Chem. Commun.* **2009**, 98.

(43). Hopkinson, M. N.; Richter, C.; Schedler, M.; Glorius, F. *Nature* **2014,** *510*, 485.

(44). Flanigan, D. M.; Romanov-Michailidis, F.; White, N. A.; Rovis, T. *Chem. Rev.* **2015,** *115*, 9307.

(45). Vedachalam, S.; Wong, Q.-L.; Maji, B.; Zeng, J.; Ma, J.; Liu, X.-W. *Adv. Synth. Catal.* **2011,** *353*, 219.

(46). Lv, H.; Jia, W.-Q.; Sun, L.-H.; Ye, S. *Angew. Chem. Int. Ed.* **2013,** *52*, 8607.

(47). Hao, L.; Du, Y.; Lv, H.; Chen, X.; Jiang, H.; Shao, Y.; Chi, Y. R. *Org. Lett.* **2012,** *14*, 2154.

(48). Atienza, R. L.; Scheidt, K. A. *Aust. J. Chem.* **2011,** *64*, 1158.

(49). Enders, D.; Grossmann, A.; Fronert, J.; Raabe, G. *Chem. Commun. (Camb)* **2010,** *46*, 6282.

(50). Read de Alaniz, J.; Rovis, T. *J. Am. Chem. Soc.* **2005,** *127*, 6284.

(51). Zhang, Y.; Du, Y.; Huang, Z.; Xu, J.; Wu, X.; Wang, Y.; Wang, M.; Yang, S.; Webster, R. D.; Chi, Y. R. *J. Am. Chem. Soc.* **2015,** *137*, 2416.

(52). He, M.; Bode, J. W. *J. Am. Chem. Soc.* **2008,** *130*, 418.

(53). Chen, X.; Fong, J. Z. M.; Xu, J.; Mou, C.; Lu, Y.; Yang, S.; Song, B.-A.; Chi, Y. R. *J. Am. Chem. Soc.* **2016,** *138*, 7212.

(54). Zhao, C.; Li, F.; Wang, J. *Angew. Chem. Int. Ed.* **2016,** *55*, 1820.

(55). He, M.; Beahm, B. J.; Bode, J. W. *Org. Lett.* **2008,** *10*, 3817.

(56). Xu, J.; Jin, Z.; Chi, Y. R. *Org. Lett.* **2013,** *15*, 5028.

(57). Huang, Z.; Huang, X.; Li, B.; Mou, C.; Yang, S.; Song, B. A.; Chi, Y. R. *J. Am. Chem. Soc.* **2016,** *138*, 7524.

(58). Fu, Z.; Wu, X.; Chi, Y. R. *Org. Chem. Front.* **2016,** *3*, 145.

(59). Sánchez-Larios, E.; Holmes, J. M.; Daschner, C. L.; Gravel, M. *Synthesis* **2011,** *2011*, 1896.

(60). Cheng, Y.; Peng, J. H.; Li, Y. J.; Shi, X. Y.; Tang, M. S.; Tan, T. Y. *J. Org. Chem.* **2011**, *76*, 1844.

(61). Sun, F.-G.; Huang, X.-L.; Ye, S. *J. Org. Chem.* **2010**, *75*, 273.

(62). Sun, F.-G.; Ye, S. Synlett. **2011**, *2011*, 1005.

(63). Sun, F.-g.; Ye, S. *Org. Biomol. Chem.* **2011**, *9*, 3632.

(64). Zhuo, S.; Zhu, T.; Zhou, L.; Mou, C.; Chai, H.; Lu, Y.; Pan, L.; Jin, Z.; Chi, Y. R. *Angew. Chem. Int. Ed.* **2019**, *58*, 1784.

Chapter 2

Catalytic Asymmetric Acetalization of Carboxylic Acids for Access to Chiral Phthalidyl Ester Prodrugs

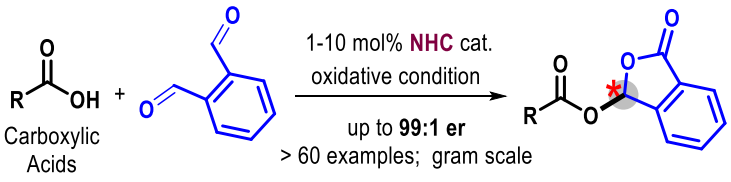

♦asymmtric acetalization

♦carboxylic acid modification ♦chiral phthalidyl ester prodrugs

2.1 Introduction

Chemical modification on medicinally significant natural products or drug molecules[1-5] is a proven strategy to develop chemical entities and prodrugs for improving drug performance or introducing alternative clinical applications[6-8]. Approximately one out of five chemical entity approvals by FDA are prodrugs in recent three years[9,10]. Carboxylic acids are among the most common moieties in pharmaceuticals. They are typically converted to the corresponding esters for better drug efficacy and/or lower side effects[11]. Among the different types of esters, phthalidyl esters as promoieties were found with impressive success[12] (**Scheme 2.1**).

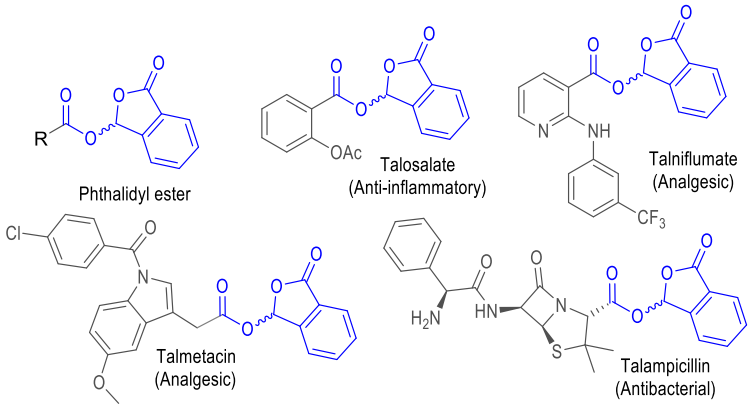

Scheme 2.1 Phthalidyl prodrugs on the market

Representative examples of phthalidyl ester prodrugs include talosalate, talniflumate, talampicilin, and talmetacin[13-15]. These phthalidyl esters contain an acetal moiety with a stereogenic carbon center that is difficult to be installed enantioselectively (**Scheme 2.2**).

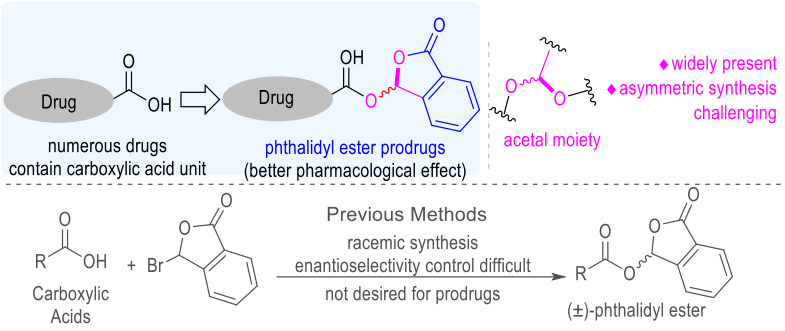

Scheme 2.2 Challenging asymmetric acetalization and phthalidyl ester synthesis

To date, phthalidyl esters are routinely prepared via reactions of carboxylic acids with 3-bromophthalides (**Scheme 2.2**)[16]. This method is efficient but unfortunately has no controls over the stereoselectivity for the newly created chiral center. It is challenging to directly modify carboxylic acid and related heteroatom functional groups in an enantioselective manner to form chiral acetal moieties and their analogs[17-19]. Thus, the phthalidyl esters are afforded as a racemic mixture of two enantiomers. Related efforts for enantioselective synthesis of phthalidyl esters also remain unsuccessful. The limited examples via kinetic resolutions used carboxylic anhydrides as the substrates and gave poor to moderate enantioselectivities with narrow substrate scopes[20].

Recent studies have further shown that such prodrugs exhibit medicinal applications. For example, talniflumate, an anti-inflammatory phthalidyl ester drug sold on the market for over thirty years, has extended its use in treatment of rheumatoid arthritis to cystic fibrosis, chronic obstructive pulmonary disease (COPD) and asthma, and is now identified as a novel inhibitor that improves responsiveness of pancreatic tumors to gefitinib[21-24]. In these cases, phthalidyl esters were used in racemic form while FDA guidelines and policies have required that each enantiomer shall be meticulously studied in pharmacology and toxicology before reaching the market[25,26]. It is worthy to note that chiral phthalidyl esters

are also found in bioactive natural products isolated from the marine plants, such as *luteorosin* and *macfarlandin A* (**Scheme 2.3**)[27]. Unfortunately, efficient methods for asymmetric access to optically enriched phthalidyl esters are not available.

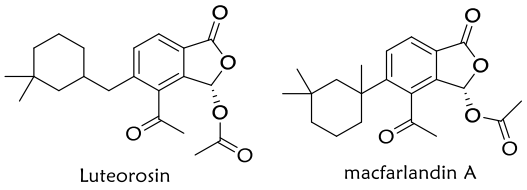

Scheme 2.3 Natural products containing phthalidyl esters

Here a highly enantioselective organocatalytic strategy for carboxylic acid functionalization and efficient access to optically enriched phthalidyl esters was disclosed (**Scheme 2.4**). This approach involves an N-heterocylcic carbene (NHC)-catalyzed activation of a phthalaldehyde that subsequently reacts with a carboxylic acid to form phthalidyl ester products. The main pathway involves a dynamic kinetic resolution process (**Scheme 2.4**). Oxidation of the one aldehyde moiety-derived Breslow intermediate generates azolium ester intermediate I. An addition of carboxylic acid to another aldehyde moiety of chiral NHC bound intermediate I affords diastereomeric intermediates II and III. Intermediate III preferentially undergoes the intermolecular annulation to give chiral phthalidyl esters with high enantiomeric ratio. The reaction enantioselectivity is controlled by the NHC catalyst.

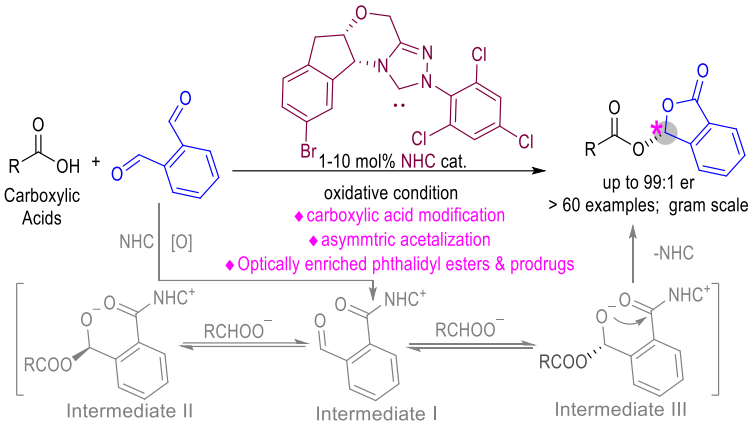

Scheme 2.4 NHC-catalyzed enantioselective acetalization and chrial phtalidyl ester synthesis

In our approach the operational condition is mild, and no transition metals are involved. A broad range of substrates and functional groups are well tolerated. Both aryl and aliphatic carboxylic acids bearing various substituents work effectively. Several natural products and drug molecules (e.g., valproic acid, chlorambucil, and naproxen) bearing carboxylic acid moieties can be enantioselectively modified using this approach. We also performed preliminary evaluations on the bioactivities of the phthalidyl ester derivatives of chlorambucil, an anti-cancer agent and chemotherapy drug. Our results show that the (*R*)-enantiomer of the phthalidyl ester derivative have better activities to inhibit the growth of Hela cells than the corresponding (*S*)-enantiomer, racemic mixture and the unmodified chlorambucil.

Our catalytic approach constitutes the first success for enantioselective addition of carboxylic acid to catalytically generated NHC-bound intermediates. Given the wide presence of carboxylic acid moieties in bioactive molecules, we expect our enantioselective approach for phthalidyl ester synthesis to bring significant values for both discovery and manufacturing of better pharmaceuticals.

2.2 Results and discussion

2.2.1 Condition optimization

We chose aspirin (acetylsalicylic acid, **1**) as a model carboxylic acid to react with *o*-phthalaldehyde (**2**) in searching for suitable NHC catalysts and conditions (**Table 2.1**). Both aspirin and the corresponding phthalidyl ester (talosalate) are commercial drugs for several decades. Extensive optimizations are shown below (Table **2.1**-**2.3**). A typical reaction was performed with azolium salt as an NHC pre-catalyst, quinone as an oxidant[28], and K_2CO_3 as the base. We firstly tested the reaction in the absence of NHC (Entry 8, **Table 2.1**). No product could generate (Entry 8, **Table 2.1**). And then NHC A[29] to G were screened to improve the er value. NHC **C**[30, 31] showed better er value with higher yield but did not satisfy our requirement (Entry 3, **Table 2.1**).

Table 2.1 Optimization: Effect of NHCs

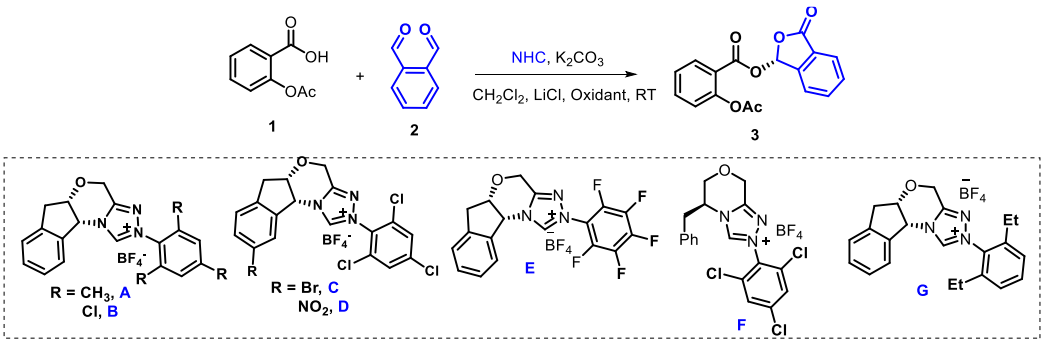

Entry	NHC	Yield (%)	e.r.
1	A	66	60:40
2	B	84	77:23
3	C	92	85:15
4	D	Trace	n.d.

5	E	75	77:23
6	F	Trace	n.d.
7	G	Trace	n.d.
8	no NHC, various Conditions	n.r.	n.d.

Reaction conditions: **1** (0.1 mmol), **2** (0.15 mmol), 0.1 equiv. NHC, 1 equiv. 3,3',5,5'-Tetra-tert-butyldiphenoquinone as oxidant, 0.6 equiv. K_2CO_3, 0.5 equiv. LiCl, CH_2Cl_2 (2 mL), rt, 12 h. Yields determined by isolation. e.r. determined by HPLC. n.r. = no reation. n.d. = not determined.

Then we moved to base and additive screening. It was frustrated that the both the bases and additive could not improve the er values at the room temperature in most of cases (Entry 1-6, Entry 9-14, **Table 2.2**). However, higher yield could be obtained in presence of combination of K_2CO_3 and LiCl[32-35].

Table 2.2 Optimization: base and additives.

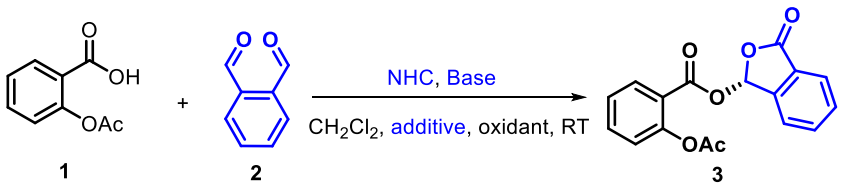

Entry	**NHC**	**Base**	**Additive**	**Yield (%)**	**e.r.**
1	**B**	$KHCO_3$	-	83	78:22
2	**B**	K_2CO_3	-	86	77:23
3	**B**	Cs_2CO_3	-	95	77:23
4	**B**	Li_2CO_3	-	Trace	n.d.
5	**B**	$LiOH{\cdot}H_2O$	-	20	77:23

6	**B**	DIPEA	-	n.d.	77:23
7	**B**	TEA	-	n.d.	75:25
8	**B**	K_2CO_3	LiCl	84	78:22
9	**C**	$NaHCO_3$	LiCl	55	82:18
10	**C**	Na_2CO_3	LiCl	61	85:15
11	**C**	$KHCO_3$	LiCl	81	85:15
12	**C**	K_2CO_3	LiCl	92	85:15
13	**C**	$LiOH{\cdot}H_2O$	-	45	84:16
14	**C**	Li_2CO_3	-	36	84:16

Reaction conditions: **1** (0.1 mmol), **2** (0.15 mmol), 0.1 equiv. NHC, 1 equiv. 3,3',5,5'-Tetra-tert-butyldiphenoquinone as oxidant, 0.6 equiv. base, 0.5 equiv. LiCl, CH_2Cl_2 (2 mL), rt, 12 h. Yields determined by isolation. e.r. determined by HPLC n.d. = not determined. TEA = Triethylamine, DIPEA = N, N-Diisopropylethylamine.

More reactions to improve the er values were conducted. It was shown that solvent may play a key role in improvement of er values. Using acetone as solvent, the er value was 43:57 (Entry 1, **Table 2.3**), which was reversed from using other solvents (e.g., 77:23 using DCM, Entry 11, **Table 2.3**). Finally, the available common solvents were screened and better er value was obtained with $CHCl_3$ as solvent. Satisfactory er values was obtained when the reaction was performed at -20 ^oC (Entry 17, **Table 2.3**).

Table 2.3 Optimization: solvents in presence **B** or **C.**

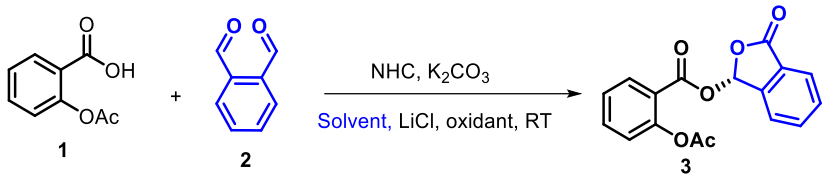

Entry	NHC	Solvent	Yield (%)	e.r.
1	**B**	acetone	n.d.	43:57
2	**B**	CCl_4	n.d.	82:18
3	**B**	ethyl acetate	n.d.	74:26
4	**B**	$PhCF_3$	n.d.	77:23
5	**B**	THF	n.d.	74:26
6	**B**	1,2-dichloroethane	n.d.	76:24
7	**B**	MeCN	n.d.	56:44
8	**B**	diethyl ether	n.d.	71:29
9	**B**	toluene	n.d.	82:18
10	**B**	$CHCl_3$	n.d.	85:15
11	**B**	CH_2Cl_2	n.d.	77:23
12	**C**	$PhCF_3$	76	84:16
13	**C**	dioxane	79	75:15
14	**C**	PhCl	n.d.	83:17
15	**C**	CH_2Cl_2	92	85:15
16	**C**	$CHCl_3$	91	90:10
17	**C**	$CHCl_3$	89	95:15[a]

Reaction conditions: **1** (0.1 mmol), **2** (0.15 mmol), 0.1 equiv. NHC, 1 equiv. 3,3',5,5'-Tetra-tert-butyldiphenoquinone as oxidant, 0.6 equiv. K_2CO_3, 0.5 equiv. LiCl, solvent (2

mL), rt, 12 h. Yields determined by isolation. e.r. determined by HPLC n.d. = not determined. [a] at -20 °C.

2.2.2 Substrate scope

With an optimized set of conditions in hand, we evaluated the generality of the present reactions (**Scheme 2.5**). We first studied aryl carboxylic acids (**4**-**21**). Various substituents (such as halogen and amine moieties) or substitution patterns for benzoic acid were all well tolerated (**4**-**14**). Multiple substituents can be present on the benzoic acid (**15**, **16**). The use of sterically bulky aryl carboxylic acid could typically give higher product er values (e.g., **16**; 97:3 er). Heteroaryl carboxylic acids worked effectively (**19**). The absolute configurations of the catalytic reaction products were confirmed based on X-ray structures of ferrocenecarboxylic acid (**20**) and *para*-iodobenzoic acid (**21**).

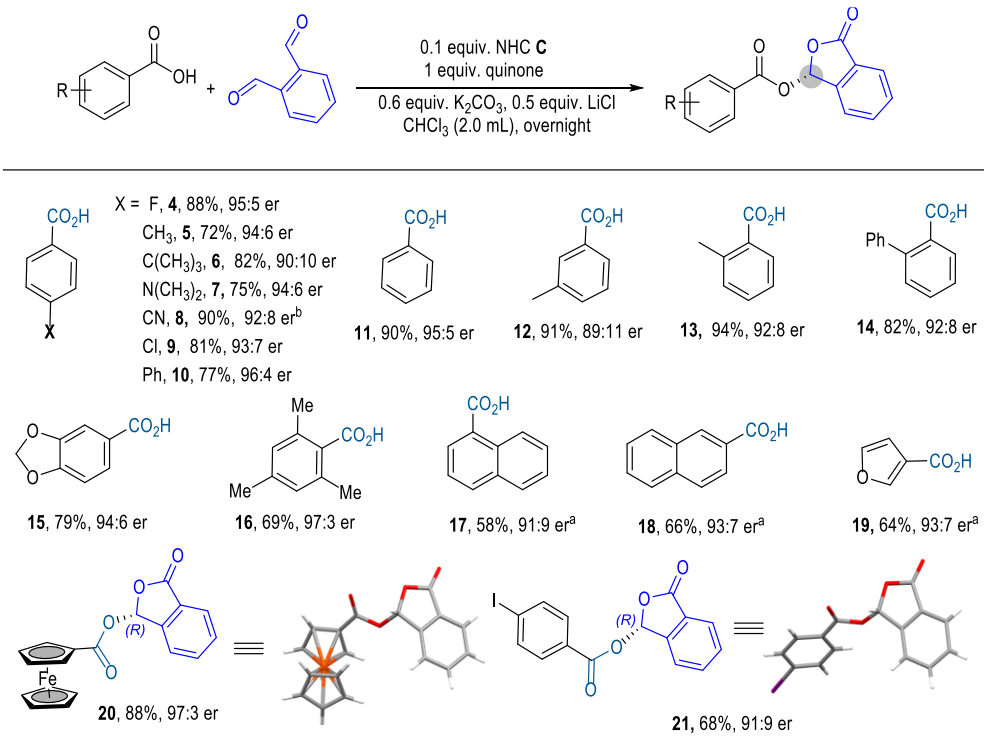

Scheme 2.5 Scope of aromatic acids

We next evaluated aliphatic acids (**22**-**44**) (**Scheme 2.6**). Notably, aliphatic acids are widely present in small molecule pharmaceuticals, peptides and proteins. They are increasingly recognized as signaling molecules and hold significant therapeutic potentials[36]. We were very delighted to find that higher enantioselectivities were obtained with aliphatic acids, when compared with aryl carboxylic acids. For example, when acetic acid is the substrate (**22**), the corresponding phthalidyl ester was obtained with 82% yield and 97:3 er. The length of the alkyl chain in the acids has little influence on the reaction yield and er values (**22**-**26**). Primary (**22**-**32**), secondary (**33**-**40**), and tertiary (**41**-**44**) alkyl carboxylic acids all worked well to give the corresponding products with excellent enantioselectivities. For cyclic (**34**-**37**, **40**, and **44**), heterocyclic (**38**, **39**, **42**), and bridging (**43**) alkyl acids, the ring size and steric hindrance have little influence on the reaction outcomes. Unsaturated carboxylic acids are effective substrates as well (**45**-**48**). The present reaction is amenable to scalable synthesis with low catalyst loadings. We demonstrated that a gram quantity of acid **32** could be effectively transformed to the corresponding ester with 97:3 er by using 1 mol% of the NHC catalyst.

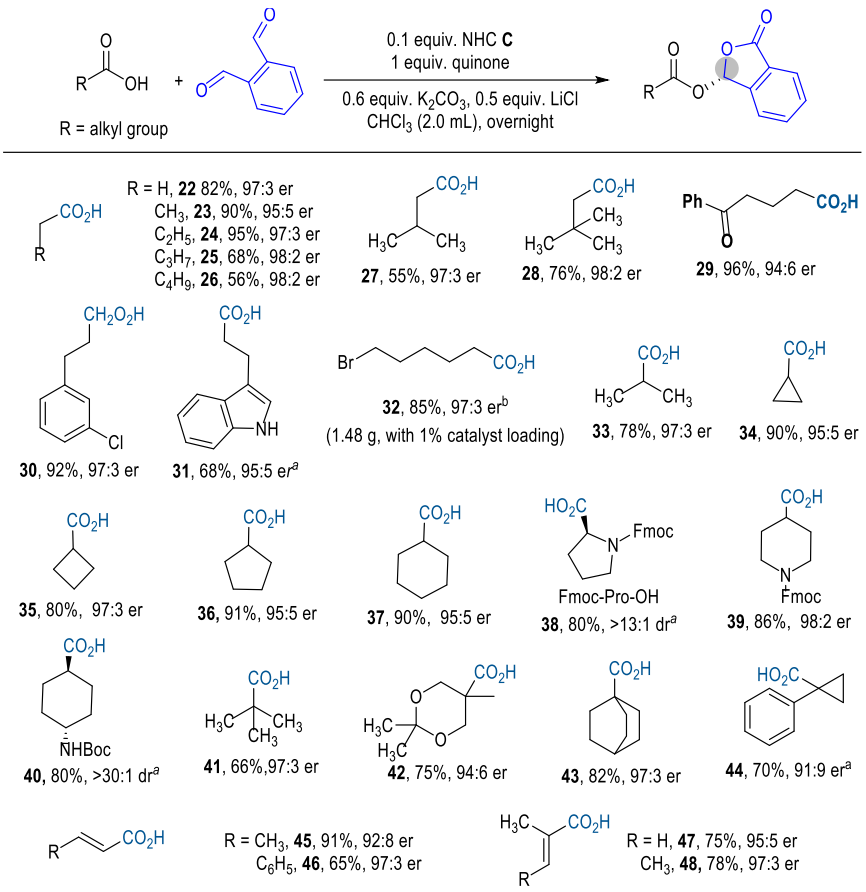

Scheme 2.6 Scope of alkyl acids

However, when we tried stronger acids, such as trifluoracetic acid, the reaction became messy and no desired product was obtained (**Scheme 2.7**). The main reasons likely include lower nucleophilicity of the trifluoroacetate anion, and the poor stabilities of the intermediates resulted from reactions between trifluoroacetate anion and the dialdehyde substrates.

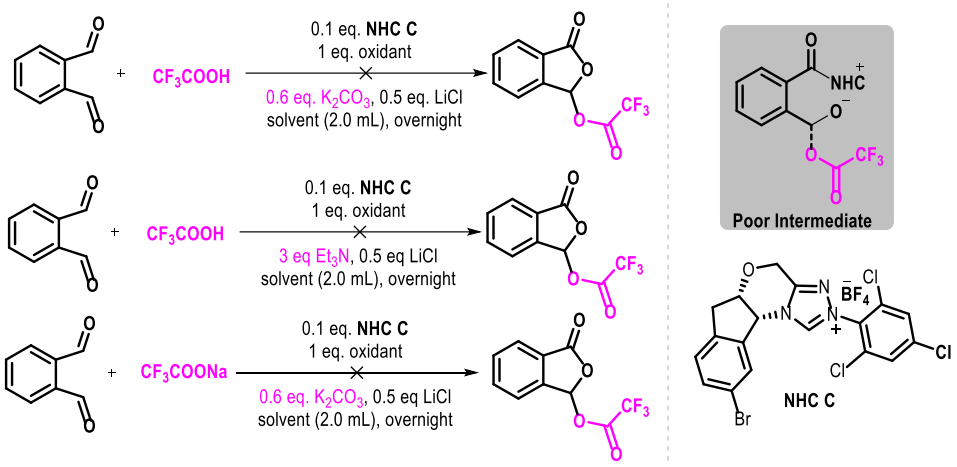

Scheme 2.7 Investigation of strong acids under our conditions

Substituted phthaldehydes tested here all reacted effectively to give the corresponding ester products with excellent er values and good yields (**49**-**52**) (**Scheme 2.8**). Regioselectivity of unsymmetrical dialdehydes was investigated (**Scheme 2.8 52a**:**52b** = 2.2:1, 95:5 er), The addition of carboxylate to aldehyde favors the sterically less congested site of the dialdehydes. For the reaction between aldehyde and NHC (to eventually form azolium ester intermediate under oxidative condition), the carbene addition step is not the rate-determine step and thus the substituents have little influence. These results clearly illustrate the broad applicability of our strategy for enantioselective modification of various carboxylic acids.

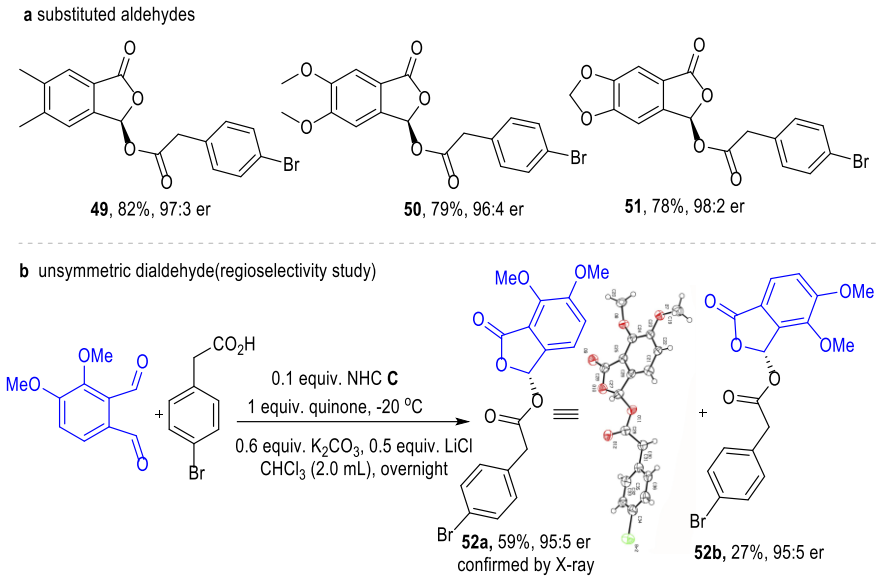

Scheme 2.8 Scope of dialdehydes and regioselectivity study

To further demonstrate the generality and utility of the present strategy, several natural products bearing carboxylic acid moieties (**Scheme 2.9**) were modified under the standard catalytic condition (**53**-**55**). Multiple commercially used drug molecules bearing carboxylic acid moieties were also modified to give the corresponding ester products (**56**-**59**, **63**). In all cases, the reaction worked effectively. The newly created chiral center during phthalidyl ester formation is well-controlled by the NHC catalyst. The chiral centers present in the natural products and drugs have nearly no influence over the stereochemistry during the catalytic reaction. For example, the use of drug *R*-**57** and *S*-**57** under otherwise identical catalytic conditions both gave the corresponding ester products with exceptionally high diastereoselectivities and identical chirality for the newly formed center. Relatively sophisticated natural products and drugs (abietic acid **55**, dehydrocholic acid **56**) with multiple fused rings and chiral centers are well tolerated under the present condition. In addition to talosalate (**3**), the present methods can be used to prepare optically enriched versions of several phthalidyl ester prodrugs sold on the market, including talmetacin, talniflumate, and talampicillin (**60**-**62**) (**Scheme 2.9 b**).

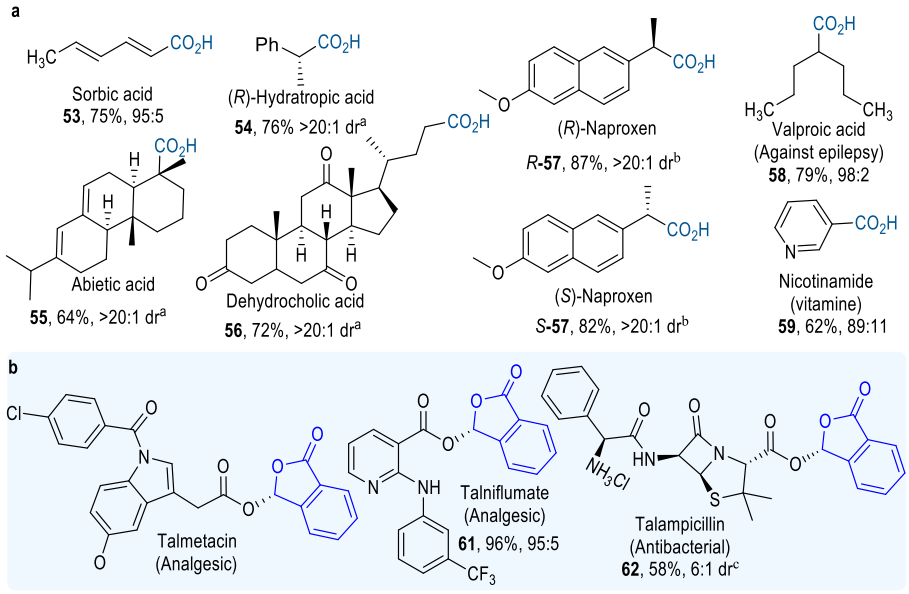

Scheme 2.9 Natural products and medicinal molecules

2.2.3 Proposed pathway and discussion

The reaction pathway was proposed in the following cycle (**Scheme 2.10**). The free carbene attacks one aldehyde group of the substrate **S-1** to generate the NHC bound intermediate I. after oxidation, intermediate **II** undergoes the reversible semi-acetalization with carboxylic acid anion **S-2** to deliver diastereomeric intermediate **III** and **IV.** Intermediate III is the favorable species for intramolecular ring closing procedure and thus provides the enantioselective product **S-3**. Intermediate **IV** poses an unfavorable structure likely for the lactonization due to the steric hindrance introduced by the chiral NHC. However, it could be converted into intermediate **III** through the intermediate **II**.

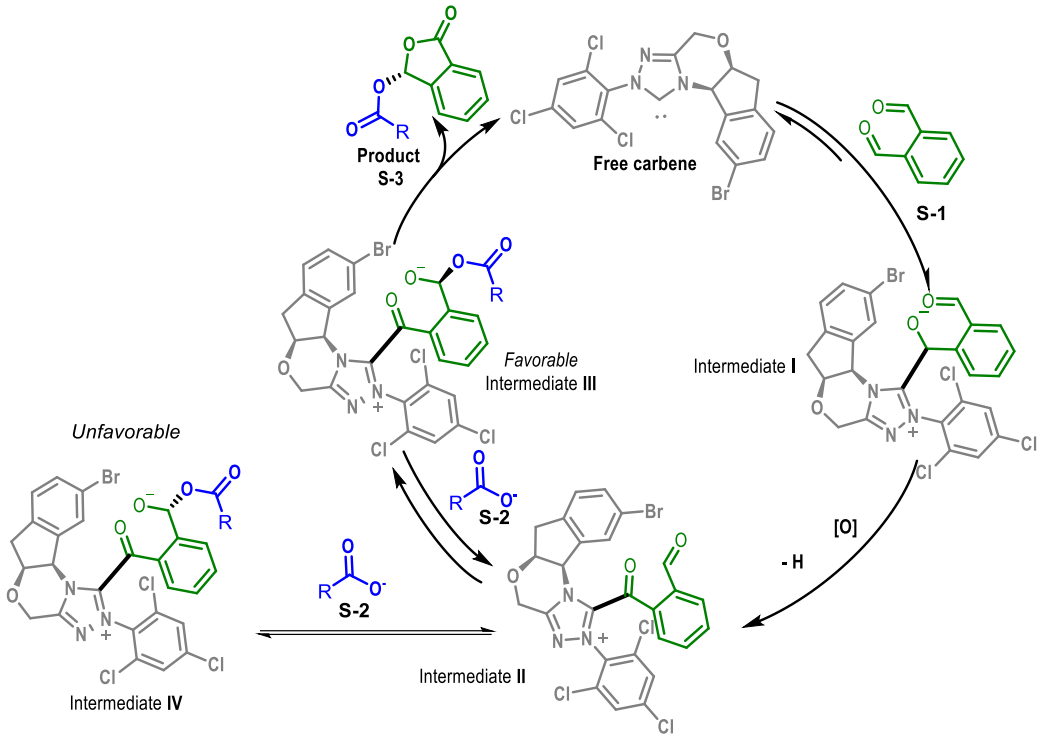

Scheme 2.10 proposed pathway

This reaction undergoes a stepwise pathway involving dynamic kinetic resolution. The enantioselective step lies in the lactonization step after semi-acetalization with carboxylic acids. This was supported by the study of regioselectivity. The aldehyde group reacted with the carboxylic acid is quite remote from the chiral center of the NHC bound intermediate II. It has very little influence on the semi-acetalization with carboxylic acids. Because of that, the sophisticated acids with steric hindrance/original chirality in not insensitive in this reaction, either.

2.2.4 Bio-evaluation

(Bioassays were carried out by Dr. Hongzhong Chen under supervision of Prof. Yanli Zhao)

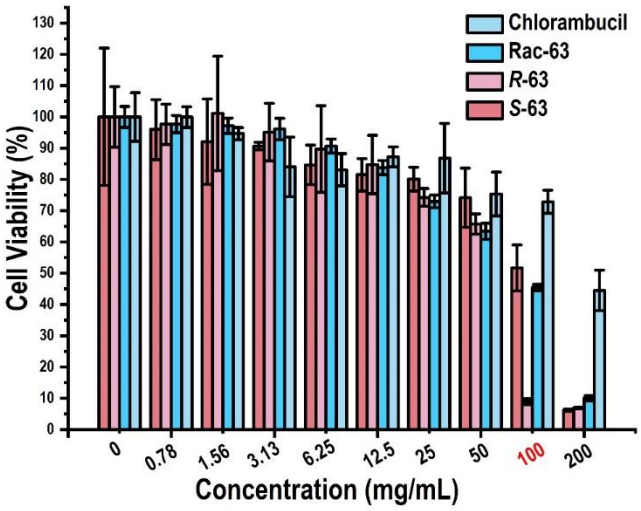

Figure 2.1 Examination of the chiral prodrug, rac-**63**, *R*-**63** and *S*-**63** using Hela cells (n = 3 biological replicates, Mean ±SD).

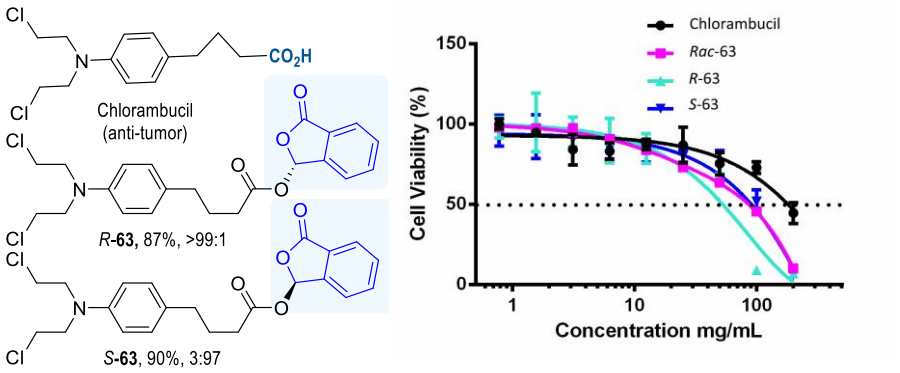

Figure 2.2 IC_{50} curve for chiral phthalidyl ester prodrugs against the growth of Hela cells (n = 3 biological replicates, Mean ±SD). IC_{50} for Chlorambucil: 157 mg/mL; *Rac*-**63**: 83.6 mg/mL; *R*-**63**: 53.6 mg/mL, *S*-**63**: 91.7 mg/mL.

It is well established that the two enantiomers of a molecule can have different pharmacological effects[37]. Chlorambucil is an anti-cancer drug with applications mainly in chronic lymphocytic leukemia (CLL), Hodgkin's lymphoma (HL) and non-Hodgkin lymphoma (NHL)[38,39]. We performed preliminary bioactivity studies using the two

phthalidyl ester enantiomers of Chlorambucil (**Figure 1.2**). Our results show that at the concentration of 100 μg/mL (**Figure 1.1**), the (*R*)-enantiomer (*R*-**63**, >99:1 er, IC_{50}: 53.6 mg/mL) phthalidyl ester is more effective to inhibit Hela cells than the corresponding (*S*)-enantiomer (*S*-**63**, 3:97 er, IC_{50}: 83.6 mg/mL), racemate (Rac-63, IC_{50}: 91.7 mg/mL) and unmodified chlorambucil (IC_{50}: 157.0 mg/mL). The different pharmacological effects might be attributed to better penetrations through cell membranes or different interactions with the target DNA brought by the chiral modifications.

2.3 Summary

In summary, we have addressed the challenges in enantioselective acetalization of carboxylic acids for quick access to optically enriched phthalidyl esters. A wide range of carboxylic acids, including natural products and pharmaceuticals, reacted effectively and stereo-selectively under our conditions. Carboxylic acids are among the most common functional groups in bioactive molecules and medicines. Phthalidyl esters are proven prodrugs of carboxylic acids. We expect our method to bring significant values for the discovery and development of better chiral prodrugs in enantiomerically enriched forms. Our study shall also benefit future development on enantioselective acetalization and related reactions for asymmetric functionalization of heteroatoms.

2.4 Experimental Section

2.4.1 General Information

Chemicals

Chemicals were commercially purchased from Sigma-Aldrich, TCI, and directly used without further purification unless otherwise stated. N-heterocyclic carbenes were synthesized following the reported procedure.

Chromatography

Analytical thin-layer chromatography (TLC) was carried out on Merck 60 F254 pre-coated silica gel plate (0.2 mm thickness). Visualization was performed using a UV lamp. Column chromatography was carried out on silica gel (60 Å, 40-63 micron) purchased from Davisil with analytical solvents as the eluent. All the yields referred to spectroscopically and chromatographically pure compounds.

Nuclear Magnetic Resonance (NMR) Spectroscopy

Proton nuclear magnetic resonance (^{1}H NMR) spectra were recorded on a Bruker BBFO (400 MHz) spectrometer or AV400 NMR (400 MHz, QNP probe). Chemical shifts were recorded in parts per million (ppm, δ) relative to tetramethylsilane (δ 0.00) or chloroform (δ = 7.26, singlet). ^{1}H NMR splitting patterns are designated as singlet (s), doublet (d), triplet (t), quartet (q), dd (doublet of doublets); m (multiplets), etc. All first-order splitting patterns were assigned on the basis of the appearance of the multiplet. Splitting patterns that could not be easily interpreted are designated as multiplet (m) or broad (br). Carbon nuclear magnetic resonance (^{13}C NMR) spectra were recorded on a Bruker BBFO (100 MHz) spectrometer. Chemical shifts are reported in ppm with the solvent resonance as the internal reference ($CDCl_3$ δ 77.0, CD_3OD δ 49.0).

High Resolution Mass Spectrometry (HRMS)

High resolution mass spectral analysis (HRMS) was performed on Finnigan MAT 95 XP mass spectrometer (Thermo Electron Corporation). The calculated values are based on the most abundant isotope.

Optical rotations

Optical rotations were measured using a 1 mL cell using a sodium lamp (sodium D line, λ = 589 nm) in the indicated solvent at the indicated temperature with a 1 dm path length on a Jasco P-1030 polarimeter and are reported as follows: $[\alpha]^{rt}_{D}$ (*c* in g per 100 mL solvent).

High Performance Liquid Chromatography (HPLC)

HPLC analysis was performed on a Shimadzu LC-15C liquid chromatograph with chiralcel IA, IB, ID, AD-H and OD-H column (Daicel Chemical Industries, Ltd.). The solvents (*n*-hexane and *iso*-propanol, HPLC-grade) used as the eluent were purchased from Sigma Aldrich. The column type and the eluent (a mixture of *n*-hexane and *iso*-propanol) are indicated for each experiment.

X-ray crystallography

X-ray crystallography analysis was performed on Bruker X8 APEX *X*-ray diffractometer.

2.4.2 General approach to chiral phthalidyl esters

To a 10 ml-round bottomed flask were added the acid (0.1 mmol), phthaldehyde (0.15 mmol), NHC C (0.01 mmol), 3,3',5,5'-Tetra-tert-butyldiphenoquinone (0.1 mmol, or 5 eq MnO_2) and LiCl (0.05 mmol), then 2 ml of $CHCl_3$ (unless otherwise noted) was added at -20 ^{o}C (unless otherwise noted) followed by addition of K_2CO_3 powder (0.06 mmol). The reaction was stirred overnight or until the red brown color faded into light yellow or

colorless. The solvent was removed under vacuum and the resulting residue was applied on the column chromatography (eluent, hexane: ethyl acetate = 3:1) to give the corresponding phthalidyl esters.

Compound *R*-**63** was also subject to the general procedure with some minor change on reaction conditions. The substrate ampicillin was protected with benzaldehyde in presence of TMEDA following the reported reference[13,40]. Then the obtained D- -benzylideneaminobenzylpenicillin salt was applied in the general procedure with acetone as solvent (eluent, hexane: ethyl acetate = 1:1). After that, the enamine-protecting group was removed from this product by dissolving it in aqueous acetone (1:1, 2 mL) and vigorously stirring this solution at pH 2.5 for 30 min (1 drop of 1 *N* HCl). Acetone was removed in vacuo and the product *R*-**63** was salted out of the aqueous phase as a sticky gum. The material was dissolved in ethyl acetate, washed with H_2O, and dried. Careful addition of dry ether to the ethyl acetate solution of the penicillin ester afforded compound *R*-**63** as an off-white amorphous solid.

2.4.3 Syhthesis of NHC C

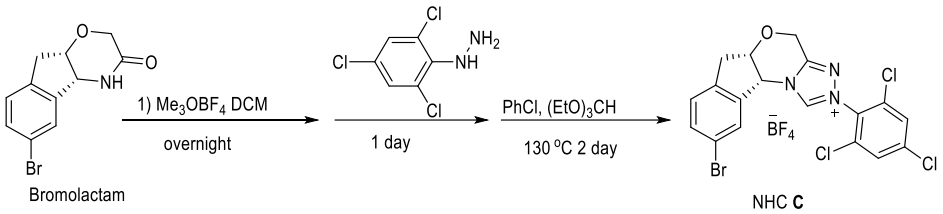

The NHC **C** was synthesized following similar procedure as other NHC catalysts. Bromolactam (4.18 g, 15.62 mmol, 1 equiv.), prepared according to Bode, is dissolved in CH_2Cl_2 (80 mL) and then Trimethyloxonium tetrafluroborate (2.30 g, 15.62 mmol, 1 equiv.) was added. The resulting mixture was stirred at room temperature overnight. 2,4,6-Trichlorophenylhydrazine (3.30 g, 15.62 mmol, 1 equiv.) was added and the reaction is

stirred for 24 hrs. After completion, CH_2Cl_2 was removed before the crude hydrazide is then taken up in chlorobenzene (60 mL) and triethylorthoformate (10 mL) and the reaction was stirred at 130 ^oC for 2 days. The reaction mixture could cool down and the NHC **C** was crystallized from the solution. The filter cake was washed by ethyl acetate and collected in 57% yield as an off-white solid.

2.4.4 Bioevaluation methods

MTT (3-(4,5-dimethylthiazol-2-yl)-2,5-diphenyltetrazolium bromide) assay was used to investigate the cytotoxicity of prodrugs including *R*-enantiomer (*R*-**63**), *S*-enantiomer (*S*-**63**) racemate (Rac-**63**) and free drug chlorambucil. The HeLa cells (obtained from ATCC, Rockville, MD, maintained in Dulbecco's Modified Eagle's Medium) were seeded in 96-well plates (100 μL of medium) and incubated for 24 h. After the cell density reached 60%-70%, the cells were fed with the prodrugs and chlorambucil at the concenration of 0, 0.78, 1.56, 3.13, 6.25, 12.5, 25, 50 100, 200 mg/mL, and incubated with 48 h. After the medium removed, the fresh medium with 10% MTT was added, and incubated with for another 4 h. The medium was removed carefully, followed by adding 100 μL of DMSO. Finally, optical densities of the samples were measured using a microplate reader with the double wavelength of 570 nm and 490 nm.

Chapter 3 will present that such methodology could be extended to the compounds with modifiable nitrogen atoms. With appropriate substrates bearing modifiable nitrogen atoms, the 3-(N-substituted) aminophthalides could be synthe

2.4.6 Characterization of Products

N-heterocyclic carbene (NHC) **C**:

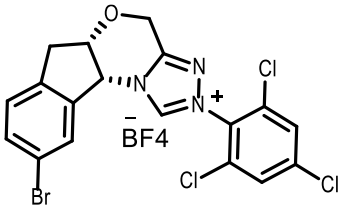

Off-white solid, 57% overall yield

^{1}H NMR (400 MHz, $CDCl_3$) δ 10.56 (s, 1H), 7.57 - 7.44 (m, 4H), 7.21 (d, J = 8.0 Hz, 1H), 6.16 (d, J = 3.9 Hz, 1H), 5.11 (t, J = 4.3 Hz, 1H), 5.06 (s, 2H), 3.32 (d, J = 4.8 Hz, 1H), 3.20-3.10 (m, 1H);

^{13}C NMR (100 MHz, $CDCl_3$) δ 150.28, 145.51, 139.44, 139.08, 137.35, 132.89, 129.34, 129.20, 127.06, 127.03, 121.49, 62.17, 60.18, 37.21.;

HRMS (ESI, m/z): calcd. for $[C_{18}H_{12}BrCl_3N_3O]^+$ 469.9224, found 469.9232;

CCDC codes: CCDC 1866589, the crystallographic data be obtained free of charge from The Cambridge Crystallographic Data Centre via www.ccdc.cam.ac.uk/data_request/cif.

Compound 3:

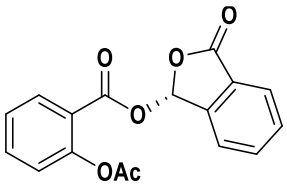

Yellow solid, 89% yield

^{1}H NMR (400 MHz, $CDCl_3$) δ 8.03 (dd, J = 8.0, 1.9 Hz, 1H), 7.97 (dd, J = 7.4, 1.6 Hz, 1H), 7.78 (t, J = 7.5 Hz, 1H), 7.73 – 7.56 (m, 4H), 7.39 – 7.29 (m, 1H), 7.20 – 7.07 (m, 1H), 2.22 (s, 3H);

^{13}C NMR (100 MHz, $CDCl_3$) δ 169.52, 167.72, 162.84, 151.19, 144.27, 135.04, 134.93, 132.18, 131.39, 126.47, 126.17, 125.85, 124.11, 123.89, 121.58, 93.18, 20.81;

IR ν_{max} (film, cm^{-1}): 2091, 1637, 1367, 1192, 970; **$[\alpha]^{21}_D$** = -35.5 (c = 3.2 in $CHCl_3$);

HRMS (ESI, m/z): calcd. for $[C_{17}H_{13}O_6]^+$ 313.0712, found 313.0711;

HPLC analysis: 95:5 er, [CHIRALPAK IB column; 0.6 mL/min; solvent system: *i*-PrOH/hexane 5:95; retention times: 28.5 min (minor), 31.2 min (major)].

Compound 4:

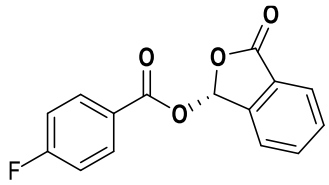

Yellow solid, 88% yield

^{1}H NMR (400 MHz, $CDCl_3$) δ 8.12 – 8.05 (m, 2H), 7.98 (dd, J = 7.3, 1.5 Hz, 1H), 7.82 – 7.75 (m, 1H), 7.72 – 7.66 (m, 3H), 7.14 (d, *J* = 8.6 Hz, 1H).;

^{13}C NMR (100 MHz, $CDCl_3$) δ 168.10, 167.77, 164.08, 144.35, 134.88, 132.91, 132.78, 131.37, 126.59, 125.88, 124.69, 124.65, 123.70, 116.04, 115.75, 93.29;

IR ν_{max} (film, cm^{-1}): 2091, 1788, 1664, 1400, 1361, 1246, 974; **$[\alpha]^{21}_D$** = -59.9 (*c* = 2.2 in $CHCl_3$);

HRMS (ESI, m/z): calcd. for $[C_{15}H_{10}FO_4]^+$ 273.0563, found 273.0562;

HPLC analysis: 95:5 er, [CHIRALPAK IB column; 0.6 mL/min; solvent system: *i*-PrOH/hexane 5:95; retention times: 16.8 min (minor), 18.7 min (major)].

Compound 5:

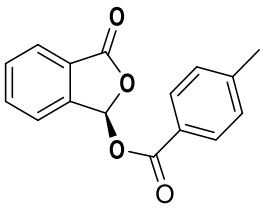

Colorless oil, 72% yield

^{1}H NMR (400 MHz, $CDCl_3$) δ 7.99 – 7.92 (m, 3H), 7.77 (t, *J* = 7.4, 1H), 7.70 – 7.66 (m, 3H), 7.25 (d, *J* = 8.1 Hz, 2H), 2.42 (s, 3H);

^{13}C NMR (100 MHz, $CDCl_3$) δ 167.96, 165.09, 145.06, 144.60, 134.84, 131.26, 130.21, 129.33, 126.64, 125.80, 125.63, 123.75, 93.22, 21.77;

IR ν_{max} (film, cm^{-1}): 2091, 1636, 1261, 1083, 955; **$[\alpha]^{21}_D$** = -27.6 (*c* = 0.5 in $CHCl_3$);

HRMS (ESI, m/z): calcd. for $[C_{16}H_{13}O_4]^+$ 269.0814, found 269.0818;

HPLC analysis: 94:6 er, [CHIRALPAK IB column; 0.6 mL/min; solvent system: *i*-PrOH/hexane 5:95; retention times: 15.4 min (minor), 16.3 min (major)].

Compound 6:

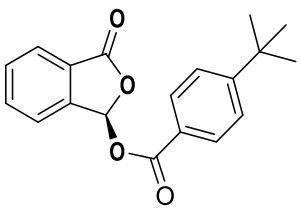

Off-white solid, 82% yield

^{1}H NMR (400 MHz, $CDCl_3$) δ 8.02 – 7.95 (m, 3H), 7.79-7.75 (m, 1H), 7.70 – 7.65 (m, 3H), 7.48 – 7.45 (m, 2H), 1.33 (s, 9H);

^{13}C NMR (100 MHz, $CDCl_3$) δ 167.92, 164.98, 157.94, 144.56, 134.79, 131.20, 130.02, 126.56, 125.73, 125.55, 125.50, 123.67, 93.16, 35.16, 30.98;

IR ν_{max} (film, cm^{-1}): 2972, 2093, 1790, 1639, 1261, 972; **$[\alpha]^{21}_D$** = -61.8 (*c* = 1.5 in $CHCl_3$);

HRMS (ESI, m/z): calcd. for $[C_{19}H_{19}O_4]^+$ 311.1283, found 311.1284;

HPLC analysis: 90:10 er, [CHIRALPAK IB column; 0.6 mL/min; solvent system: *i*-PrOH/hexane 5:95; retention times: 13.3 min (minor), 13.9 min (major)].

Compound 7:

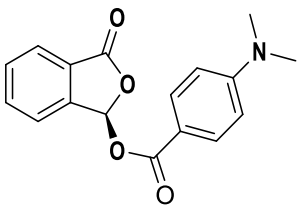

off-white solid, 75% yield

^{1}H NMR (400 MHz, $CDCl_3$) δ 7.98 – 7.87 (m, 3H), 7.75 (td, *J* = 7.5, 1.2 Hz, 1H), 7.70 – 7.61 (m, 3H), 6.65 – 6.58 (m, 2H), 3.05 (s, 6H);

^{13}C NMR (100 MHz, $CDCl_3$) δ 168.21, 165.14, 153.93, 145.06, 134.65, 132.02, 130.98, 126.72, 125.62, 123.70, 114.45, 110.65, 93.04, 39.96;

IR ν_{max} (film, cm^{-1}): 2093, 1776, 1636, 1267, 1184, 961; **$[\alpha]^{21}_D$** = -72.7 (*c* = 2.2 in $CHCl_3$);

HRMS (ESI, m/z): calcd. for $[C_{17}H_{16}O_4]^+$ 298.1079, found 298.1079;

HPLC analysis: 94:6 er, [CHIRALPAK IB column; 0.6 mL/min; solvent system: *i*-PrOH/hexane 5:95; retention times: 42.2 min (major), 46.5 min (minor)].

Compound 8:

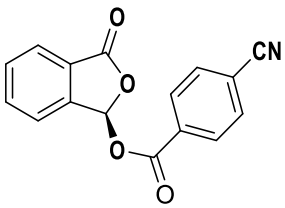

Light yellow solid, 90% yield

^{1}H NMR (400 MHz, $CDCl_3$) δ 8.19 – 8.14 (m, 2H), 7.99 (d, *J* = 7.5 Hz, 1H), 7.84 – 7.75 (m, 3H), 7.74-7.66 (m, 3H);

^{13}C NMR (100 MHz, $CDCl_3$) δ 167.49, 163.56, 143.87, 135.02, 132.38, 132.20, 131.59, 130.58, 126.47, 126.00, 123.70, 117.58, 117.46, 93.49;

IR ν_{max} (film, cm^{-1}): 2096, 1780, 1738, 1643, 1260, 976; **$[\alpha]^{21}_D$** = -41.1 (*c* = 1.9 in $CHCl_3$);

HRMS (ESI, m/z): calcd. for $[C_{16}H_{10}NO_4]^+$ 280.0610, found 280.0618;

HPLC analysis: 92:8 er, [CHIRALPAK IB column; 0.6 mL/min; solvent system: *i*-PrOH/hexane 5:95; retention times: 35.2 min (minor), 41.3 min (major)].

Compound 9:

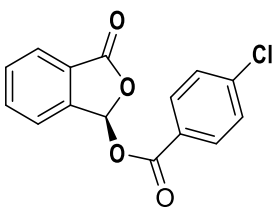

Light yellow solid, 81% yield

^{1}H NMR (400 MHz, $CDCl_3$) δ 8.01-7.97 (m, 3H), 7.78 (t, *J* = 7.5, 1H), 7.72 – 7.66 (m, 3H), 7.46 – 7.42 (m, 2H);

^{13}C NMR (100 MHz, $CDCl_3$) δ 167.73, 164.25, 144.26, 140.71, 134.90, 131.50, 131.40, 129.02, 126.85, 126.57, 125.90, 123.71, 93.32;

IR ν_{max} (film, cm^{-1}): 2091, 1786, 1635, 1260, 1092, 976; **$[\alpha]^{21}_D$** = -58.1 (*c* = 0.5 in $CHCl_3$);

HRMS (ESI, m/z): calcd. for $[C_{15}H_{10}O_4Cl]^+$ 280.0610, found 280.0618;

HPLC analysis: 93:7 er, [CHIRALPAK IB column; 0.6 mL/min; solvent system: *i*-PrOH/hexane 5:95; retention times: 17.8 min (minor), 19.6 min (major)].

Compound 10:

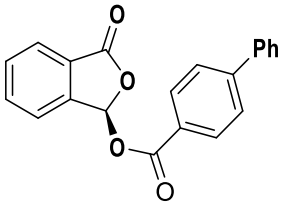

Yellow solid, 77% yield

^{1}H NMR (400 MHz, $CDCl_3$) δ 8.15 – 8.10 (m, 2H), 8.01 – 7.97 (m, 1H), 7.81 – 7.75 (m, 1H), 7.74 – 7.65 (m, 5H), 7.64 – 7.59 (m, 2H), 7.50 – 7.44 (m, 2H), 7.43 – 7.37 (m, 1H);

^{13}C NMR (100 MHz, $CDCl_3$) δ 167.89, 164.95, 146.82, 144.50, 139.61, 134.86, 131.30, 130.69, 128.96, 128.40, 127.28, 127.23, 127.02, 126.62, 125.84, 123.74, 93.29;

IR ν_{max} (film, cm^{-1}): 2092, 1782, 1634, 1258, 1088, 970; **$[\alpha]^{21}_D$** = -46.7 (*c* = 0.8 in $CHCl_3$);

HRMS (ESI, m/z): calcd. for $[C_{21}H_{15}O_4]^+$ 331.0970, found 331.0975;

HPLC analysis: 96:4 er, [CHIRALPAK IB column; 0.6 mL/min; solvent system: *i*-PrOH/hexane 5:95; retention times: 26.1 min (minor), 26.8 min (major)]

Compound 11:

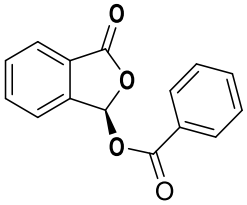

Off-white solid, 90% yield

^{1}H NMR (400 MHz, $CDCl_3$) δ 8.03 (dd, J = 8.0, 1.9 Hz, 1H), 7.97 (dd, J = 7.4, 1.6 Hz, 1H), 7.78 (t, J = 7.5 Hz, 1H), 7.73 – 7.56 (m, 4H), 7.39 – 7.29 (m, 1H), 7.20 – 7.07 (m, 1H), 2.22 (s, 3H);

^{13}C NMR (100 MHz, $CDCl_3$) δ 169.52, 167.72, 162.84, 151.19, 144.27, 135.04, 134.93, 132.18, 131.39, 126.47, 126.17, 125.85, 124.11, 123.89, 121.58, 93.18, 20.81;

IR ν_{max} (film, cm^{-1}): 2091, 1782, 1630, 1261, 970; **$[\alpha]^{21}_D$** = -45.9 (c = 0.8 in $CHCl_3$);

HRMS (ESI, m/z): calcd. for $[C_{15}H_{11}O_4]^+$ 255.0657, found 255.0658;

HPLC analysis: 95:5 er, [CHIRALPAK IB column; 0.6 mL/min; solvent system: *i*-PrOH/hexane 5:95; retention times: 16.1 min (minor), 17.1 min (major)].

Compound 12:

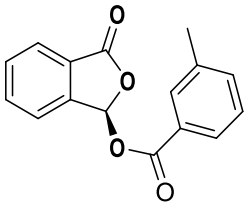

Yellow solid, 91% yield

^{1}H NMR (400 MHz, $CDCl_3$) δ 8.00 – 7.95 (m, 1H), 7.90 – 7.83 (m, 2H), 7.80-7.76 (m, 1.0 Hz, 1H), 7.72 – 7.66 (m, 3H), 7.42 (d, J = 7.5 Hz, 1H), 7.34 (t, J = 7.7 Hz, 1H), 2.39 (s, 3H);

^{13}C NMR (100 MHz, $CDCl_3$) δ 167.89, 165.21, 144.52, 138.48, 134.82, 131.26, 130.59, 128.47, 128.28, 127.31, 126.61, 125.80, 123.74, 93.26, 21.17;

IR ν_{max} (film, cm^{-1}): 2090, 1786, 1734, 1635, 1269, 972; **$[\alpha]^{21}_D$** = -45.4 (c = 1.5 in $CHCl_3$);

HRMS (ESI, m/z): calcd. for $[C_{16}H_{13}O_4]^+$ 269.0814, found 269.0816;

HPLC analysis: 89:11 er, [CHIRALPAK IB column; 0.6 mL/min; solvent system: *i*-PrOH/hexane 5:95; retention times: 13.9 min (minor), 14.4 min (major)]

Compound 13:

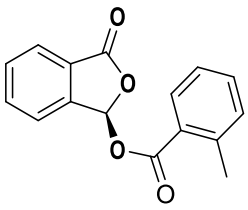

Off-white solid, 94% yield

^{1}H NMR (400 MHz, $CDCl_3$) δ 8.04 – 7.95 (m, 1H), 7.92 (dd, *J* = 7.9, 1.4 Hz, 1H), 7.81 – 7.74 (m, 1H), 7.72 – 7.63 (m, 3H), 7.45 (td, *J* = 7.5, 1.5 Hz, 1H), 7.31 – 7.19 (m, 2H), 2.65 (s, 3H);

^{13}C NMR (100 MHz, $CDCl_3$) δ 167.96, 165.43, 144.59, 141.58, 134.81, 133.17, 131.98, 131.23, 131.15, 127.31, 126.65, 125.89, 125.84, 123.63, 93.04, 21.91;

IR ν_{max} (film, cm^{-1}): 2089, 1780, 1734, 1635, 1240, 1053, 972; **$[\alpha]^{21}_{D}$** = -64.6 (*c* = 1.4 in $CHCl_3$);

HRMS (ESI, m/z): calcd. for $[C_{16}H_{13}O_4]^+$ 269.0814, found 269.0810;

HPLC analysis: 92:8 er, [CHIRALPAK IB column; 0.6 mL/min; solvent system: *i*-PrOH/hexane 5:95; retention times: 16.0 min (minor), 20.8 min (major)]

Compound 14:

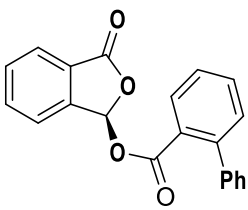

Off-white solid, 82% yield

^{1}H NMR (400 MHz, $CDCl_3$) δ 7.91 (dd, *J* = 7.8, 1.4 Hz, 1H), 7.86 – 7.83 (m, 1H), 7.64 – 7.54 (m, 3H), 7.43 (td, J = 7.6, 1.3 Hz, 1H), 7.38 – 7.31 (m, 5H), 7.30 – 7.25 (m, 2H), 7.10 – 7.07 (m, 1H);

^{13}C NMR (100 MHz, $CDCl_3$) δ 167.71, 166.93, 143.84, 143.05, 140.94, 134.45, 132.17, 131.00, 130.90, 130.37, 128.85, 128.35, 128.09, 127.33, 127.32, 126.22, 125.49, 123.49, 92.94.;

IR ν_{max} (film, cm^{-1}): 2091, 1790, 1637, 1265, 1234, 1047, 970, 744; **$[\alpha]^{21}_D$** = -17.1 (*c* = 1.1 in $CHCl_3$);

HRMS (ESI, m/z): calcd. for $[C_{21}H_{15}O_4]^+$ 331.0970, found 331.0975;

HPLC analysis: 92:8 er, [CHIRALPAK IB column; 0.6 mL/min; solvent system: *i*-PrOH/hexane 5:95; retention times: 23.1 min (minor), 34.5 min (major)]

Compound 15:

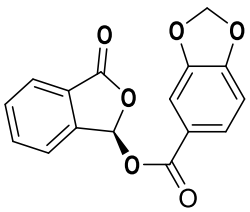

Off-white solid, 79% yield

^{1}H NMR (400 MHz, $CDCl_3$) δ 7.97 (d, *J* = 7.7 Hz, 1H), 7.83 – 7.74 (m, 1H), 7.67 (m, 4H), 7.46 (d, *J* = 1.7 Hz, 1H), 6.84 (d, *J* = 8.2 Hz, 1H), 6.05 (s, 2H);

^{13}C NMR (100 MHz, $CDCl_3$) δ 167.88, 164.32, 152.61, 147.94, 144.52, 134.81, 131.25, 126.62, 126.43, 125.80, 123.69, 122.18, 109.79, 108.17, 102.04, 93.22;

IR ν_{max} (film, cm^{-1}): 2091, 1643, 1260, 1151, 972; **$[\alpha]^{21}_D$** = -21.3 (*c* = 0.4 in $CHCl_3$);

HRMS (ESI, m/z): calcd. for $[C_{16}H_{11}O_6]^+$ 299.0556, found 299.0562;

HPLC analysis: 94:6 er, [CHIRALPAK IA column; 0.6 mL/min; solvent system: *i*-PrOH/hexane 5:95; retention times: 32.1 min (minor), 40.8 min (major)]

Compound 16:

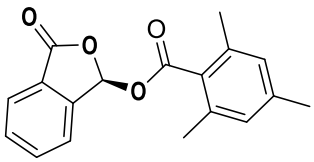

Yellow solid, 69% yield

^{1}H NMR (400 MHz, $CDCl_3$) δ 7.96 – 7.92 (m, 1H), 7.75 (t, J = 7.3, 1H), 7.69 (s, 1H), 7.65 (t, J = 7.0 Hz, 2H), 6.86 (s, 2H), 2.35 (s, 6H), 2.27 (s, 3H);

^{13}C NMR (100 MHz, $CDCl_3$) δ 168.22, 167.86, 144.27, 140.42, 135.82, 134.77, 131.24, 128.66, 128.51, 126.50, 125.81, 123.43, 92.91, 21.11, 19.98;

IR ν_{max} (film, cm^{-1}): 2085, 1789, 1732, 1638, 1163, 972; **$[\alpha]^{21}_D$** = -46.7 (c = 0.8 in $CHCl_3$);

HRMS (ESI, m/z): calcd. for $[C_{21}H_{15}O_4]^+$ 331.0970, found 331.0975;

HPLC analysis: 97:3 er, [CHIRALPAK ID column; 0.6 mL/min; solvent system: *i*-PrOH/hexane 5:95; retention times: 17.7 min (minor), 19.4 min (major)].

Compound 17:

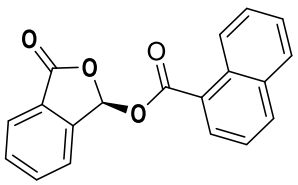

Off-white solid, 58% yield

^{1}H NMR (400 MHz, $CDCl_3$) δ 9.03 (dd, J = 8.7, 1.0 Hz, 1H), 8.23 (dd, J = 7.4, 1.3 Hz, 1H), 8.07 (dt, J = 8.2, 1.1 Hz, 1H), 7.98 (dd, J = 7.6, 1.0 Hz, 1H), 7.92 – 7.89 (m, 1H), 7.82 – 7.64 (m, 6H), 7.59 - 7.55 (m, 1H), 7.47 (dd, J = 8.2, 7.4 Hz, 1H);

^{13}C NMR (100 MHz, $CDCl_3$) δ 167.97, 165.37, 144.55, 134.86, 134.84, 133.81, 131.56, 131.46, 131.27, 128.71, 128.41, 126.64, 126.51, 125.85, 125.47, 124.48, 124.35, 123.69, 93.19;

IR ν_{max} (film, cm^{-1}): 2092, 1788, 1732, 1639, 1238, 972, 777; **$[\alpha]^{21}_D$** = -80.4 (c = 2.0 in $CHCl_3$);

HRMS (ESI, m/z): calcd. for $[C_{19}H_{13}O_4]^+$ 305.0814, found 305.0818;

HPLC analysis: 91:9 er, [CHIRALPAK IB column; 0.6 mL/min; solvent system: *i*-PrOH/hexane 5:95; retention times: 20.9 min (minor), 24.7 min (major)].

Compound 18:

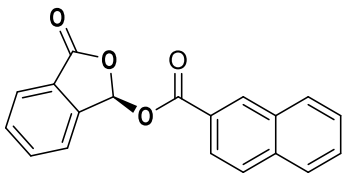

Off-white solid, 66% yield

^{1}H NMR (400 MHz, $CDCl_3$) δ 8.61 (d, J = 1.7 Hz, 1H), 8.04 (dd, J = 8.5, 1.7 Hz, 1H), 8.00 – 7.97 (m, 1H), 7.93 – 7.85 (m, 3H), 7.81 – 7.66 (m, 4H), 7.60 (ddd, J = 8.2, 6.8, 1.4 Hz, 1H), 7.53 (ddd, J = 8.1, 6.9, 1.3 Hz, 1H);

^{13}C NMR (100 MHz, $CDCl_3$) δ 167.91, 165.22, 144.51, 135.94, 134.88, 132.30, 132.11, 131.31, 129.45, 128.87, 128.46, 127.79, 126.92, 126.62, 125.83, 125.51, 125.11, 123.80, 93.38;

IR ν_{max} (film, cm^{-1}): 2093, 1784, 1732, 1636, 1276, 974, 750; **$[\alpha]^{21}_D$** = -72.9 (c = 4.4 in $CHCl_3$);

HRMS (ESI, m/z): calcd. for $[C_{19}H_{13}O_4]^+$ 305.0814, found 305.0819;

HPLC analysis: 93:7 er, [CHIRALPAK IB column; 0.6 mL/min; solvent system: *i*-PrOH/hexane 5:95; retention times: 20.9 min (minor), 24.7 min (major)].

Compound 19:

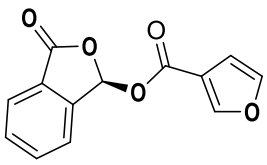

Off-white solid, 64% yield

^{1}H NMR (400 MHz, $CDCl_3$) δ 8.06 (dd, J = 1.6, 0.8 Hz, 1H), 7.97 (dt, J = 7.5, 1.0 Hz, 1H), 7.78 (td, J = 7.5, 1.1 Hz, 1H), 7.71 – 7.64 (m, 2H), 7.62 (s, 1H), 7.46 (t, J = 1.7 Hz, 1H), 6.78 (dd, J = 2.0, 0.8 Hz, 1H);

^{13}C NMR (100 MHz, $CDCl_3$) δ 167.80, 161.27, 149.06, 144.29, 144.21, 134.84, 131.30, 126.56, 125.81, 123.65, 117.80, 109.76, 92.76;

IR ν_{max} (film, cm^{-1}): 2085, 1784, 1639, 1301, 1284, 1161, 974; **$[\alpha]^{21}_D$** = -61.2 (c = 0.7 in $CHCl_3$);

HRMS (ESI, m/z): calcd. for $[C_{13}H_9O_5]^+$ 245.0450, found 245.0457;

HPLC analysis: 93:7 er, [CHIRALPAK IB column; 0.6 mL/min; solvent system: *i*-PrOH/hexane 5:95; retention times: 18.5 min (minor), 19.7 min (major)].

Compound 20:

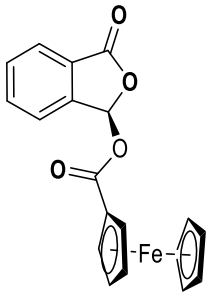

Yellow solid, 88% yield

^{1}H NMR (400 MHz, $CDCl_3$) δ 7.98 (dd, J = 7.6, 1.0 Hz, 1H), 7.78 (td, J = 7.5, 1.1 Hz, 1H), 7.71 – 7.61 (m, 3H), 4.90 (dt, J = 2.6, 1.3 Hz, 1H), 4.78 (dt, J = 2.6, 1.3 Hz, 1H), 4.50 (td, J = 2.6, 1.3 Hz, 1H), 4.46 (td, J = 2.6, 1.4 Hz, 1H), 4.24 (s, 5H);

^{13}C NMR (100 MHz, $CDCl_3$) δ 170.52, 168.06, 144.75, 134.75, 131.14, 126.77, 125.78, 123.52, 92.70, 72.37, 72.24, 70.71, 70.40, 70.20, 68.43;

IR ν_{max} (film, cm^{-1}): 2091, 1782, 1636, 1265, 1107, 966; **$[\alpha]^{21}_D$** = -157.3 (c = 0.8 in $CHCl_3$);

HRMS (ESI, m/z): calcd. for $[C_{20}H_{17}FeO_4]^+$ 377.0476, found 377.0514;

HPLC analysis: 97:3 er, [CHIRALPAK IB column; 0.6 mL/min; solvent system: *i*-PrOH/hexane 5:95; retention times: 23.2 min (minor), 24.4 min (major)].

CCDC codes: CCDC 1866428, the crystallographic data be obtained free of charge from The Cambridge Crystallographic Data Centre via www.ccdc.cam.ac.uk/data_request/cif.

Compound 21:

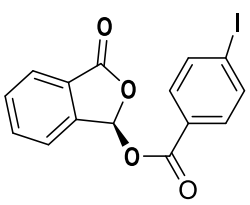

Off-white solid, 68% yield

^{1}H NMR (400 MHz, $CDCl_3$) δ 7.98 (d, J = 7.5 Hz, 1H), 7.86 – 7.64 (m, 8H);

^{13}C NMR (100 MHz, $CDCl_3$) δ 167.71, 164.67, 144.24, 138.02, 134.91, 131.41, 127.86, 126.56, 125.90, 123.71, 102.25, 93.33;

IR ν_{max} (film, cm^{-1}): 2093, 1782, 1738, 1639, 1584, 1256, 976, 748; **$[\alpha]^{21}_{D}$** = -40.8023 (c = 1.8 in $CHCl_3$);

HRMS (ESI, m/z): calcd. for $[C15H_{10}IO_4]^+$ 380.9624, found 380.9636;

HPLC analysis: 91:9 er, [CHIRALPAK IA column; 0.6 mL/min; solvent system: *i*-PrOH/hexane 5:95; retention times: 23.6 min (minor), 32.4 min (major)].

CCDC codes: CCDC 1866429, the crystallographic data be obtained free of charge from The Cambridge Crystallographic Data Centre via www.ccdc.cam.ac.uk/data_request/cif.

Compound 22:

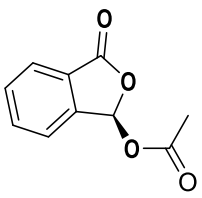

Colorless oil, 82% yield

^{1}H NMR (400 MHz, $CDCl_3$) δ 7.94 (d, J = 7.5 Hz, 2H), 7.84 – 7.72 (m, 2H), 7.64 (m, 4H), 7.43 (s, 1H), 2.20 (s, 3H);

^{13}C NMR (100 MHz, $CDCl_3$) δ 169.40, 167.78, 144.26, 134.77, 131.24, 126.49, 125.80, 123.51, 92.63, 20.81;

IR ν_{max} (film, cm^{-1}): 2091, 1628, 1570,1356, 1217; **$[\alpha]^{21}_D$** = -32.4 (c = 0.6 in $CHCl_3$);

HRMS (ESI, m/z): calcd. for $[C_{10}H_9O_4]^+$ 193.0512, found 193.0423;

HPLC analysis: 97:3 er, [CHIRALPAK IB column; 0.6 mL/min; solvent system: *i*-PrOH/hexane 5:95; retention times: 16.8 min (minor), 18.8 min (major)].

Compound 23:

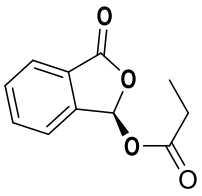

Colorless oil, 90% yield

^{1}H NMR (400 MHz, $CDCl_3$) δ 7.93 (d, J = 7.6 Hz, 1H), 7.75 (t, J = 7.5, 1H), 7.66 (t, J = 7.5, 1H), 7.59 (d, J = 7.6 Hz, 1H), 7.46 (s, 1H), 2.46 (q, J = 7.5 Hz, 2H), 1.21 (t, J = 7.5 Hz, 3H);

^{13}C NMR (100 MHz, $CDCl_3$) δ 172.91, 167.84, 144.37, 134.74, 131.18, 126.51, 125.75, 123.47, 92.60, 27.40, 8.65;

IR ν_{max} (film, cm^{-1}): 2089, 1634, 1357, 1284, 1144, 968; **$[\alpha]^{21}_D$** = -71.6 (c = 1.5 in $CHCl_3$);

HRMS (ESI, m/z): calcd. for $[C_{11}H_{11}O_4]^+$ 207.0657, found 207.0664;

HPLC analysis: 95:5 er, [CHIRALPAK IB column; 0.6 mL/min; solvent system: *i*-PrOH/hexane 5:95; retention times: 13.7 min (minor), 15.6 min (major)].

Compound 24:

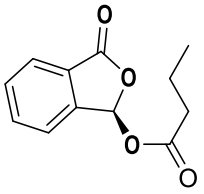

Colorless oil, 95% yield

^{1}H NMR (400 MHz, $CDCl_3$) δ 7.94 (dt, J = 7.6, 1.0 Hz, 1H), 7.75 (td, J = 7.5, 1.1 Hz, 1H), 7.66 (td, J = 7.4, 1.0 Hz, 1H), 7.59 (m, 1H), 7.46 (s, 1H), 2.42 (t, J = 7.3 Hz, 2H), 1.72 (m, 2H), 0.99 (t, J = 7.4 Hz, 3H);

^{13}C NMR (100 MHz, $CDCl_3$) δ 172.09, 167.87, 144.42, 134.75, 131.18, 126.52, 125.77, 123.45, 92.55, 35.84, 18.07, 13.50;

IR ν_{max} (film, cm^{-1}): 2965, 1638, 1568, 1261, 1099, 787; **$[\alpha]^{21}_D$** = -37.0 (c = 1.1 in $CHCl_3$);

HRMS (ESI, m/z): calcd. for $[C_{12}H_{12}O_4]^+$ 221.0814, found 221.0811;

HPLC analysis: 97:3 er, [CHIRALPAK IB column; 0.6 mL/min; solvent system: *i*-PrOH/hexane 5:95; retention times: 11.0 min (minor), 12.7 min (major)].

Compound 25:

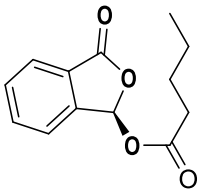

Yellow solid, 68% yield

^{1}H NMR (400 MHz, $CDCl_3$) δ 7.93 (d, J = 7.6 Hz, 1H), 7.76 (td, J = 7.5, 1.0 Hz, 1H), 7.66 (dd, J = 11.0, 4.0 Hz, 1H), 7.59 (d, J = 7.6 Hz, 1H), 7.45 (s, 1H), 2.44 (t, J = 7.5 Hz, 2H), 1.73 – 1.61 (m, 2H), 1.45 – 1.32 (m, 2H), 0.93 (t, J = 7.3 Hz, 3H);

^{13}C NMR (100 MHz, $CDCl_3$) δ 172.25, 167.86, 144.40, 134.75, 131.17, 126.49, 125.73, 123.45, 92.54, 33.70, 26.54, 22.06, 13.59;

IR ν_{max} (film, cm^{-1}): 2091, 1638, 1466, 1356, 1054, 970; **$[\alpha]^{21}_D$** = -15.6 (c = 1 in $CHCl_3$);

HRMS (ESI, m/z): calculated for $[C_{13}H_{15}O_4]^+$: 235.0965, found: 235.0970.

HPLC analysis: 98:2 er, [CHIRALPAK OD-H column; 0.7 mL/min; solvent system: *i*-PrOH/hexane 20:80; retention times: 7.8 min (minor), 8.9 min (major)].

Compound 26:

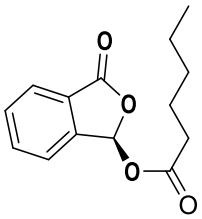

Yellow solid, 65% yield

^{1}H NMR (400 MHz, $CDCl_3$) δ 7.94 (d, J = 7.6 Hz, 1H), 7.75 (td, J = 7.5, 1.0 Hz, 1H), 7.65 (t, J = 7.3 Hz, 1H), 7.58 (d, J = 7.6 Hz, 1H), 7.45 (s, 1H), 2.43 (t, J = 7.5 Hz, 2H), 1.74 – 1.63 (m, 2H), 1.39 – 1.29 (m, 4H), 0.94 – 0.86 (m, 3H);

^{13}C NMR (100 MHz, $CDCl_3$) δ 172.28, 167.88, 144.43, 134.75, 131.18, 126.53, 125.77, 123.46, 92.57, 33.97, 31.09, 24.20, 22.20, 13.82;

IR ν_{max} (film, cm^{-1}): 2874, 2091, 1782, 1643, 1355, 1284, 1213, 972; **$[\alpha]^{21}_D$** = -13.1 (c = 1 in $CHCl_3$);

HRMS (ESI, m/z): calculated for $[C_{14}H_{17}O_4]^+$: 249.1121, found: 249.1121.

HPLC analysis: 98:2 er, [CHIRALPAK OD-H column; 0.7 mL/min; solvent system: *i*-PrOH/hexane 20:80; retention times: 7.6 min (minor), 8.7 min (major)].

Compound 27:

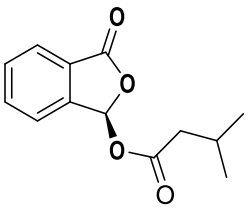

Yellow oil, 75% yield

^{1}H NMR (400 MHz, $CDCl_3$) δ 7.94 (d, J = 7.6 Hz, 1H), 7.76 (td, J = 7.5, 1.0 Hz, 1H), 7.66 (t, J = 7.5 Hz, 1H), 7.58 (d, J = 7.6 Hz, 1H), 7.45 (s, 1H), 2.73 – 2.58 (m, 1H), 1.24 (s, 3H), 1.22 (s, 3H);

^{13}C NMR (100 MHz, $CDCl_3$) δ 175.53, 167.90, 144.47, 134.77, 131.16, 126.51, 125.74, 123.40, 92.62, 33.87, 18.58, 18.56;

IR ν_{max} (film, cm^{-1}): 2964, 2935, 2874, 2081, 1782, 1643, 1470, 1360, 1284, 976; **$[\alpha]^{21}_D$** = -16.9 (c = 1 in $CHCl_3$);

HRMS (ESI, m/z): calculated for $[C_{13}H_{15}O_4]^+$: 235.0965, found: 235.0970;

HPLC analysis: 97:3 er, [CHIRALPAK OD-H column; 0.7 mL/min; solvent system: *i*-PrOH/hexane 20:80; retention times: 7.4 min (minor), 8.6 min (major)].

Compound 28:

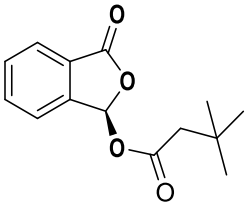

Yellow oil, 76% yield

^{1}H NMR (400 MHz, $CDCl_3$) δ 7.93 (d, J = 7.6 Hz, 1H), 7.75 (td, J = 7.5, 1.0 Hz, 1H), 7.66 (t, J = 7.5 Hz, 1H), 7.58 (d, J = 7.6 Hz, 1H), 7.46 (s, 1H), 2.32 (s, 2H), 1.07 (s, 10H);

^{13}C NMR (100 MHz, $CDCl_3$) δ 170.63, 167.89, 144.48, 134.74, 131.14, 126.51, 125.74, 123.41, 92.40, 47.44, 31.00, 29.51;

IR ν_{max} (film, cm^{-1}): 2963, 2872, 2081, 1790, 1643, 1215, 1117, 974; **$[\alpha]^{21}_D$** = -15.4 (c = 1 in $CHCl_3$);

HRMS (ESI, m/z): calculated for $[C_{14}H_{17}O_4]^+$: 249.1121, found: 249.1122;

HPLC analysis: 98:2 er, [CHIRALPAK OD-H column; 0.7 mL/min; solvent system: *i*-PrOH/hexane 20:80; retention times: 7.0 min (minor), 7.8 min (major)].

Compound 29:

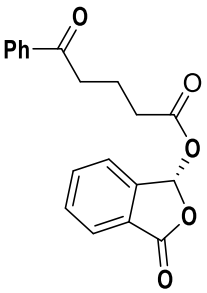

Yellow solid, 96% yield

^{1}H NMR (400 MHz, $CDCl_3$) δ 7.98 – 7.89 (m, 3H), 7.74 (td, J = 7.5, 1.0 Hz, 1H), 7.65 (t, J = 7.3 Hz, 1H), 7.63 – 7.53 (m, 2H), 7.50 – 7.42 (m, 3H), 3.19 – 3.01 (m, 2H), 2.67 – 2.48 (m, 2H), 2.14 (p, J = 7.1 Hz, 2H);

^{13}C NMR (100 MHz, $CDCl_3$) δ 199.05, 171.79, 167.78, 144.21, 136.64, 134.78, 133.16, 131.21, 128.61, 127.95, 126.43, 125.73, 123.51, 92.57, 37.00, 33.05, 18.86;

IR ν_{max} (film, cm^{-1}): 2091, 1782, 1762, 1635, 1130, 1053, 970; **$[\alpha]^{21}_D$** = 0.9 (c = 1 in $CHCl_3$);

HRMS (ESI, m/z): calculated for $[C_{19}H_{17}O_5]^+$: 325.1071, found: 325.1083;

HPLC analysis: 93:7 er, [CHIRALPAK OD-H column; 0.7 mL/min; solvent system: *i*-PrOH/hexane 20:80; retention times: 7.0 min (minor), 7.8 min (major)].

Compound 30:

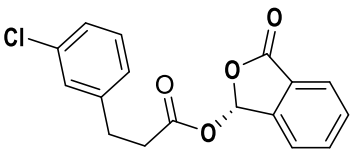

Yellow solid, 92% yield

^{1}H NMR (400 MHz, $CDCl_3$) δ 7.94 – 7.91 (m, 1H), 7.74 (t, J = 7.5, 1H), 7.65 (t, J = 7.5, 1H), 7.49 (d, J = 7.6 Hz, 1H), 7.42 (s, 1H), 7.23 – 7.18 (m, 3H), 7.09 (d=t, J = 6.9, 1H), 2.98 (t, J = 8.0 Hz, 2H), 2.78 – 2.73 (m, 2H);

^{13}C NMR (100 MHz, $CDCl_3$) δ 171.00, 167.70, 144.12, 141.68, 134.79, 134.29, 131.24, 129.85, 128.45, 126.72, 126.51, 126.38, 125.76, 123.47, 92.66, 35.22, 30.09;

IR ν_{max} (film, cm^{-1}): 2085, 1780, 1635, 1360, 1285, 1134, 974; **$[\alpha]^{21}_D$** = -31.9 (*c* = 4.3 in $CHCl_3$);

HRMS (ESI, m/z): calculated for $[C_{17}H_{14Cl}O_4]^+$: 317.0581, found: 317.0585;

HPLC analysis: 97:3 er, [CHIRALPAK IB column; 0.6 mL/min; solvent system: *i*-PrOH/hexane 5:95; retention times: 26.3 min (minor), 29.2 min (major)].

Compound 31:

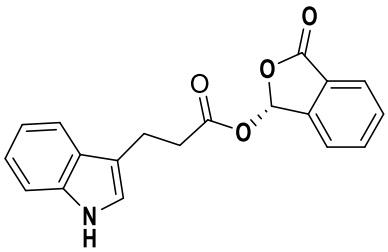

Yellow oil, 68% yield

^{1}H NMR (400 MHz, $CDCl_3$) δ 8.09 (br, 1H), 7.89 (d, *J* = 7.4 Hz, 1H), 7.70 – 7.54 (m, 3H), 7.42 – 7.32 (m, 3H), 7.19 (t, *J* = 7.5 Hz, 1H), 7.10 (t, *J* = 7.4 Hz, 1H), 7.01 (s, 1H), 3.15 (t, *J* = 7.4 Hz, 2H), 2.83 (t, *J* = 7.4 Hz, 2H);

^{13}C NMR (100 MHz, $CDCl_3$) δ 171.87, 167.95, 144.21, 136.22, 134.73, 131.12, 126.97, 126.33, 125.64, 123.46, 122.05, 121.74, 119.35, 118.49, 114.01, 111.21, 92.60, 34.79, 20.31;

IR ν_{max} (film, cm^{-1}): 2091, 1636, 1355, 1261, 1215, 962; **$[\alpha]^{21}_D$** = -58.0 (*c* = 1 in $CHCl_3$);

HRMS (ESI, m/z): calculated for $[C_{19}H_{16}NO_4]^+$: 322.1074, found: 322.1062;

HPLC analysis: 95:5 er, [CHIRALPAK OD-H column; 0.7 mL/min; solvent system: *i*-PrOH/hexane 20:80; retention times: 31.6 min (minor), 38.8 min (major)].

Compound 32:

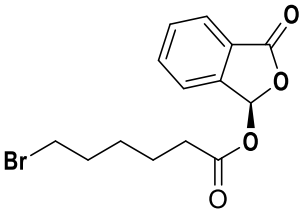

Yellow oil, 85% yield

^{1}H NMR (400 MHz, $CDCl_3$) δ 7.94 (d, J = 7.6 Hz, 1H), 7.76 (td, J = 7.5, 1.1 Hz, 1H), 7.70 – 7.63 (m, 1H), 7.60 (d, J = 7.6 Hz, 1H), 7.45 (s, 1H), 3.41 (t, J = 6.7 Hz, 2H), 2.46 (t, J = 7.4 Hz, 2H), 1.89 (m, 2H), 1.72 (m, 2H), 1.57 – 1.47 (m, 2H);

^{13}C NMR (100 MHz, $CDCl_3$) δ 171.86, 167.78, 144.25, 134.78, 131.21, 126.44, 125.75, 123.46, 92.56, 33.74, 33.32, 32.20, 27.41, 23.62;

IR ν_{max} (film, cm^{-1}): 2090, 1757, 1637, 1465, 1356, 1053, 972; **$[\alpha]^{21}_{D}$** = -36.9 (c = 0.4 in $CHCl_3$);

HRMS (ESI, m/z): calculated for $[C_{14}H_{16}BrO_4]^+$: 327.0232, found: 327.0234;

HPLC analysis: 97:3 er, [CHIRALPAK IB column; 0.6 mL/min; solvent system: *i*-PrOH/hexane 5:95; retention times: 21.8 min (minor), 29.1 min (major)].

Compound 33:

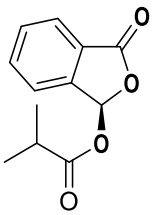

Yellow oil, 78% yield

^{1}H NMR (400 MHz, $CDCl_3$) δ 7.94 (d, J = 7.6 Hz, 1H), 7.76 (td, J = 7.5, 1.0 Hz, 1H), 7.66 (t, J = 7.5 Hz, 1H), 7.58 (d, J = 7.6 Hz, 1H), 7.45 (s, 1H), 2.73 – 2.58 (m, 1H), 1.24 (s, 3H), 1.22 (s, 3H);

^{13}C NMR (100 MHz, $CDCl_3$) δ 175.53, 167.90, 144.47, 134.77, 131.16, 126.51, 125.74, 123.40, 92.62, 33.87, 18.58, 18.56;

IR ν_{max} (film, cm^{-1}): 2093, 1784, 1643, 1360, 1285, 1053, 974; **$[\alpha]^{21}_D$** = -19.8 (*c* = 1 in $CHCl_3$);

HRMS (ESI, m/z): calculated for $[C_{12}H_{13}O_4]^+$: 221.0808, found: 221.0821;

HPLC analysis: 97:3 er, [CHIRALPAK OD-H column; 0.7 mL/min; solvent system: *i*-PrOH/hexane 20:80; retention times: 7.4 min (minor), 8.2 min (major)].

Compound 34:

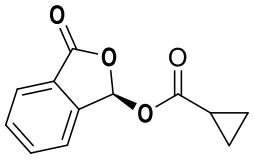

White solid, 90% yield

^{1}H NMR (400 MHz, $CDCl_3$) δ 7.94 (d, *J* = 7.5, 1H), 7.76 (td, *J* = 7.5, 1.1 Hz, 1H), 7.66 (t, *J* = 7.5, 1H), 7.61 (d, *J* = 7.6, 1H), 7.44 (s, 1H), 1.72-1.66 (m, 1H), 1.18-1.12 (m, 2H), 1.03 – 0.98 (m, 2H);

^{13}C NMR (100 MHz, $CDCl_3$) δ 173.48, 167.86, 144.40, 134.73, 131.16, 126.54, 125.73, 123.52, 92.63, 12.75, 9.64, 9.56;

IR ν_{max} (film, cm^{-1}): 2924, 2855, 1784, 1643, 1470, 1260, 750; **$[\alpha]^{21}_D$** = -62.7 (*c* = 1.6 in $CHCl_3$);

HRMS (ESI, m/z): calculated for $[C_{12}H_{11}O_4]^+$: 219.0657, found: 219.0654;

HPLC analysis: 95:6 er, [CHIRALPAK IB column; 0.6 mL/min; solvent system: *i*-PrOH/hexane 5:95; retention times: 15.0 min (minor), 16.3 min (major)].

Compound 35:

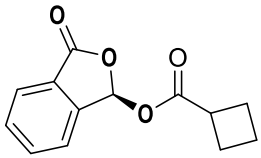

Yellow oil, 80% yield

^{1}H NMR (400 MHz, $CDCl_3$) δ 7.93 (d, J = 7.6 Hz, 1H), 7.75 (t, J = 7.5 Hz, 1H), 7.65 (t, J = 7.5 Hz, 1H), 7.58 (d, J = 7.6 Hz, 1H), 7.45 (s, 1H), 3.23 (p, J = 8.5 Hz, 1H), 2.43 – 2.30 (m, 2H), 2.30 – 2.19 (m, 2H), 2.09 – 1.88 (m, 2H);

^{13}C NMR (100 MHz, $CDCl_3$) δ 173.86, 167.91, 144.46, 134.75, 131.16, 126.52, 125.74, 123.45, 92.65, 37.67, 25.15, 24.94, 18.35;

IR ν_{max} (film, cm^{-1}): 2962, 2872, 2087, 1643, 1470, 1358, 1141, 970; **$[\alpha]^{21}_{D}$** = -10.4 (c = 1 in $CHCl_3$);

HRMS (ESI, m/z): calculated for $[C_{13}H_{13}O_4]^+$: 233.0808, found: 233.0806

HPLC analysis: 97:3 er, [CHIRALPAK OD-H column; 0.7 mL/min; solvent system: *i*-PrOH/hexane 20:80; retention times: 7.4 min (minor), 8.2 min (major)].

Compound 36:

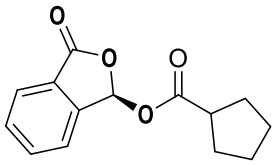

colorless oil, 91% yield

^{1}H NMR (400 MHz, $CDCl_3$) δ 7.93 (dt, J = 7.5, 1.0 Hz, 1H), 7.75 (td, J = 7.5, 1.1 Hz, 1H), 7.65 (td, J = 7.5, 1.0 Hz, 1H), 7.58 (d, J = 7.6, 1H), 7.45 (s, 1H), 2.89 – 2.78 (m, 1H), 2.00 – 1.81 (m, 4H), 1.79 – 1.68 (m, 2H), 1.66 – 1.56 (m, 2H);

^{13}C NMR (100 MHz, $CDCl_3$) δ 175.20, 167.92, 144.54, 134.73, 131.13, 126.55, 125.74, 123.40, 92.66, 43.49, 29.87, 29.79, 25.82, 25.78;

IR ν_{max} (film, cm^{-1}): 3030, 2965, 2872, 2099, 1769, 1643, 1470, 1360, 1284, 748; **$[\alpha]^{21}_D$** = -44.2 (*c* = 1.9 in $CHCl_3$);

HRMS (ESI, m/z): calculated for $[C_{14}H_{15}O_4]^+$: 247.0970, found: 247.0975

HPLC analysis: 95:5 er, [CHIRALPAK IB column; 0.6 mL/min; solvent system: *i*-PrOH/hexane 5:95; retention times: 12.1 min (minor), 13.2 min (major)].

Compound 37:

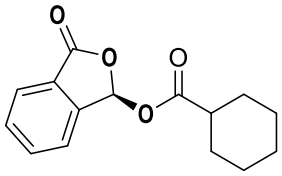

Light yellow semisolid, 90% yield

^{1}H NMR (400 MHz, $CDCl_3$) δ 7.93 (dt, *J* = 7.6, 1.0 Hz, 1H), 7.75 (td, *J* = 7.5, 1.1 Hz, 1H), 7.68 – 7.63 (m, 1H), 7.59 – 7.56 (m, 1H), 7.45 (s, 1H), 2.41 (tt, *J* = 11.2, 3.6 Hz, 1H), 1.99 – 1.91 (m, 2H), 1.82 – 1.72 (m, 2H), 1.68 – 1.62 (m, 1H), 1.57 - 1.44 (m, 2H), 1.36 – 1.20 (m, 3H);

^{13}C NMR (100 MHz, $CDCl_3$) δ 174.41, 167.90, 144.54, 134.72, 131.12, 126.53, 125.73, 123.39, 92.55, 42.86, 28.66, 28.60, 25.54, 25.18, 25.16;

IR ν_{max} (film, cm^{-1}): 3066, 3005, 2947, 2855, 2100, 1738, 1635, 1470, 1310, 894; **$[\alpha]^{21}_D$** = -42.8 (*c* = 2.3 in $CHCl_3$);

HRMS (ESI, m/z): calculated for $[C_{15}H_{17}O_4]^+$: 261.1127, found: 261.1133

HPLC analysis: 95:5 er, [CHIRALPAK IB column; 0.6 mL/min; solvent system: *i*-PrOH/hexane 5:95; retention times: 12.1 min (minor), 13.2 min (major)].

Compound 38:

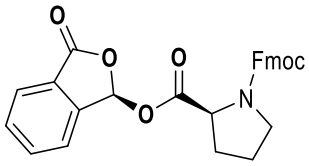

Light yellow oil, 80% yield

^{1}H NMR (400 MHz, $CDCl_3$) δ 7.95 – 7.88 (m, 1H), 7.87 – 7.70 (m, 3H), 7.69 – 7.55 (m, 4H), 7.49 (s, 1H), 7.45 – 7.22 (m, 5H), 4.55 – 4.17 (m, 4H), 3.78 – 3.61 (m, 1H), 3.59 – 3.48 (m, 1H), 2.35 – 2.18 (m, 1H), 2.17 – 1.89 (m, 3H);

^{13}C NMR (100 MHz, $CDCl_3$) δ 171.33, 171.17, 167.85, 154.94, 154.15, 144.19, 144.00, 143.97, 143.79, 143.50, 141.31, 141.28, 134.96, 134.76, 131.36, 131.29, 127.73, 127.08, 127.05, 127.00, 126.32, 125.82, 125.66, 125.17, 125.13, 125.05, 124.93, 123.87, 123.53, 119.99, 92.89, 92.81, 67.66, 58.93, 58.59, 47.28, 47.15, 47.06, 46.57, 30.85, 29.58, 24.32, 23.39;

IR ν_{max} (film, cm^{-1}): 2857, 2090, 1788, 1664, 1417, 1354, 1146, 974; **$[\alpha]^{21}_D$** = 2.1 (*c* = 1 in $CHCl_3$);

HRMS (ESI, m/z): calculated for $[C_{28}H_{24}NO_6]^+$: 470.1598, found: 470.1602;

HPLC analysis: >13:1 dr, [CHIRALPAK OD-H column; 0.7 mL/min; solvent system: *i*-PrOH/hexane 30:70; retention times: 65.6 min (major), 84.5 min (minor)].

Compound 39:

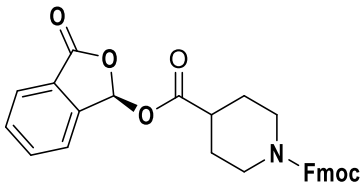

Yellow solid, 86% yield

^{1}H NMR (400 MHz, $CDCl_3$) δ 7.94 (d, *J* = 7.6 Hz, 1H), 7.79 – 7.71 (m, 3H), 7.69 – 7.62 (m, 1H), 7.60 – 7.53 (m, 3H), 7.44 (s, 1H), 7.39 (t, *J* = 7.5 Hz, 2H), 7.30 (td, *J* = 7.4, 1.0 Hz, 2H), 4.43 (br, 2H), 4.22 (t,

J = 6.6 Hz, 1H), 4.08 – 3.94 (m, 2H), 2.91 (t, *J* = 11.4 Hz, 2H), 2.58 (tt, *J* = 10.8, 3.9 Hz, 1H), 1.89 (br, 2H), 1.64 (br, 2H);

^{13}C NMR (100 MHz, $CDCl_3$) δ 172.75, 167.67, 154.96, 144.11, 143.88, 141.25, 134.81, 131.29, 127.61, 126.97, 126.36, 125.79, 124.82, 123.33, 119.90, 92.63, 67.15, 47.29, 42.92, 42.90, 40.62, 27.37;

IR ν_{max} (film, cm^{-1}): 2087, 1784, 1645, 1446, 1284, 974; **$[\alpha]^{21}_D$** = -5.7 (*c* = 2 in $CHCl_3$);

HRMS (ESI, m/z): calculated for $[C_{29}H_{26}NO_6]^+$: 484.1755, found: 484.1753;

HPLC analysis: 98:2 er, [CHIRALPAK OD-H column; 0.7 mL/min; solvent system: *i*-PrOH/hexane 30:70; retention times: 31.2 min (minor), 54.4 min (major)].

Compound 40:

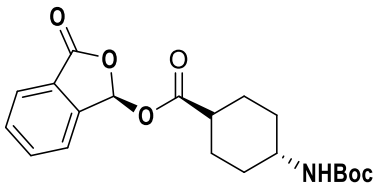

Colorless semisolid, 80% yield

^{1}H NMR (400 MHz, $CDCl_3$) δ 7.93 (d, *J* = 7.6 Hz, 1H), 7.76 (td, *J* = 7.5, 1.0 Hz, 1H), 7.67 (dt, *J* = 7.5, 3.7 Hz, 1H), 7.58 (d, *J* = 7.6 Hz, 1H), 7.43 (s, 1H), 4.49 (br, 1H), 3.42 (br, 1H), 2.33 (tt, *J* = 12.0, 3.2 Hz, 1H), 2.11 – 2.04 (m, 4H), 1.65 – 1.51 (m, 2H), 1.43 (s, 9H), 1.20 – 1.05 (m, 2H);

^{13}C NMR (100 MHz, $CDCl_3$) δ 173.74, 167.77, 155.05, 144.25, 134.78, 131.17, 126.35, 125.68, 123.35, 92.53, 42.02, 32.15, 32.11, 28.29, 27.42, 27.36;

IR ν_{max} (film, cm^{-1}): 2089, 1784, 1651, 1365, 1169, 1047, 974; **$[\alpha]^{21}_D$** = -8.5 (*c* = 2 in $CHCl_3$);

HRMS (ESI, m/z): calculated for $[C_{20}H_{26}NO_6]^+$: 376.1755, found: 376.1772;

HPLC analysis: >30:1 dr, [CHIRALPAK OD-H column; 0.7 mL/min; solvent system: *i*-PrOH/hexane 20:80; retention times: 10.9 min (minor), 13.1 min (major)].

Compound 41:

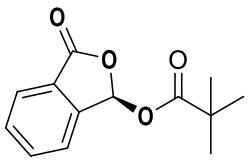

Colorless semisolid, 66% yield

^{1}H NMR (400 MHz, $CDCl_3$) δ 7.94 (dd, J = 7.6, 1.0 Hz, 1H), 7.75 (tt, J = 7.5, 1.0 Hz, 1H), 7.66 (t, J = 7.5 Hz, 1H), 7.56 (d, J = 7.6 Hz, 1H), 7.43 (s, 1H), 1.25 (s, 9H);

^{13}C NMR (100 MHz, $CDCl_3$) δ 176.99, 167.96, 144.63, 134.76, 131.13, 126.59, 125.77, 123.32, 92.82, 38.95, 26.82;

IR ν_{max} (film, cm^{-1}): 2089, 1782, 1636, 1274, 1215, 1120, 974; **$[\alpha]^{21}_{D}$** = -48.7 (c = 1.2 in $CHCl_3$);

HRMS (ESI, m/z): calculated for $[C_{13}H_{14}O_4]^+$: 235.0970, found: 235.0967;

HPLC analysis: 97:3 er, [CHIRALPAK IA column; 0.6 mL/min; solvent system: *i*-PrOH/hexane 5:95; retention times: 10.8 min (minor), 12.2 min (major)].

Compound 42:

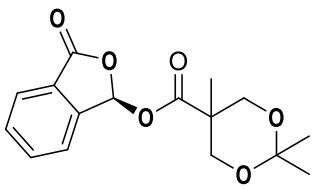

Yellow solid, 75% yield

^{1}H NMR (400 MHz, $CDCl_3$) δ 7.94 (d, J = 7.6, 1H), 7.76 (t, J = 7.5, 1H), 7.67 (t, J = 7.5, 1H), 7.61 (d, J = 7.6 Hz, 1H), 7.50 (s,

1H), 4.24 (dd, *J* = 11.7, 1.7 Hz, 1H), 4.16 (dd, *J* = 11.8, 1.8 Hz, 1H), 3.67 (dd, *J* = 11.8, 2.8 Hz, 2H), 1.43 (s, 3H), 1.39 (s, 3H), 1.20 (s, 3H);

^{13}C NMR (100 MHz, $CDCl_3$) δ 172.93, 167.76, 144.27, 134.88, 131.26, 126.39, 125.74, 123.50, 98.20, 92.93, 65.79, 65.65, 42.29, 25.60, 21.52, 18.05;

IR ν_{max} (film, cm^{-1}): 2085, 1790, 1751, 1636, 1213, 1080, 976; **$[\alpha]^{21}_D$** = -29.7 (*c* = 1 in $CHCl_3$);

HRMS (ESI, m/z): calculated for $[C_{16}H_{19}O_6]^+$: 307.1182, found: 307.1180;

HPLC analysis: 94:6 er, [CHIRALPAK IB column; 0.6 mL/min; solvent system: *i*-PrOH/hexane 5:95; retention times: 16.8 min (minor), 18.2 min (major)].

Compound 43:

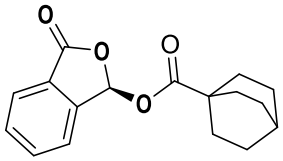

Yellow solid, 82% yield

^{1}H NMR (400 MHz, $CDCl_3$) δ 7.94 (d, *J* = 7.6 Hz, 1H), 7.75 (td, *J* = 7.5, 1.1 Hz, 1H), 7.65 (t, *J* = 7.3 Hz, 1H), 7.56 (d, *J* = 7.6 Hz, 1H), 7.44 (s, 1H), 2.02 (m, 3H), 1.93 (m, 6H), 1.78 – 1.65 (m, 6H);

^{13}C NMR (100 MHz, $CDCl_3$) δ 176.01, 167.99, 144.70, 134.73, 131.08, 126.56, 125.72, 123.36, 92.67, 40.89, 38.39, 36.26, 27.68;

IR ν_{max} (film, cm^{-1}): 2934, 2852, 2091, 1788, 1636, 1121, 970; **$[\alpha]^{21}_D$** = -46.7 (*c* = 2.8 in $CHCl_3$);

HRMS (ESI, m/z): calculated for $[C_{17}H_{19}O_4]^+$: 287.1283, found: 287.1275;

HPLC analysis: 97:3 er, [CHIRALPAK IA column; 0.6 mL/min; solvent system: *i*-PrOH/hexane 5:95; retention times: 13.1 min (minor), 14.3 min (major)].

Compound 44:

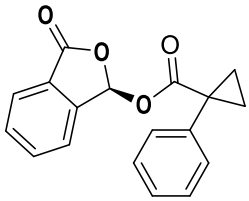

Yellow solid, 70% yield

^{1}H NMR (400 MHz, $CDCl_3$) δ 7.88 (d, J = 7.6 Hz, 1H), 7.69 (td, J = 7.5, 1.0 Hz, 1H), 7.60 (t, J = 7.5 Hz, 1H), 7.50 (d, J = 7.6 Hz, 1H), 7.39 (s, 1H), 7.37 – 7.31 (m, 2H), 7.31 – 7.19 (m, 3H), 1.77 – 1.64 (m, 2H), 1.37 – 1.26 (m, 2H);

^{13}C NMR (100 MHz, $CDCl_3$) δ 173.20, 167.82, 144.28, 138.10, 134.72, 131.09, 130.38, 128.23, 127.49, 126.44, 125.65, 123.35, 93.08, 29.00, 17.39, 17.16;

IR ν_{max} (film, cm^{-1}): 2093, 1996, 1782, 1638, 1275, 1146, 974; **$[\alpha]^{21}_{D}$** = -1.3 (c = 1 in $CHCl_3$);

HRMS (ESI, m/z): calculated for $[C_{18}H_{15}O_4]^+$: 295.0965, found: 295.0963;

HPLC analysis: 91:9 er, [CHIRALPAK OD-H column; 0.7 mL/min; solvent system: *i*-PrOH/hexane 30:70; retention times: 10.8 min (minor), 15.6 min (major)].

Compound 45:

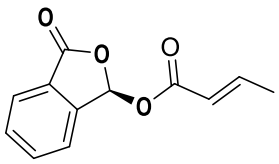

Yellow solid, 91% yield

^{1}H NMR (400 MHz, $CDCl_3$) δ 7.94 (d, J = 7.6 Hz, 1H), 7.75 (td, J = 7.5, 1.1 Hz, 1H), 7.70 – 7.56 (m, 2H), 7.51 (s, 1H), 7.14 (dq, J = 15.7, 6.9 Hz, 1H), 5.90 (dq, J = 15.7, 1.8 Hz, 1H), 1.93 (dd, J = 6.9, 1.8 Hz, 3H);

^{13}C NMR (100 MHz, $CDCl_3$) δ 167.91, 164.52, 148.38, 144.52, 134.72, 131.15, 126.55, 125.73, 123.57, 121.06, 92.71, 18.26;

IR ν_{max} (film, cm^{-1}): 2980, 2922, 1784, 1732, 1651, 1284, 972; **$[\alpha]^{21}_D$** = -64.0 (*c* = 3.0 in $CHCl_3$);

HRMS (ESI, m/z): calculated for $[C_{12}H_{11}O_4]^+$: 219.0657, found: 219.0654;

HPLC analysis: 92:8 er, [CHIRALPAK IB column; 0.6 mL/min; solvent system: *i*-PrOH/hexane 5:95; retention times: 15.4 min (minor), 16.8 min (major)].

Compound 46:

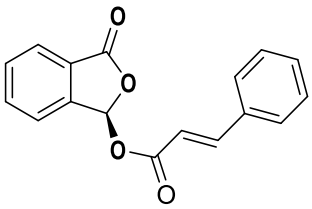

Yellow solid, 65% yield

^{1}H NMR (400 MHz, $CDCl_3$) δ 7.96 (d, *J* = 7.5 Hz, 1H), 7.85 – 7.73 (m, 2H), 7.67 (t, *J* = 7.9 Hz, 2H), 7.59 (s, 1H), 7.56 – 7.48 (m, 2H), 7.46 – 7.35 (m, 3H), 6.46 (d, *J* = 16.0 Hz, 1H);

^{13}C NMR (100 MHz, $CDCl_3$) δ 167.90, 165.16, 147.67, 144.47, 134.80, 133.76, 131.23, 131.01, 128.99, 128.36, 126.56, 125.77, 123.66, 115.99, 92.91;

IR ν_{max} (film, cm^{-1}): 2093, 1782, 1636, 1307, 1142, 1051, 968; **$[\alpha]^{21}_D$** = -27.7 (*c* = 1 in $CHCl_3$);

HRMS (ESI, m/z): calculated for $[C_{17}H_{13}O_4]^+$: 281.0808, found: 281.0812;

HPLC analysis: 97:3 er, [CHIRALPAK OD-H column; 0.7 mL/min; solvent system: *i*-PrOH/hexane 30:70; retention times: 17.1 min (major), 25.3 min (minor)].

Compound 47:

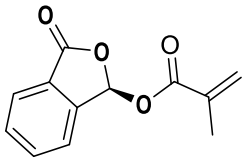

Light yellow solid, 75% yield

^{1}H NMR (400 MHz, $CDCl_3$) δ 7.95 (d, J = 7.6 Hz, 1H), 7.76 (t, J = 7.5 Hz, 1H), 7.71 – 7.60 (m, 2H), 7.50 (s, 1H), 6.19 (s, 1H), 5.72 (d, J = 1.3 Hz, 1H), 1.99 (s, 3H);

^{13}C NMR (100 MHz, $CDCl_3$) δ 167.87, 165.63, 144.42, 134.88, 134.80, 131.22, 128.24, 126.54, 125.76, 123.60, 93.08, 18.06;

IR ν_{max} (film, cm^{-1}): 2090, 1784, 1636, 1307, 1283, 1132, 974; **$[\alpha]^{21}_D$** = -38.1 (c = 1 in $CHCl_3$);

HRMS (ESI, m/z): calculated for $[C_{12}H_{11}O_4]^+$: 219.0652, found: 219.0650;

HPLC analysis: 95:5 er, [CHIRALPAK OD-H column; 0.7 mL/min; solvent system: *i*-PrOH/hexane 20:80; retention times: 7.8 min (minor), 8.5 min (major)].

Compound 48:

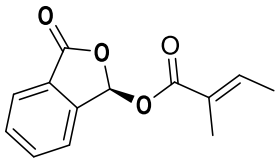

Off-white solid, 78% yield

^{1}H NMR (400 MHz, $CDCl_3$) δ 7.94 (d, J = 7.6 Hz, 1H), 7.75 (t, J = 7.5 Hz, 1H), 7.66 (t, J = 7.5 Hz, 1H), 7.61 (d, J = 7.6 Hz, 1H), 7.52 (s, 1H), 7.01 – 6.93 (m, 1H), 1.88 (s, 3H), 1.82 (d, J = 6.6 Hz, 3H);

^{13}C NMR (100 MHz, $CDCl_3$) δ 167.96, 166.13, 144.70, 140.70, 134.70, 131.09, 127.32, 126.61, 125.70, 123.59, 93.06, 14.59, 11.92;

IR ν_{max} (film, cm^{-1}): 2938, 2087, 1771, 1645, 1260, 976; **$[\alpha]^{21}_D$** = -53.8 (c = 0.6 in $CHCl_3$);

HRMS (ESI, m/z): calculated for $[C_{13}H_{13}O_4]^+$: 233.0814, found: 233.0819;

HPLC analysis: 97:3 er, [CHIRALPAK IB column; 0.6 mL/min; solvent system: *i*-PrOH/hexane 5:95; retention times: 17.1 min (minor), 18.5 min (major)].

Compound 49:

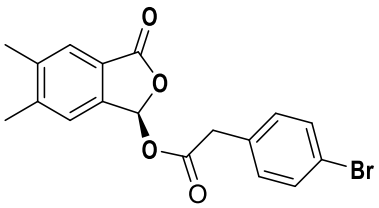

Yellow solid, 82% yield

^{1}H NMR (400 MHz, $CDCl_3$) δ 7.67 (s, 1H), 7.49 – 7.45 (m, 2H), 7.34 (s, 1H), 7.27 (s, 1H), 7.18 – 7.15 (m, 2H), 3.68 (s, 2H), 2.39 (s, 3H), 2.38 (s, 3H);

^{13}C NMR (100 MHz, $CDCl_3$) δ 169.75, 168.00, 145.22, 142.18, 140.81, 131.84, 131.58, 131.04, 126.14, 124.16, 124.10, 121.61, 92.92, 40.29, 20.77, 20.14;

IR ν_{max} (film, cm^{-1}): 2092, 1772, 1643, 1261, 1217, 968; **$[\alpha]^{21}_D$** = -12.0 (*c* = 0.8 in $CHCl_3$);

HRMS (ESI, m/z): calcd. for $[C_{18}H_{16}BrO_4]^+$ 375.0226, found 375.0221;

HPLC analysis: 97:3 er, [CHIRALPAK ADH column; 0.6 mL/min; solvent system: *i*-PrOH/hexane 15:85; retention times: 18.3 min (minor), 34.6 min (major)]

Compound 50:

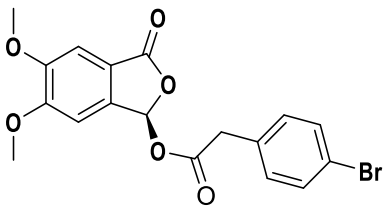

Yellow solid, 79% yield

^{1}H NMR (400 MHz, $CDCl_3$) δ 7.48 – 7.46 (m, 2H), 7.32 (s, 1H), 7.29 (s, 1H), 7.21 – 7.15 (m, 2H), 6.87 (s, 1H), 3.96 (s, 3H), 3.95 (s, 3H), 3.69 (s, 1H);

^{13}C NMR (100 MHz, $CDCl_3$) δ 169.85, 167.93, 155.27, 152.08, 138.43, 131.85, 131.60, 131.04, 121.64, 118.52, 106.16, 104.66, 92.73, 56.55, 56.43, 40.33;

IR ν_{max} (film, cm^{-1}): 1789.9, 1737.9, 1643.4, 1259.5, 1089.8, 976.0; **$[\alpha]^{21}_D$** = -6.0 (*c* = 0.7 in $CHCl_3$);

HRMS (ESI, m/z): calcd. for $[C_{18}H_{16}BrO_6]^+$ 407.0125, found 407.0127;

HPLC analysis: 96:4 er, [CHIRALPAK IB column; 0.6 mL/min; solvent system: *i*-PrOH/hexane 15:85; retention times: 31.1 min (minor), 42.3 min (major)]

Compound 51:

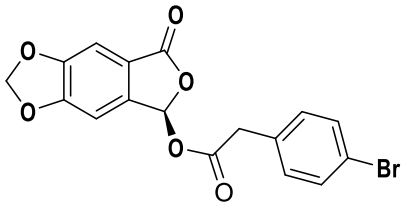

White solid, 78% yield

^{1}H NMR (400 MHz, $CDCl_3$) δ 7.49 – 7.45 (m, 2H), 7.27 (s, 1H), 7.21 (s, 1H), 7.18 – 7.15 (m, 2H), 6.86 (s, 1H), 6.16 (s, 2H), 3.68 (s, 2H);

^{13}C NMR (100 MHz, $CDCl_3$) δ 169.69, 167.10, 154.11, 150.90, 140.47, 131.88, 131.48, 131.00, 121.67, 120.49, 104.54, 103.23, 103.07, 92.44, 40.29;

IR ν_{max} (film, cm^{-1}): 2960.7, 2924.1, 1637.6, 1338.6, 1037.7, 769.6; **$[\alpha]^{21}_D$** = -21.8 (*c* = 0.7 in $CHCl_3$);

HRMS (ESI, m/z): calcd. for $[C_{17}H_{12}BrO_6]^+$ 390.9812, found 390.9815;

HPLC analysis: 98:2 er, [CHIRALPAK IB column; 0.6 mL/min; solvent system: *i*-PrOH/hexane 15:85; retention times: 31.4 min (minor), 42.4 min (major)]

Compound 52a:

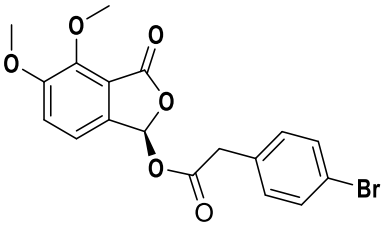

Colorless oil, 59% yield

^{1}H NMR (400 MHz, $CDCl_3$) δ 7.47 (d, J = 8.5 Hz, 2H), 7.29 (s, 1H), 7.24 – 7.10 (m, 4H), 4.13 (s, 3H), 3.93 (s, 3H), 3.67 (s, 2H).;

^{13}C NMR (100 MHz, $CDCl_3$) δ 169.75, 165.23, 154.31, 148.56, 136.39, 131.84, 131.59, 131.01, 121.61, 119.16, 118.09, 117.84, 92.13, 62.49, 56.80, 40.34;

IR ν_{max} (film, cm^{-1}): 2852.7, 2088.9, 1784.2, 1635.6, 14987, 1265, 983.7; **$[\alpha]^{21}_{D}$** = -5.0 (*c* = 1.0 in $CHCl_3$);

HRMS (ESI, m/z): calcd. for $[C_{18}H_{16}BrO_6]^+$ 407.0125, found 407.0123;

HPLC analysis: 95:5 er, [CHIRALPAK IB column; 0.6 mL/min; solvent system: *i*-PrOH/hexane 15:85; retention times: 27.9 min (minor), 38.8 min (major)]

CCDC codes: CCDC 1893685, the crystallographic data be obtained free of charge from The Cambridge Crystallographic Data Centre via www.ccdc.cam.ac.uk/data_request/cif. (Note: recrystallized in ethyl acetate / ethanol but in racemic form)

Compound 52b:

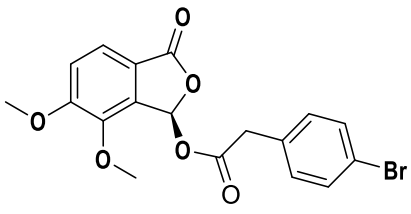

Colorless oil, 27% yield

^{1}H NMR (400 MHz, $CDCl_3$) δ 7.63 (d, J = 8.2 Hz, 1H), 7.50 – 7.44 (m, 3H), 7.16 (dd, J = 12.4, 8.1 Hz, 3H), 3.97 (s, 3H), 3.75 (s, 3H), 3.69 (s, 2H);

^{13}C NMR (100 MHz, $CDCl_3$) δ 169.18, 167.28, 157.51, 144.26, 135.44, 131.85, 131.64, 131.1, 121.95, 121.58, 119.2, 115.50, 60.67, 56.54, 40.42;

IR ν_{max} (film, cm^{-1}): 2856.6, 2088.9, 1772.6, 1645.3, 1635.6, 1278.8; **$[\alpha]^{21}_D$** = -75.6 (*c* = 0.5 in $CHCl_3$);

HRMS (ESI, m/z): calcd. for $[C_{18}H_{16}BrO_6]^+$ 407.0125, found 407.0121;

HPLC analysis: 95:5 er, [CHIRALPAK IB column; 0.6 mL/min; solvent system: *i*-PrOH/hexane 15:85; retention times: 24.9 min (minor), 25.6 min (major)]

Compound 53:

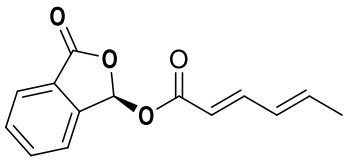

Yellow solid, 75% yield

^{1}H NMR (400 MHz, $CDCl_3$) δ 7.94 (d, *J* = 7.6 Hz, 1H), 7.75 (td, *J* = 7.5, 1.0 Hz, 1H), 7.69 – 7.59 (m, 2H), 7.52 (s, 1H), 7.42 – 7.32 (m, 1H), 6.25 – 6.19 (m, 2H), 5.80 (d, *J* = 14.9 Hz, 1H), 1.88 (d, *J* = 4.9 Hz, 3H);

^{13}C NMR (100 MHz, $CDCl_3$) δ 167.92, 165.37, 147.95, 144.57, 141.72, 134.71, 131.11, 129.54, 126.55, 125.67, 123.61, 116.69, 92.74, 18.73;

IR ν_{max} (film, cm^{-1}): 2093, 1778, 1771, 1643, 1236, 1124, 970; **$[\alpha]^{21}_D$** = - 29.0 (*c* = 1 in $CHCl_3$);

HRMS (ESI, m/z): calculated for $[C_{14}H_{13}O_4]^+$: 245.0808, found: 245.0817;

HPLC analysis: 95:5 er, [CHIRALPAK OD-H column; 0.7 mL/min; solvent system: *i*-PrOH/hexane 20:80; retention times: 11.3 min (minor), 12.9 min (major)].

Compound 54:

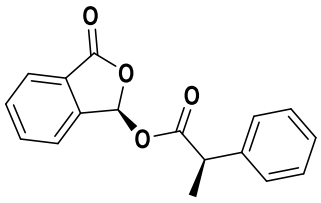

Colorless glassy solid, 76% yield

^{1}H NMR (400 MHz, $CDCl_3$) δ 7.90 (d, J = 7.2 Hz, 1H), 7.69 – 7.57 (m, 2H), 7.38 (s, 1H), 7.36 – 7.24 (m, 6H), 3.79 (q, J = 7.1 Hz, 1H), 1.57 (d, J = 7.2 Hz, 3H);

^{13}C NMR (100 MHz, $CDCl_3$) δ 173.09, 167.81, 144.20, 139.34, 134.71, 131.14, 128.75, 127.49, 127.44, 126.38, 125.67, 123.29, 92.81, 45.23, 18.12;

IR ν_{max} (film, cm^{-1}): 2093, 1788, 1759, 1643, 1358, 1284, 1140, 974; **$[\alpha]^{21}_{D}$** = - 0.22 (c = 1 in $CHCl_3$);

HRMS (ESI, m/z): calculated for $[C_{17}H_{15}O_4]^+$: 283.0965, found: 283.0964;

Compound 55:

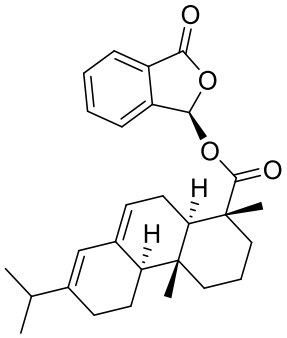

Off-white solid, 64 % yield

^{1}H NMR (400 MHz, $CDCl_3$) δ 7.93 (d, J = 7.6 Hz, 1H), 7.74 (td, J = 7.5, 1.0 Hz, 1H), 7.65 (t, J = 7.3 Hz, 1H), 7.54 (d, J = 7.6 Hz, 1H), 7.41 (s, 1H), 5.76 (s, 1H), 5.38– 5.33 (m, 1H), 2.22 (dq, J = 13.6, 6.8 Hz, 1H), 2.11 – 1.97 (m, 4H), 1.94 – 1.66 (m, 6H), 1.63 – 1.55 (m, 2H), 1.30 (s, 3H), 1.25 – 1.09 (m, 2H), 1.00 (dd, J = 6.8, 3.9 Hz, 6H), 0.82 (s, 3H);

^{13}C NMR (100 MHz, $CDCl_3$) δ 177.02, 167.93, 145.34, 144.62, 135.35, 134.73, 131.11, 126.65, 125.77, 123.35, 122.33, 120.30, 93.01, 50.68, 46.83, 44.72, 38.04, 36.82, 34.84, 34.48, 27.36, 25.49, 22.40, 21.35, 20.78, 17.93, 16.87, 14.01;

IR ν_{max} (film, cm^{-1}): 2987, 2087, 1784, 1697, 1643, 1284, 974; **$[\alpha]^{21}_D$** = -34.9 (*c* = 1 in $CHCl_3$);

HRMS (ESI, m/z): calculated for $[C_{28}H_{35}O_4]^+$: 435.2530, found: 435.2527.;

Compound 56:

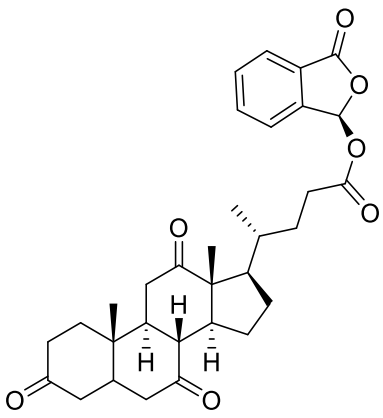

Off-white solid, 72 % yield

^{1}H NMR (400 MHz, $CDCl_3$) δ 7.93 (d, *J* = 7.6 Hz, 1H), 7.76 (td, *J* = 7.5, 0.9 Hz, 1H), 7.66 (t, *J* = 7.4 Hz, 1H), 7.60 (d, *J* = 7.6 Hz, 1H), 7.45 (s, 1H), 2.98 – 2.80 (m, 3H), 2.58 – 2.47 (m, 1H), 2.45 – 2.08 (m, 9H), 2.08 – 1.78 (m, 6H), 1.62 (td, *J* = 14.3, 4.8 Hz, 1H), 1.51 – 1.40 (m, 4H), 1.38 – 1.20 (m, 3H), 1.08 (s, 3H), 0.84 (d, *J* = 6.6 Hz, 3H);

^{13}C NMR (100 MHz, $CDCl_3$) δ 211.85, 208.98, 208.64, 172.47, 167.81, 144.28, 134.73, 131.16, 126.40, 125.69, 123.44, 92.51, 56.79, 51.70, 48.87, 46.72, 45.50, 45.46, 44.89, 42.69, 38.53, 36.38, 35.92, 35.28, 35.15, 31.14, 29.98, 27.57, 25.02, 21.81, 18.49, 11.74;

IR ν_{max} (film, cm^{-1}): 2091, 1782, 1643, 1530, 1358, 1215, 971; **$[\alpha]^{21}_D$** = 9.3 (*c* = 2 in $CHCl_3$);

HRMS (ESI, m/z): calculated for $[C_{32}H_{39}O_7]^+$: 535.2690, found: 535.2696;

Compound *R*-57

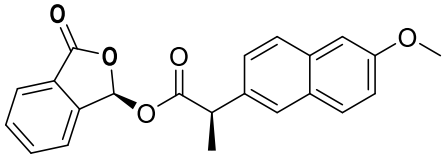

White solid, 87% yield

^{1}H NMR (400 MHz, $CDCl_3$) δ 7.92 – 7.85 (m, 1H), 7.74 – 7.65 (m, 3H), 7.62 – 7.52 (m, 2H), 7.42 – 7.36 (m, 2H), 7.28 – 7.22 (m, 1H), 7.19 – 7.10 (m, 2H), 3.92 (s, 4H), 1.64 (d, *J* = 7.1 Hz, 3H);

^{13}C NMR (100 MHz, $CDCl_3$) δ 173.25, 167.81, 157.81, 144.22, 134.69, 134.43, 133.84, 131.11, 129.25, 128.88, 127.34, 126.40, 126.13, 125.93, 125.68, 123.34, 119.16, 105.61, 92.88, 55.31, 45.18, 18.21;

IR ν_{max} (film, cm^{-1}): 2854, 2081, 1636, 1261, 1263, 972, 850; **$[\alpha]^{21}_{D}$** = -19.7 (*c* = 1.5 in $CHCl_3$);

HRMS (ESI, m/z): calculated for $[C_{22}H_{19}O_5]^+$: 363.1232, found: 363.1230;

HPLC analysis: > 40:1 dr [CHIRALPAK IB column; 0.6 mL/min; solvent system: *i*-PrOH/hexane 5:95; retention times: 26.3 min (major), 35.1 min (minor)].

Compound *S*-57

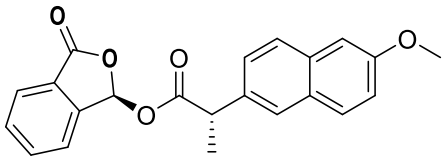

White solid, 82% yield

^{1}H NMR (400 MHz, $CDCl_3$) δ 7.89 (dt, *J* = 7.4, 1.0 Hz, 1H), 7.73 – 7.59 (m, 5H), 7.51 (dq, *J* = 7.7, 0.8 Hz, 1H), 7.42 (s, 1H), 7.37 (dd, *J* = 8.4, 1.9 Hz, 1H), 7.17 – 7.09 (m, 2H), 3.91 (s, 4H), 1.63 (d, *J* = 7.1 Hz, 3H);

^{13}C NMR (100 MHz, $CDCl_3$) δ 173.17, 167.75, 157.80, 144.29, 134.71, 134.14, 133.85, 131.18, 129.28, 128.89, 127.41, 126.55, 126.16, 125.91, 125.75, 123.45, 119.13, 105.62, 93.03, 55.32, 45.42, 18.44;

IR ν_{max} (film, cm^{-1}): 2854, 2081, 1636, 1261, 1263, 972, 850; **$[\alpha]^{21}_D$** = - 25.9 (*c* = 1.3 in $CHCl_3$);

HRMS (ESI, m/z): calculated for $[C_{22}H_{19}O_5]^+$: 363.1232, found: 363.1226;

HPLC analysis: >20:1 [CHIRALPAK IB column; 0.6 mL/min; solvent system: *i*-PrOH/hexane 5:95; retention times: 27.3 min (major), 28.9 min (minor)].

Compound 58:

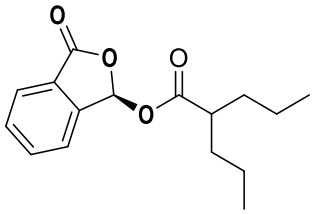

White solid, 79% yield

^{1}H NMR (400 MHz, $CDCl_3$) δ 7.94 (d, *J* = 7.6 Hz, 1H), 7.75 (td, *J* = 7.5, 1.1 Hz, 1H), 7.69 – 7.62 (m, 1H), 7.57 – 7.52 (m, 1H), 7.47 (s, 1H), 2.52 – 2.41 (m, 1H), 1.73 – 1.61 (m, 2H), 1.54 – 1.42 (m, 2H), 1.42 – 1.26 (m, 4H), 0.91 (td, *J* = 7.3, 2.5 Hz, 6H);

^{13}C NMR (100 MHz, $CDCl_3$) δ 175.00, 167.95, 144.60, 134.75, 131.15, 126.60, 125.78, 123.34, 92.54, 45.10, 34.26, 34.21, 20.53, 20.48, 13.92, 13.90;

IR ν_{max} (film, cm^{-1}): 3055, 2986, 2034, 2117, 1788, 1643, 1265, 895; **$[\alpha]^{21}_D$** = -1.9 (*c* = 1 in $CHCl_3$);

HRMS (ESI, m/z): calculated for $[C_{16}H_{21}O_4]^+$: 277.1434, found: 277.1435;

HPLC analysis: 98:2 er, [CHIRALPAK OD-H column; 0.7 mL/min; solvent system: *i*-PrOH/hexane 20:80; retention times: 9.8 min (minor), 11.9 min (major)].

Compound 59

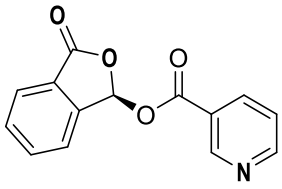

White solid, 62% yield

^{1}H NMR (400 MHz, $CDCl_3$) δ 9.23 (dd, J = 2.2, 0.9 Hz, 1H), 8.83 (dd, J = 4.9, 1.7 Hz, 1H), 8.33 (dt, J = 8.0, 2.0 Hz, 1H), 7.99 (dt, J = 7.7, 1.1 Hz, 1H), 7.80 (td, J = 7.5, 1.2 Hz, 1H), 7.75 – 7.67 (m, 3H), 7.43 (ddd, J = 8.0, 4.9, 0.9 Hz, 1H);

^{13}C NMR (100 MHz, $CDCl_3$) δ 167.59, 163.87, 154.35, 151.24, 143.96, 137.51, 134.98, 131.51, 126.47, 125.95, 124.51, 123.69, 123.45, 93.25;

IR ν_{max} (film, cm^{-1}): 2857, 2093, 1784, 1638, 1261, 1097, 974, 783; **$[\alpha]^{21}_{D}$** = - 31.5 (c = 0.7 in $CHCl_3$);

HRMS (ESI, m/z): calculated for $[C_{14}H_{10}NO_4]^+$: 256.0610, found: 256.0607;

HPLC analysis: 88:12 er, [CHIRALPAK IB column; 0.6 mL/min; solvent system: *i*-PrOH/hexane 5:95; retention times: 50.8 min (minor), 55.9 min (major)].

Compound 60

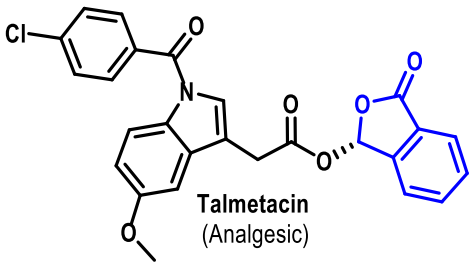

Light yellow solid, 80% yield

^{1}H NMR (400 MHz, $CDCl_3$) δ 7.94 (d, J = 7.7 Hz, 1H), 7.72 (td, J = 7.5, 1.2 Hz, 1H), 7.68 – 7.64 (m, 3H), 7.51 – 7.45 (m, 3H), 7.43 (s, 1H), 6.92 – 6.88 (m, 2H), 6.68 (dd, J = 9.0, 2.5 Hz, 1H), 3.78 (s, 2H), 3.77 (s, 3H), 2.37 (s, 3H);

^{13}C NMR (100 MHz, $CDCl_3$) δ 169.33, 168.25, 167.69, 156.07, 144.11, 139.42, 136.28, 134.82, 133.69, 131.34, 131.18, 130.77, 130.18, 129.15, 126.43, 125.84, 123.50, 115.00, 111.96, 111.18, 101.07, 93.04, 55.66, 30.17, 13.39;

IR ν_{max} (film, cm^{-1}): 2091, 1784, 1637, 1478, 1355, 1215, 974, 750; **$[\alpha]^{21}_D$** = - 29.0 (*c* = 3.2 in $CHCl_3$);

HRMS (ESI, m/z): calculated for $[C_{27}H_{21}ClNO_6]^+$: 490.1057, found: 490.1052;

HPLC analysis: 98:2 er, [CHIRALPAK IB column; 0.6 mL/min; solvent system: *i*-PrOH/hexane 5:95; retention times: 54.6 min (major), 57.3 min (minor)].

Compound 61

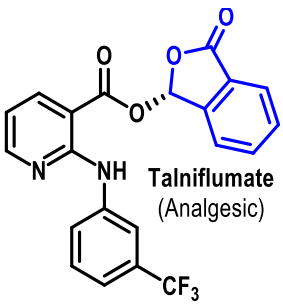

Yellow solid, 96% yield

^{1}H NMR (400 MHz, $CDCl_3$) δ 10.16 (s, 1H), 8.45 (dd, *J* = 4.6, 2.0 Hz, 1H), 8.19 (dd, *J* = 7.9,2.0 Hz, 1H), 8.11 (s, 1H), 7.99 (d, *J* = 7.5 Hz, 1H), 7.87 (d, *J* = 8.1 Hz, 1H), 7.82 (dt, *J* = 6.9, 1.0 Hz, 1H), 7.71 (t, *J* = 7.5 Hz, 2H), 7.66 (s, 1H), 7.46 (t, *J* = 8.0 Hz, 1H), 7.33 (d, *J* =7.7 Hz, 1H), 6.76 (dd, *J* = 7.9, 4.7 Hz, 1H);

^{13}C NMR (100 MHz, $CDCl_3$) δ 167.6, 116.1, 156.1, 154.4, 144.0, 140.8, 139.8, 135.0, 131.6, 129.3, 126.0, 124.0, 123.7, 119.64, 119.60, 117.62, 117.58, 114.2, 105.5, 93.2;

IR ν_{max} (film, cm^{-1}): 2093, 1786, 1630, 1446, 1328, 1126, 970; **$[\alpha]^{21}_D$** = - 44.0 (*c* = 2.2 in $CHCl_3$);

HRMS (ESI, m/z): calculated for $[C_{21}H_{13}F3NO_4]^+$: 400.0833, found: 400.0821;

HPLC analysis: 95:5 er, [CHIRALPAK IB column; 0.6 mL/min; solvent system: *i*-PrOH/hexane 5:95; retention times: 24.5 min (minor), 25.9 min (major)].

Compound 62

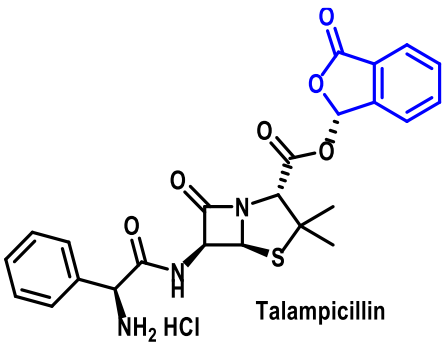

Off-white solid, 48% yield (two steps)

^{1}H NMR (400 MHz, MeOD) δ 7.95 – 7.88 (m, 3H), 7.83 (tdd, J = 7.6, 2.5, 1.3 Hz, 2H), 7.76 – 7.67 (m, 5H), 7.55 – 7.41 (m, 16H), 5.58 (ddd, J = 5.6, 4.0, 1.1 Hz, 2H), 5.46 (ddd, J = 15.9, 4.1, 1.1 Hz, 2H), 5.02 (d, J = 2.3 Hz, 2H), 4.50 (dd, J = 5.1, 1.1 Hz, 2H), 1.51 – 1.38 (m, 11H);**IR ν_{max}** (film, cm^{-1}): 2629, 2085, 1782, 1771, 1643, 1358, 1151, 980. The data was consistent with the reported literature [2-3]. **$[\alpha]^{21}_D$** = 185 (c = 0.5 in MeOH);

HRMS (ESI, m/z): calculated for $[C_{24}H_{24}N_3O_6S]^+$: 482.1386, found: 482.1386;

HPLC analysis: 6:1 dr, drHIRALPAK IB column; 0.6 mL/min; solvent system: *i*-PrOH/hexane 5:95; retention times: 26.7 min (minor), 37.8 min (major)].

Compound 63

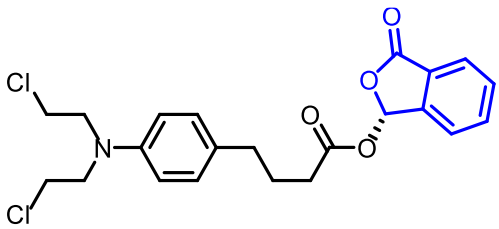

Yellow gum, 87% yield

^{1}H NMR (400 MHz, $CDCl_3$) δ 7.93 (d, J = 7.5 Hz, 1H), 7.74 (t, J = 7.5 Hz, 1H), 7.65 (t, J = 7.5 Hz, 1H), 7.57 (d, J = 7.6 Hz, 1H), 7.44 (s, 1H), 7.05 (d, J = 8.3 Hz, 2H), 6.65 – 6.60 (m, 2H), 3.78 – 3.54 (m, 8H), 2.59 (t, J = 7.5 Hz, 2H), 2.43 (t, J = 7.5 Hz, 2H), 1.96 (p, J = 7.5 Hz, 2H);

^{13}C NMR (100 MHz, $CDCl_3$) δ 172.02, 167.81, 144.42, 144.34, 134.75, 131.21, 130.06, 129.68, 126.51, 125.79, 123.45, 112.23, 92.58, 53.59, 40.48, 33.73, 33.26, 26.27;

IR ν_{max} (film, cm^{-1}): 2085, 1884, 1636, 1355, 1259, 1107, 1012; **$[\alpha]^{21}_D$** = - 16.7 (*c* = 0.6 in $CHCl_3$);

HRMS (ESI, m/z): calculated for $[C_{21}H_{22}Cl_2NO_4]^+$: 422.0926, found: 422.0921;

HPLC analysis: >99:1 er, [CHIRALPAK IB column; 0.6 mL/min; solvent system: *i*-PrOH/hexane 5:95; retention times: 59.6 min (major), 66.9 min (minor)].

2.4.7 X-ray Crystallographic Information

X-ray crystallographic data for NHC C, compound 21 and 22 are available free of charge from the Cambridge Crystallographic Data Centre under CCDC 1866589, 1866428 and 1866429, respectively.

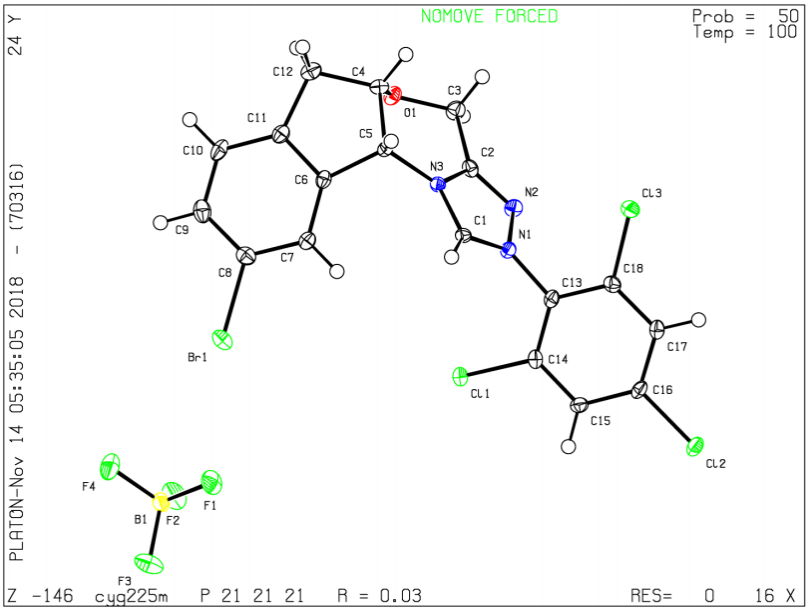

Figure 2.3 X-ray crystallographic structure for NHC **C**

A colorless block-like specimen of $C_{18}H_{12}BBrCl_3F_4N_3O$, approximate dimensions 0.240 mm x 0.300 mm x 0.380 mm, was used for the X-ray crystallographic analysis. The X-ray intensity data were measured. The total exposure time was 0.07 hours. The frames were

integrated with the Bruker SAINT software package using a narrow-frame algorithm. The integration of the data using an orthorhombic unit cell yielded a total of 20753 reflections to a maximum θ angle of 31.02° (0.69 Å resolution), of which 6466 were independent (average redundancy 3.210, completeness = 99.5%, R_{int} = 4.64%, R_{sig} = 5.44%) and = 5577 (86.25%) were greater than $2\sigma(F^2)$. The final cell constants of a = 9.4659(2) Å, b = 12.1057(2) Å, c = 17.7599(5) Å, volume = 2035.13(8) $Å^3$, are based upon the refinement of the XYZ-centroids of 8378 reflections above 20 σ(I) with 5.463° < 2θ < 61.76°. Data were corrected for absorption effects using the Multi-Scan method (SADABS). The ratio of minimum to maximum apparent transmission was 0.793. The calculated minimum and maximum transmission coefficients (based on crystal size) are 0.4540 and 0.5890. The structure was solved and refined using the Bruker SHELXTL Software Package, using the space group P 21 21 21, with Z = 4 for the formula unit, $C_{18}H_{12}BBrCl_3F_4N_3O$. The final anisotropic full-matrix least-squares refinement on F^2 with 280 variables converged at R1 = 3.19%, for the observed data and wR2 = 6.56% for all data. The goodness-of-fit was 1.036. The largest peak in the final difference electron density synthesis was 0.438 $e^-/Å^3$ and the largest hole was -0.391 $e^-/Å^3$ with an RMS deviation of 0.090 $e^-/Å^3$. On the basis of the final model, the calculated density was 1.826 g/cm^3 and F(000), 1104e^-.

Table 2.5 Data collection and structure refinement for NHC **C**

Theta range for data collection	2.29 to 31.02°
Index ranges	-12<=h<=13, -12<=k<=17, -22<=l<=25
Reflections collected	20753
Independent reflections	6466 [R(int) = 0.0464]
Coverage of independent reflections	99.5%

Absorption correction	Multi-Scan
Max. and min. transmission	0.5890 and 0.4540
Structure solution technique	direct methods
Structure solution program	XS, VERSION 2013/1
Refinement method	Full-matrix least-squares on F^2
Refinement program	SHELXL-2016/6 (Sheldrick, 2016)
Function minimized	$\Sigma\ w(F_o^2 - F_c^2)^2$
Data / restraints / parameters	6466 / 0 / 280
Goodness-of-fit on F^2	1.036
Δ/σ_{max}	0.001
Final R indices	5577 data; I>2σ(I) R1 = 0.0319, wR2 = 0.0618
	all data R1 = 0.0434, wR2 = 0.0656
Weighting scheme	$w=1/[\sigma^2(F_o^2)+(0.0264P)^2+0.0178P]$ where $P=(F_o^2+2F_c^2)/3$
Absolute structure parameter	-0.005(4)
Largest diff. peak and hole	0.438 and -0.391 eÅ^{-3}
R.M.S. deviation from mean	0.090 eÅ^{-3}

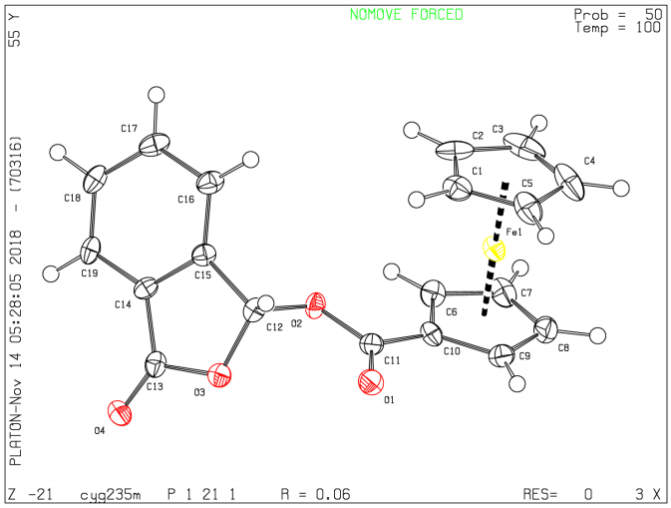

Figure 2.4 X-ray crystallographic structure for Compound **21**

An orange needle-like specimen of $C_{19}H_{14}FeO_4$, approximate dimensions 0.040 mm x 0.100 mm x 0.220 mm, was used for the X-ray crystallographic analysis. The X-ray

intensity data were measured. The total exposure time was 0.17 hours. The frames were integrated with the Bruker SAINT software package using a narrow-frame algorithm. The integration of the data using a monoclinic unit cell yielded a total of 19246 reflections to a maximum θ angle of 30.57° (0.70 Å resolution), of which 4727 were independent (average redundancy 4.072, completeness = 99.8%, R_{int} = 9.70%, R_{sig} = 10.14%) and 3310 (70.02%) were greater than $2\sigma(F^2)$. The final cell constants of a = 9.7860(9) Å, b = 7.6741(6) Å, c = 11.0882(10) Å, β = 111.807(3)°, volume = 773.12(12) $Å^3$, are based upon the refinement of the XYZ-centroids of 3520 reflections above 20 σ(I) with 6.622° < 2θ < 51.00°. Data were corrected for absorption effects using the Multi-Scan method (SADABS). The ratio of minimum to maximum apparent transmission was 0.723. The calculated minimum and maximum transmission coefficients (based on crystal size) are 0.8110 and 0.9610. The structure was solved and refined using the Bruker SHELXTL Software Package, using the space group P 1 21 1, with Z = 2 for the formula unit, $C_{19}H_{14}FeO_4$. The final anisotropic full-matrix least-squares refinement on F^2 with 217 variables converged at R1 = 6.05%, for the observed data and wR2 = 13.37% for all data. The goodness-of-fit was 1.032. The largest peak in the final difference electron density synthesis was 0.955 $e^-/Å^3$ and the largest hole was -0.683 $e^-/Å^3$ with an RMS deviation of 0.107 $e^-/Å^3$. On the basis of the final model, the calculated density was 1.556 g/cm^3 and F(000), 372 e^-.

Table 2.6 Data collection and structure refinement for Compound **21**

Theta range for data collection	2.24 to 30.57°
Index ranges	-14<=h<=13, -10<=k<=10, -15<=l<=15
Reflections collected	19246
Independent reflections	4727 [R(int) = 0.0970]
Coverage of independent reflections	99.8%
Absorption correction	Multi-Scan
Max. and min. transmission	0.9610 and 0.8110

Structure solution technique	direct methods
Structure solution program	XT, VERSION 2014/5
Refinement method	Full-matrix least-squares on F^2
Refinement program	SHELXL-2016/6 (Sheldrick, 2016)
Function minimized	$\Sigma\ w(F_o^2 - F_c^2)^2$
Data / restraints / parameters	4727 / 1 / 217
Goodness-of-fit on F^2	1.032
Final R indices	3310 data; I>2σ(I) R1 = 0.0605, wR2 = 0.1145
	all data R1 = 0.1015, wR2 = 0.1337
Weighting scheme	$w=1/[\sigma^2(F_o^2)+(0.0461P)^2+0.7294P]$ where $P=(F_o^2+2F_c^2)/3$
Absolute structure parameter	0.020(15)
Largest diff. peak and hole	0.955 and -0.683 eÅ^{-3}
R.M.S. deviation from mean	0.107 eÅ^{-3}

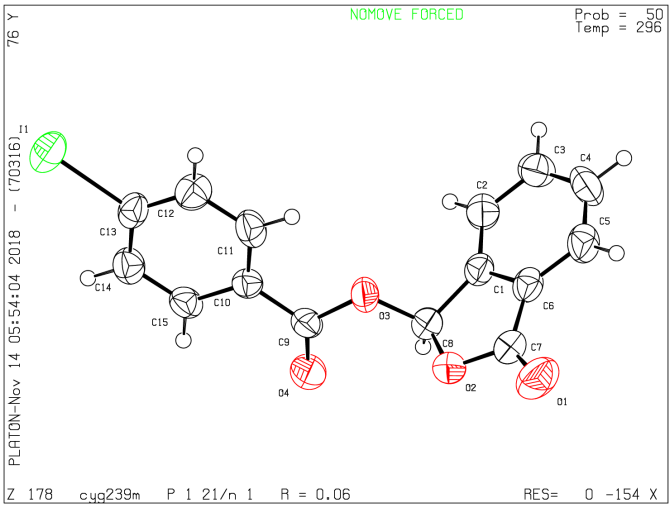

Figure 2.5 X-ray crystallographic structure for Compound **22**

A colorless needle-like specimen of $C_{15}H_9IO_4$, approximate dimensions 0.020 mm x 0.030 mm x 0.240 mm, was used for the X-ray crystallographic analysis. The X-ray intensity data were measured.The total exposure time was 0.27 hours. The frames were integrated with the Bruker SAINT software package using a narrow-frame algorithm. The integration of the data using a monoclinic unit cell yielded a total of 14436 reflections to a maximum θ

angle of 28.69° (0.74 Å resolution), of which 3458 were independent (average redundancy 4.175, completeness = 99.5%, R_{int} = 7.48%, R_{sig} = 6.96%) and 1872 (54.14%) were greater than $2\sigma(F^2)$. The final cell constants of a = 4.2761(3) Å, b = 17.1430(14) Å, c = 18.3924(13) Å, β = 90.734(3)°, volume = 1348.15(17) $Å^3$, are based upon the refinement of the XYZ-centroids of 2091 reflections above 20 σ(I) with 4.752° < 2θ < 48.04°. Data were corrected for absorption effects using the Multi-Scan method (SADABS). The ratio of minimum to maximum apparent transmission was 0.866. The calculated minimum and maximum transmission coefficients (based on crystal size) are 0.5980 and 0.9540. The structure was solved and refined using the Bruker SHELXTL Software Package, using the space group P 1 21/n 1, with Z = 4 for the formula unit, $C_{15}H_9IO_4$. The final anisotropic full-matrix least-squares refinement on F^2 with 181 variables converged at R1 = 5.57%, for the observed data and wR2 = 15.02% for all data. The goodness-of-fit was 1.044. The largest peak in the final difference electron density synthesis was 1.170 $e^-/Å^3$ and the largest hole was -0.857 $e^-/Å^3$ with an RMS deviation of 0.112 $e^-/Å^3$. On the basis of the final model, the calculated density was 1.873 g/cm^3 and F(000), 736 e^-.

Table 2.7 Data collection and structure refinement for Compound **22**

Theta range for data collection	2.62 to 28.69°
Index ranges	-4<=h<=5, -22<=k<=23, -24<=l<=24
Reflections collected	14436
Independent reflections	3458 [R(int) = 0.0748]
Coverage of independent reflections	99.5%
Absorption correction	Multi-Scan
Max. and min. transmission	0.9540 and 0.5980
Structure solution technique	direct methods
Structure solution program	XT, VERSION 2014/5
Refinement method	Full-matrix least-squares on F^2

Refinement program	SHELXL-2016/6 (Sheldrick, 2016)
Function minimized	$\Sigma\ w(F_o^2 - F_c^2)^2$
Data / restraints / parameters	3458 / 0 / 181
Goodness-of-fit on F^2	1.044
Final R indices	1872 data; $I>2\sigma(I)$ R1 = 0.0557, wR2 = 0.1207
	all data R1 = 0.1233, wR2 = 0.1502
Weighting scheme	$w=1/[\sigma^2(F_o^2)+(0.0548P)^2+1.8341P]$ where $P=(F_o^2+2F_c^2)/3$
Largest diff. peak and hole	1.170 and -0.857 eÅ^{-3}
R.M.S. deviation from mean	0.112 eÅ^{-3}

2.5 References

(1). Fiori, K. W.; Puchlopek, A. L. A.; Miller, S. J. *Nat. Chem.* **2009,** *1*, 630.

(2). Wadzinski, T. J.; Steinauer, A.; Hie, L. N.; Pelletier, G.; Schepartz, A.; Miller, S. J. *Nat. Chem.* **2018,** *10*, 644.

(3). Monaco, M. R.; Poladura, B.; de Los Bernardos, M. D.; Leutzsch, M.; Goddard, R.; List, B. *Angew. Chem. Int. Ed.* **2014,** *53*, 7063.

(4). Galvez, A. O.; Schaack, C. P.; Noda, H.; Bode, J. W. *J. Am. Chem. Soc.* **2017,** *139*, 1826.

(5). Cheng, G. L.; Li, T. J.; Yu, J. Q. *J. Am. Chem. Soc.* **2015,** *137*, 10950.

(6). Rautio, J.; Kumpulainen, H.; Heimbach, T.; Oliyai, R.; Oh, D.; Jarvinen, T.; Savolainen, J. *Nat. Rev. Drug Discov.* **2008,** *7*, 255.

(7). Yoganathan, S.; Miller, S. J. *J. Med. Chem.* **2015,** *58*, 2367.

(8). Lewis, C. A.; Miller, S. J. *Angew. Chem. Int. Ed.* **2006,** *45*, 5616.

(9). Rautio, J.; Meanwell, N. A.; Di, L.; Hageman, M. J. *Nat. Rev. Drug Discov.* **2018,** *17*, 559.

(10). Ettmayer, P.; Amidon, G. L.; Clement, B.; Testa, B. *J. Med. Chem.* **2004,** *47*, 2393.

(11). Huttunen, K. M.; Raunio, H.; Rautio, J. *Pharmacol. Rev.* **2011,** *63*, 750.

(12). Stella, V. J.; Charman, W. N. A.; Naringrekar, V. H. *Drugs* **1985,** *29*, 455.

(13). Clayton, J. P.; Cole, M.; Elson, S. W.; Ferres, H.; Hanson, J. C.; Mizen, L. W.; Sutherland, R. *J. Med. Chem.* **1976,** *19*, 1385.

(14). Castaer, J.; Prous, J. *Drugs Fut.* **1986,** *11*, 394.

(15). Kim, H. J.; Han, Y. H.; Chung, S. J.; Lee, M. H.; Shim, C. K. *Arch. Pharm. Res.* **1996,** *19*, 297.

(16). Nandakumar, M.; Sankar, E.; Mohanakrishnan, A. K. *Synlett* **2014,** *25*, 509.

(17). Coric, I.; Vellalath, S.; List, B. *J. Am. Chem. Soc.* **2010,** *132*, 8536.

(18). Coric, I.; List, B. *Nature* **2012,** *483*, 315.

(19). Kim, J. H.; Coric, I.; Vellalath, S.; List, B. *Angew. Chem. Int. Ed.* **2013,** *52*, 4474.

(20). Niedek, D.; Schuler, S. M. M.; Eschmann, C.; Wende, R. C.; Seitz, A.; Keul, F.; Schreiner, P. R. *Synthesis-Stuttgart* **2017,** *49*, 371.

(21). Knight, D. *Curr. Opin. Investig. Drugs* **2004,** *5*, 557.

(22). Walker, N. M.; Simpson, J. E.; Levitt, R. C.; Boyle, K. T.; Clarke, L. L. *J. Pharmacol. Exp. Ther.* **2006,** *317*, 275.

(23). Rao, C. V.; Janakiram, N. B.; Madka, V.; Kumar, G.; Scott, E. J.; Pathuri, G.; Bryant, T.; Kutche, H.; Zhang, Y. T.; Biddick, L.; Gali, H.; Zhao, Y. D.; Lightfoot, S.; Mohammed, A. *Cancer Res.* **2016,** *76*, 1965.

(24). Rao, C. V.; Janakiram, N. B.; Mohammed, A. *Clinical Cancer Research* **2017,** *23*, 1373.

(25). FDA *Chirality* **1992,** *4*, 338.

(26). Daniels, J. M.; Nestmann, E. R.; Kerr, A. *Drug. Inf. J.* **1997,** *31*, 639.

(27). Cimino, G.; Crispino, A.; Gavagnin, M.; Sodano, G. *J. Nat. Prod.* **1990,** *53*, 102.

(28). De Sarkar, S.; Grimme, S.; Studer, A. *J. Am. Chem. Soc.* **2010,** *132*, 1190.

(29). He, M.; Struble, J. R.; Bode, J. W. *J. Am. Chem. Soc.* **2006,** *128*, 8418.

(30). de Alaniz, J. R.; Kerr, M. S.; Moore, J. L.; Rovis, T. *J. Org. Chem.* **2008,** *73*, 2033.

(31). Kuwano, S.; Harada, S.; Kang, B.; Oriez, R.; Yamaoka, Y.; Takasu, K.; Yamada, K. *J. Am. Chem. Soc.* **2013,** *135*, 11485.

(32). Raup, D. E. A.; Cardinal-David, B.; Holte, D.; Scheidt, K. A. *Nat. Chem.* **2010,** *2*, 766.

(33). Dugal-Tessier, J.; O'Bryan, E. A.; Schroeder, T. B. H.; Cohen, D. T.; Scheidt, K. A. *Angew. Chem. Int. Ed.* **2012,** *51*, 4963.

(34). Mo, J. M.; Shen, L.; Chi, Y. R. *Angew. Chem. Int. Ed.* **2013,** *52*, 8588.

(35). Bera, S.; Samanta, R. C.; Daniliuc, C. G.; Studer, A. *Angew. Chem. Int. Ed.* **2014,** *53*, 9622.

(36). Proschak, E.; Heitel, P.; Kalinowsky, L.; Merk, D. *J. Med. Chem.* **2017,** *60*, 5235.

(37). Brooks, W. H.; Guida, W. C.; Daniel, K. G. *Curr. Top. Med. Chem.* **2011,** *11*, 760.

(38). Ezdinli, E. Z.; Stutzman, L. *J. Am. Med. Assoc.* **1965,** *191*, 444.

(39). Burger, J. A.; O'Brien, S. *Nat. Rev. Clin. Oncol.* **2018,** *15*, 510.

(40). I. Isaka, K. N., T. Kashiwagi, A. Koda, H. Horiguchi, H. Matsui, K. Takahashi & M. Murakami. *Chem. Pharm. Bull.* **1976,** *24*, 102.

Chapter 3

Carbene Catalyzed Enantioselective Synthesis of 3- （*N*-substitued）*AminoPhthalides*

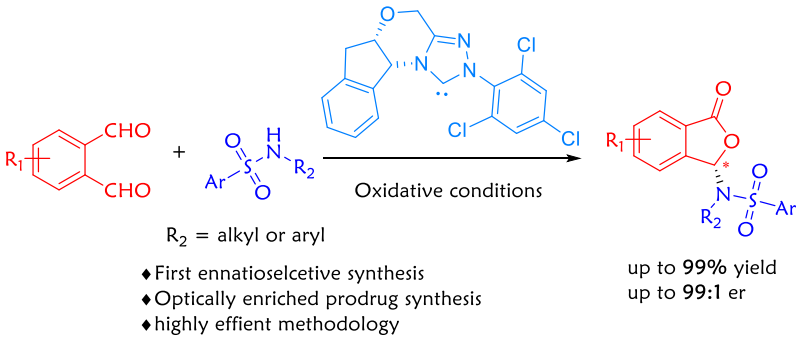

R_2 = alkyl or aryl

- First ennatioselcetive synthesis
- Optically enriched prodrug synthesis
- highly effient methodology

up to **99%** yield
up to **99:1** er

3.1 Introduction

The natural products, especially small molecules, have been the mainstay of the drug discovery. More than 60% of the medicines on market origin from the natural product.[1-2] In particular, phthalides have played a vital role in the discovery of new drug molecule. Phthalides are commonly found in naturally occurring substances and exhibit a diverse range of biological activities, which have proven to be useful for circulatory and heart diseases.[3] A broad spectrum of phthalides have been found from natural substances. 3-(*O*-Substituted) phthalides derivatives, such as phthalidyl esters, are well established marketed drugs, and we have demonstrated the chiral synthesis of phthalidyl esters in the **Chapter 2**.[4-5]

Apart from these, as we demonstrated in the introduction, nitrogen is extremely prevalent in nature products[6-7], and 3-(*N*-substituted) aminophthalides have also been used to develop new drugs. 5-Fluoro uracil modified by phthalidyl group was used to test antitumor activity.[8] Histamine was also developed as diphthalidyl prodrugs for histamine H3 receptor agonist [9] (**Scheme 3.1**).

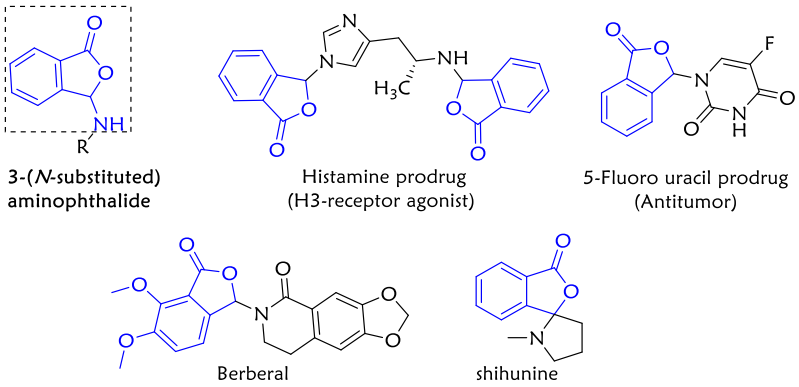

Scheme 3.1 3-(*N*-substituted) aminophthalide and phthalidyl prodrugs

The aminophthalides also exist as natural products. Berberal is an alkaloid isolated from *berberis heterobotrys*, which is used for the treatment of skin diseases, rheumatism, infertility, and so on. The leaves and fruit of them also act as an antiscorbutic in traditional

medicine.[10] Another one with the aminophthalide moiety is *shihunine*, which was tested against Gaucher disease and Parkinson disease.[11-12]

Reported synthetic procedures for the synthesis of 3-(*N*-substituted) aminophthalides are established in racemic form from 2-formylbenzoic acid or 3-bromophthalides using amine as nucleophile (**Scheme 3.2**).[13-14]

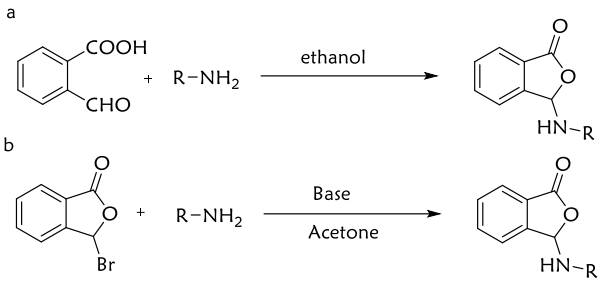

Scheme 3.2 Reported synthesis of the 3-(*N*-substituted) aminophthalides.

However, there is no report of the enantioselective synthesis of 3-(*N*-substituted) aminophthalide derivatives up to date. Recently, our group has developed acetalization of acids to access chiral phthalidyl ester prodrugs using *N*-heterocyclic carbene as a catalyst (also see **Chapter 2** for details). Inspired by this work, here we disclose chiral *N*-heterocyclic carbene catalyzed synthesis of 3-sulfonamide substituted optically enriched aminophthalide derivatives from phthalaldehydes. Our reaction offers 3-sulfonamide or cyclic sulfonamide substituted optically enriched phthalide derivatives with excellent yield (up to 99%) and excellent enantiomeric ratio (up to 99:1). One antibacterial drug, sulfamethoxazole, was modified by the present method and tested against the growth of *E. Coli.*

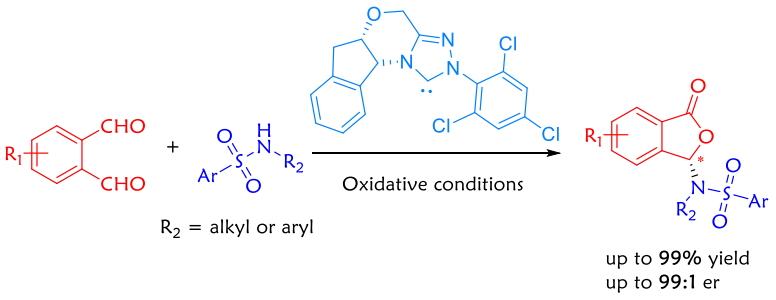

Scheme 3.3 Our approaches to aminophthalides

3.2 Results and Discussion

3.2.1 Condition optimization

Our initial studies used phthalaldehyde **1a** and *N*-phenylbenzenesulfonamide **2a** as model substrates. The key results from detail optimization were depicted in **Table 3.1**. The initial reaction was performed in the presence of dichloromethane and 10 mol% morpholine based N-heterocyclic carbene precatalyst **A,** 100 mol% DBU as a base and 100 mol% 3,3',5,5'-tetra-tert-butyldiphenoquinone(DQ) as oxidant, which afforded product **3aa** with the moderate yield and the moderate enantiomeric ratio (entry 1). By replacing the precatalyst with **B,** *N*-substituted phenyl ring at the trizolium ring was found to offer good yield albeit with diminised enantioselectivity (entry 2). Use of precatalyst **C** bearing 4-metheoxy phenyl group at trizolium ring resulted in improvement of enantiomeric ratio (e.r 60:40) and yield of the reaction. Replacing Precatalyst **C** with precatalyst **D** containing electron withdrawing pentafluorophenyl ring offered further improvement of enantiomeric ratio with lower yield (entry 4). Furthermore, the use of *N*-mesityl substituted precatalyst **E** enhanced the er value while the yield remained moderate (entry 5). Finally, precatalyst **F** bearing *N*-(2,4,6-trichlorophenyl) group offered better yield and better er value. Further screening of bases such as inorganic bases provided better enantiomeric ratio (entry 6) over organic bases, Cs_2CO_3 offering excellent enantiomeric ratio and good yield (entry 7). A moderately weak inorganic base such as $LiOH{\cdot}H_2O$, offered excellent yield and excellent enantiomeric ratio (entry 8). Screening of different solvents other than using dicholoromethane resulted in lowering the er value (entry 9 and 10).

Table 3.1 Condition optimization

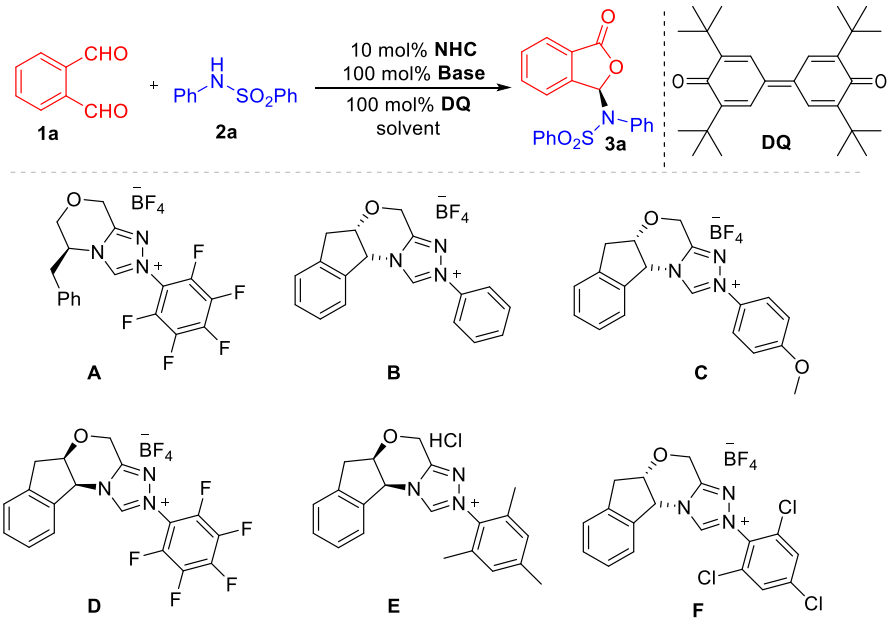

Entry	NHCs	Bases	Solvents	Yields(%)	e.r.
1	**A**	DBU	CH_2Cl_2	68	10:90
2	**B**	DBU	CH_2Cl_2	84	53:47
3	**C**	DBU	CH_2Cl_2	88	60:40
4	**D**	DBU	CH_2Cl_2	66	16:84
5	**E**	DBU	CH_2Cl_2	68	10:90
6	**F**	DBU	CH_2Cl_2	80	93:7
7	**F**	Cs_2CO_3	CH_2Cl_2	79	96:4
8	**F**	$LiOH.H_2O$	CH_2Cl_2	92	99:1
9	**F**	$LiOH.H_2O$	$PhCF_3$	80	97:3
10	**F**	$LiOH.H_2O$	THF	74	92:8

Reaction condition: **1** (1 equiv.), **2** (1.5 equiv.), NHC (0.1 equiv.), Base (1.0 equiv.), DQ (1 equiv.) (3,3',5,5'-tetra-tert-butyldiphenoquinone), solvent (2 mL). DBU = 1,8-Diazabicyclo [5.4.0] undec-7-ene. The yield determined by isolation. e.r. determined by HPLC.

3.2.2 Substrate Scope

With the best conditions in hand, Substrate scope of our reaction with respect to different aromatic sulfonamide was explored. Sulfonamide containing different functional groups in phenyl ring such as, halogen, cyano, nitro, alkoxy, alkyl, alkenyl and, alkynyl groups have worked well in the reaction to furnish 3-(*N*-substituted) aminophthalide derivatives with excellent enantiomeric ratio and high yield (product **3aa** to **3ai**). The product **3ah** was obtained with low yield, presumably due to the presence of bulky -SMe group at the *ortho* postion of the phenyl ring. It is noted that there is no significant effect of the substituents at different positions of the phenyl group on the er value. Substituted pyridines containing sulfonamide also worked in the reaction to afford 3-substituted aminophthalide in good yield and excellent e.r. value. (product **3aj**).

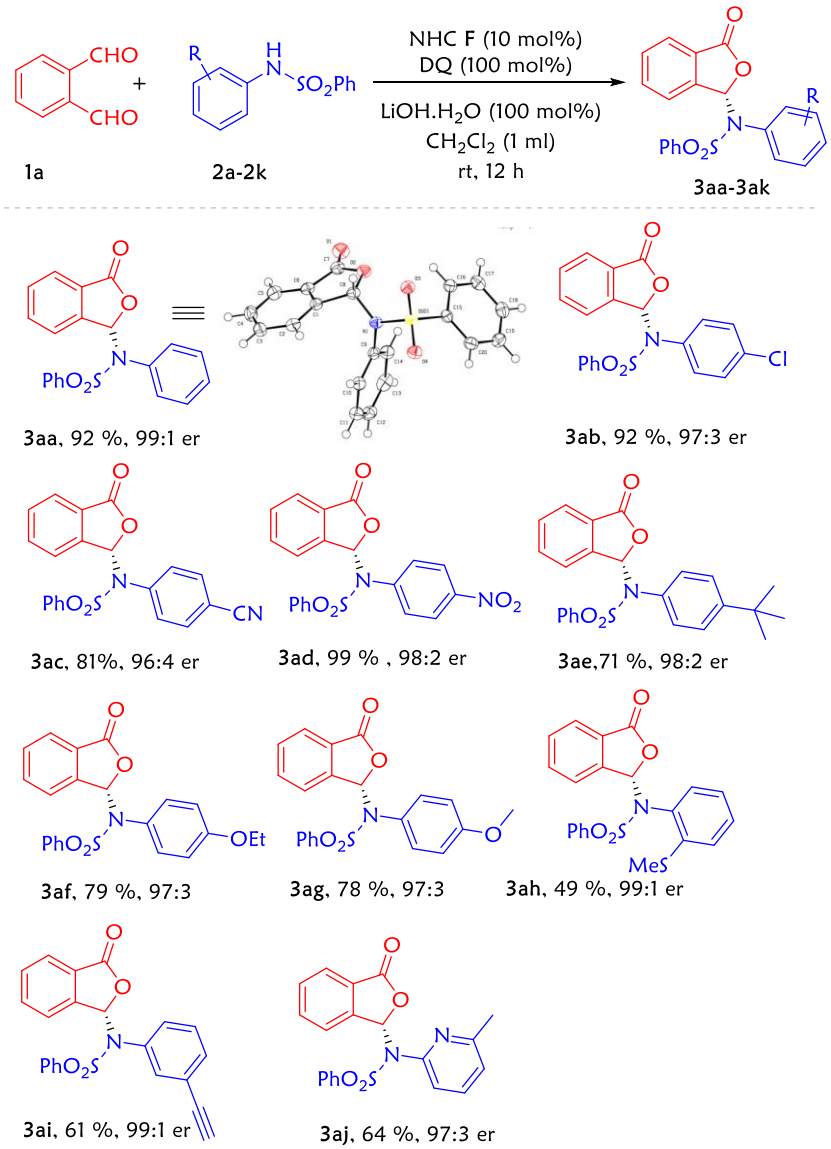

Reaction condition: **1a**(1 equiv.), **2a** (1.5 equiv), NHC **F** (10 mol%), **DQ** (1 equiv.), CH_2Cl_2 (2 mL), 12 h. The yield determined by isolation. e.r. determined by HPLC. **DQ** = 3,3',5,5'-tetra-tert-butyldiphenoquinone, er = enantiomeric ratio.

Scheme 3.4 Scope of substrates.

We also determined the X-ray crystallographic structure of the product **3aa.** The structure was depicted in the **Scheme 3.4**.(see also **Experimental Section 3.4.5**). Further exploration of the substrate scope, including N-alkyl-substituted sulfonamides as well as substituted phthalaldehydes, is currently underway.

3.2.3 Proposed pathway and disccusion

A proposed pathway was the present reaction is described in **Scheme 3.5**. One of aldehyde moiety of phthalaldehyde is activated by the carbene catalyst, and the resulting Breslow intermediate is then oxidized by the oxidant to form acyl azolium intermediate **I**. In presence of base, the addition of sulfonamide nucleophile to another aldehyde moiety and afford two diastereomeric intermediates **IIa** and **IIb,** which poses an dynamic equilibrium. The intermediate **IIa** is favorable in the intramolecule transesterification while intermediate **IIb** is unfavorable for this step. The enantioselective phthalidyl amines generate.

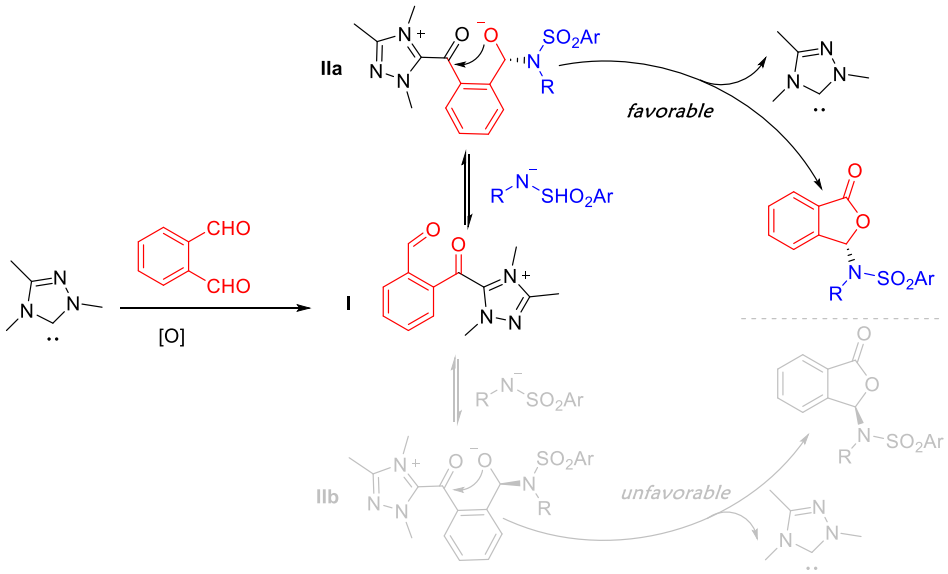

Scheme 3.5 Proposed pathway

The catalyst utilized in this reaction is different from the catalyst used in the reaction with carboxylic acids in **Chapter 2**. The only difference between the two catalyts lies in the Br group at the aromatic ring of the aminoindane core unit.The enantioselectivity determining step for both reactions happens at the lactonizaton, The reaction site is far from the Br group. Thus, the substitution by Br group brings less/no difference of steric hindrance between two NHC bound intermediates. However, it changes the electronic

properties of NHCs and makes the corresponding NHC a suitable leaving group for respective reaction such as leaving rate and electron withdrawing ability. Moreover, the different properties between oxygen and nitrogen, the difference between carboxylic acid and disubstituted sulfonamides also contribute to the different performance of the NHCs.

3.3 Summary

In summary, we have developed carbene catalyzed first enantioselective synthesis of 3-(*N*-substituted) aminophthalide derivatives with high yield and excellent enantiomeric ratio, which could be used to modify various medicinally significant molecules containing nitrogen atoms. Broad substrate scope with respect to different sulfonamides has been achieved. The present method also allows making phthalide substituted enantiopure drug molecules that could show better biological activity.

3.4 Experimental Section

3.4.1 General Information

Please refer to the Chapter 2.4.1

3.4.2 General procedure: synthesis of the Benzosulfonamides[15]

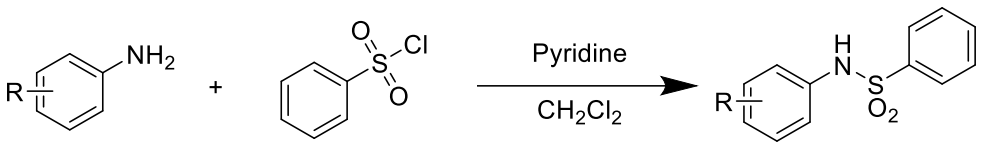

To a mixture of **amine** (1.00 eq) and pyridine (3.00 eq) solvated in CH_2Cl_2 (50 mL), **benzenesulfonyl chloride** (1.10 eq) was added portionwise. The resulting mixture stirred at room temperature, when complete (monitered by TLC), was quenched using 2*N* HCl. Mixture washed with CH_2Cl_2 organic fractions combined, was evaporated in vacuo. Crude product was then isolated by column chromatography. The resulting benzosulfonamide product was collected from fractions, solvent evaporated, and isolated as solid.

3.4.3 General procedure: synthesis of 3-(*N*-substituted) aminophthalides

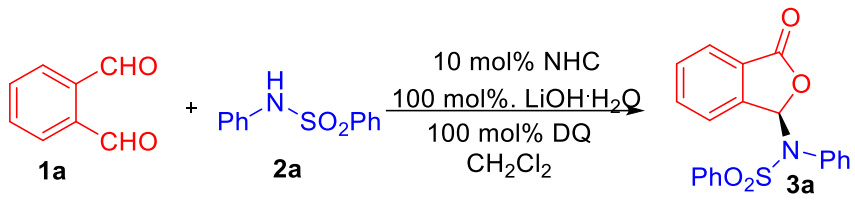

To a stirred solution of the phthalaldehydes (1.0 equiv.), benzosulfonamides (1.5 equiv.), NHC **F** (0.1 equiv.), **DQ** (1.0 equiv.) in CH_2Cl_2 (2 mL) was added $LiOH{\cdot}H_2O$ (1.0 equiv.). The mixture was stirred for overnight and then evaporated to dryness. The resulting residual was applied onto the silica chromatography with hexane/ethyl acetate (3:2 to 2:3) to afford the desried products.

3.4.4 Characteristization of products

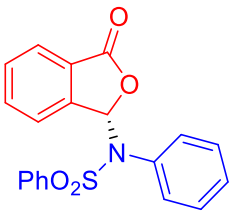

Compound 3aa: White solid, 92% yield;**^{1}H NMR** (400 MHz, $CDCl_3$) δ 7.79 (d, J = 7.4 Hz, 2H), 7.67 – 7.60 (m, 5H), 7.52 (t, J = 7.8 Hz, 2H), 7.41 (dt, J = 8.0, 4.1 Hz, 1H), 7.13 (t, J = 7.4 Hz, 1H), 7.05 (t, J = 7.6 Hz, 2H), 6.88 (d, J = 7.6 Hz, 2H). **^{13}C NMR** (101 MHz, CDCl3) δ 168.35, 143.74, 139.04, 138.04, 136.44, 134.43, 133.59, 133.38, 133.01, 131.16, 130.52, 129.33, 129.03, 128.94, 128.46, 127.24, 125.45, 125.38, 123.81, 121.73, 87.98 ppm.

HRMS (ESI, m/z): calcd. for $C_{20}H_{16}NO_4S^+$ 366.0795, found 366.0796.

HPLC analysis: 99:1 e.r. (Chiralcel IA, 10:90 *i*-PrOH/Hexane, 0.6 mL/min), R_t (major)= 23.2 min, R_t (minor) = 28.5 min.

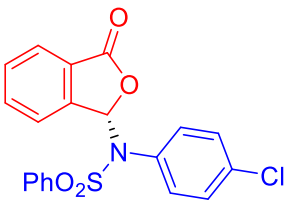

Compound 3ab: White solid, 92% yield; **^{1}H NMR** (400 MHz, $CDCl_3$) δ 7.79 (dd, J = 8.4, 1.1 Hz, 2H), 7.70 – 7.59 (m, 5H), 7.53 (t, J = 7.8 Hz, 2H), 7.45 (t, J = 7.4 Hz, 1H), 7.03 (d, J = 8.8 Hz, 2H), 6.82 (d, J = 8.7 Hz, 2H). **^{13}C NMR** (101 MHz, $CDCl_3$) δ 167.99, 143.52, 137.76, 135.56, 134.59, 133.77, 132.37, 131.96, 130.73, 129.25, 129.14, 128.43, 127.14, 125.58, 123.61, 87.73 ppm.

HRMS (ESI, m/z): calcd. for $C_{20}H_{15}ClNO_4S^+$ 400.0405, found 400.0402.

HPLC analysis: 97:3 e.r. (Chiralcel IA, 10:90 *i*-PrOH/Hexane, 0.6 mL/min), R_t (major) = 16.6 min, R_t (minor) = 28.4 min.

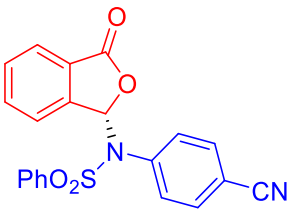

Compound 3ac: Yellow solid, 81% yield; **^{1}H NMR** (400 MHz, $CDCl_3$) δ 7.78 (dd, J = 8.4, 1.1 Hz, 2H), 7.72 – 7.59 (m, 5H), 7.58 – 7.53 (m, 2H), 7.47 (t, J = 7.4 Hz, 1H), 7.38 (d, J = 8.7 Hz, 2H), 7.04 (d, J = 8.6 Hz, 2H).**^{13}C NMR** (101 MHz, $CDCl_3$) δ 167.70, 143.15, 138.00, 137.48, 134.80, 134.07, 132.82, 131.87, 130.98, 129.30, 128.36, 127.04, 125.75, 123.52, 117.45, 113.47, 87.55 ppm.

HRMS (ESI, m/z): calcd. for $C_{21}H_{15}N_2O_4S^+$ 391.0747, found 391.0744.

HPLC analysis: 96:4 e.r. (Chiralcel IA, 10:90 *i*-PrOH/Hexane, 0.6 mL/min), R_t (major) = 29.8 min, R_t (minor) = 66.9 min.

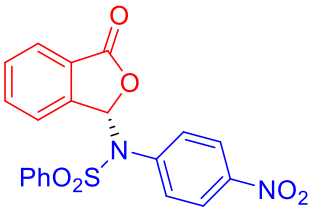

Compound 3ad: Yellow solid, 93% yield; **^{1}H NMR** (400 MHz, $CDCl_3$) δ 7.93 (d, J = 9.0 Hz, 2H), 7.81 – 7.77 (m, 2H), 7.72 – 7.60 (m, 5H), 7.56 (t, J = 7.8 Hz, 2H), 7.46 (t, J = 7.3

Hz, 1H), 7.11 (d, *J* = 8.9 Hz, 2H). ^{13}C NMR (101 MHz, $CDCl_3$) δ 167.66, 147.85, 143.09, 139.67, 137.41, 134.87, 134.14, 132.00, 131.03, 129.36, 128.37, 127.02, 125.79, 124.16, 123.53, 87.53.

HRMS (ESI, m/z): calcd. for $C_{20}H_{15}N_2O_6S^+$ 411.0645, found 411.0644.

HPLC analysis: 97:3 e.r. (Chiralcel IA, 10:90 *i*-PrOH/Hexane, 0.6 mL/min), R_t (major) = 26.4 min, R_t (minor) = 51.5 min.

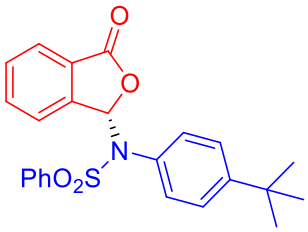

Compound 3ae: Yellow solid, 71% yield; **^{1}H NMR** (400 MHz, $CDCl_3$) δ 7.82 – 7.78 (m, 2H), 7.64 (dd, *J* = 9.1, 5.8 Hz, 5H), 7.52 (t, *J* = 7.8 Hz, 2H), 7.41 (dt, *J* = 7.9, 4.1 Hz, 1H), 7.04 (d, *J* = 8.7 Hz, 2H), 6.78 (d, *J* = 8.6 Hz, 2H), 1.13 (s, 9H). **^{13}C NMR** (101 MHz, $CDCl_3$) δ 168.36, 152.39, 143.91, 138.32, 134.34, 133.44, 130.55, 130.41, 130.37, 128.96, 128.41, 127.24, 125.81, 125.30, 123.73, 88.04, 34.51, 31.03.

HRMS (ESI, m/z): calcd. for $C_{24}H_{24}NO_6S^+$ 422.1421, found 422.1422.

HPLC analysis: 98:2 e.r. (Chiralcel IA, 10:90 *i*-PrOH/Hexane, 0.6 mL/min), R_t (major) = 13.3 min, R_t (minor) = 18.6 min.

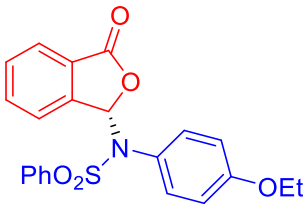

Compound 3af: off white solid, 97% yield; **^{1}H NMR** (400 MHz, $CDCl_3$) *δ* 7.82 – 7.77 (m, 2H), 7.64 (dd, *J* = 14.6, 7.0 Hz, 5H), 7.51 (t, *J* = 7.8 Hz, 2H), 7.44 – 7.39 (m, 1H), 6.75 (d, *J* = 8.5 Hz, 2H), 6.52 (d, *J* = 9.1 Hz, 2H), 3.83 (q, *J* = 7.0 Hz, 2H), 1.30 (t, *J* = 7.0 Hz, 3H).

^{13}C NMR (101 MHz, $CDCl_3$) δ 168.31, 159.28, 143.94, 138.14, 134.36, 133.45, 132.31, 130.44, 128.96, 128.46, 127.27, 125.37, 125.32, 123.70, 114.46, 88.05, 63.46, 14.61.

HRMS (ESI, m/z): calcd. for $C_{22}H_{20}NO_5S^+$ 410.1057, found 410.1058.

HPLC analysis: 97:3 e.r. (Chiralcel IA, 10:90 iPrOH/Hexane, 0.6 mL/min), R_t (major) = 19.1 min, R_t (minor) = 33.9 min

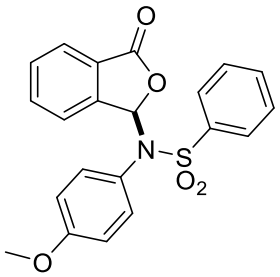

Compound 3ag: White solid, 78% yield; **^{1}H NMR** (400 MHz, $CDCl_3$) *δ* 7.82 – 7.78 (m, 2H), 7.68 – 7.59 (m, 5H), 7.51 (tt, *J* = 6.7, 1.4 Hz, 2H), 7.42 (ddd, *J* = 7.9, 5.3, 3.0 Hz, 1H), 6.81 – 6.74 (m, 2H), 6.56 – 6.51 (m, 2H). **^{13}C NMR** (101 MHz, $CDCl_3$) δ 168.25, 159.83, 143.92, 138.13, 134.33, 133.43, 132.31, 130.42, 128.95, 128.44, 127.26, 125.51, 125.37, 123.67, 114.02, 88.01, 55.18.

HRMS (ESI, m/z): calcd. for $C_{21}H_{18}NO_5S^+$ 396.0900, found 396.0903.

HPLC analysis: 97:3 e.r. (Chiralcel IA, 10:90 *i*-PrOH/Hexane, 0.6 mL/min), R_t (major) = 22.6 min, R_t (minor) = 38.4 min

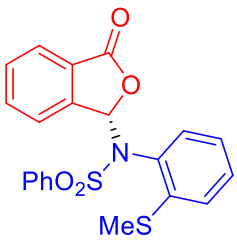

Compound 3ah: Yellow solid, 49% yield; **^{1}H NMR** (400 MHz, $CDCl_3$) δ 8.15 (d, *J* = 7.8 Hz, 1H), 7.86 – 7.81 (m, 2H), 7.67 (dd, *J* = 10.7, 4.2 Hz, 1H), 7.56 (ddd, *J* = 13.7, 12.3, 6.9 Hz, 5H), 7.40 (t, *J* = 7.5 Hz, 1H), 7.10 (dtd, *J* = 9.6, 8.0, 1.4 Hz, 2H), 6.77 – 6.71 (m, 1H), 6.54 (dd, *J* = 8.0, 1.2 Hz, 1H), 2.38 (s, 3H). **^{13}C NMR** (101 MHz, $CDCl_3$) δ 168.25, 142.78,

138.00, 133.72, 133.48, 131.50, 130.68, 130.21, 129.91, 129.02, 128.94, 127.09, 126.88, 124.85, 124.64, 124.45, 88.85, 15.91.

HRMS (ESI, m/z): calcd. for $C_{21}H_{18}NO_4S_2^+$ 412.0672, found 412.0674.

HPLC analysis: 99:1 e.r. (Chiralcel IA, 10:90 *i*-PrOH/Hexane, 0.6 mL/min), R_t (major) = 24.7 min, R_t (minor) = 37.6 min

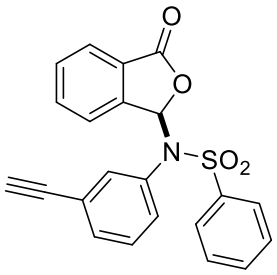

Compound 3ai: White solid, 61% yield; **^{1}H NMR** (400 MHz, $CDCl_3$) δ 7.81 – 7.77 (m, 2H), 7.70 – 7.58 (m, 4H), 7.57 – 7.50 (m, 2H), 7.47 – 7.40 (m, 2H), 7.26 – 7.23 (m, 1H), 7.07 (d, *J* = 1.9 Hz, 1H), 6.99 (t, *J* = 7.9 Hz, 1H), 6.81 (ddd, *J* = 8.1, 2.2, 1.2 Hz, 1H), 3.01 (s, 1H). **^{13}C NMR** (101 MHz, $CDCl_3$) δ 167.94, 143.43, 137.76, 134.86, 134.52, 133.71, 133.65, 132.93, 131.22, 130.62, 129.06, 128.86, 128.39, 127.12, 125.47, 123.63, 123.17, 87.71, 81.84, 78.56.

HRMS (ESI, m/z): calcd. for $C_{22}H_{16}NO_4S^+$ 390.0795, found 390.0799.

HPLC analysis: 99:1 e.r. (Chiralcel IA, 10:90 *i*-PrOH/Hexane, 0.6 mL/min), R_t (major) = 21.0 min, R_t (minor) = 27.3 min.

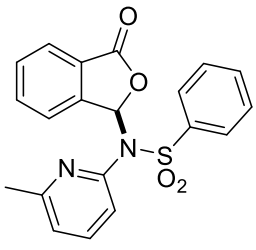

Compound 3aj: Yellow solid, 64% yield;**^{1}H NMR** (400 MHz, $CDCl_3$) δ 7.89 – 7.83 (m, 2H), 7.72 (d, *J* = 7.7 Hz, 1H), 7.61 – 7.31 (m, 7H), 7.06 (d, *J* = 7.9 Hz, 1H), 6.77 (d, *J* = 7.6 Hz, 1H), 2.09 (s, 3H). **^{13}C NMR** (101 MHz, $CDCl_3$) δ 168.58, 158.00, 148.42, 143.69,

138.59, 137.75, 133.74, 133.39, 130.06, 128.78, 128.42, 128.26, 124.66, 123.33, 122.15, 119.64, 87.43, 23.56.

HRMS (ESI, m/z): calcd. for $C_{20}H_{17}N_2O_4S^+$ 381.0904, found 381.0905.

HPLC analysis: 97:3 e.r. (Chiralcel IA, 10:90 *i*-PrOH/Hexane, 0.6 mL/min), R_t (major) = 21.8 min, R_t (minor) = 25.2 min.

3.4.5 X-ray Structure for Compound 3aa

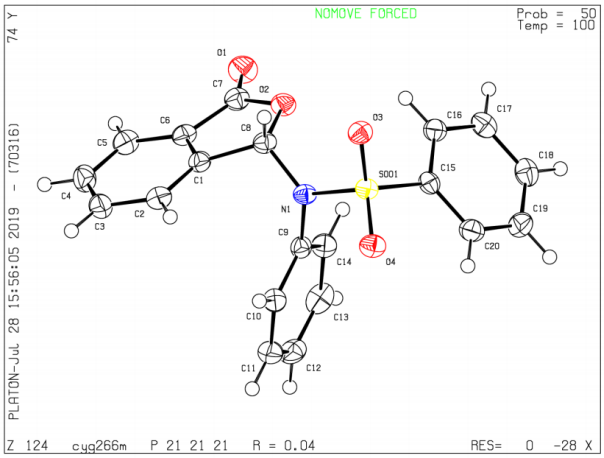

Table 3.2 Data collection and structure refinement for Compound **3aa**

Theta range for data collection	2.40 to 28.31°	
Index ranges	-8<=h<=8, -21<=k<=19, -22<=l<=20	
Reflections collected	15120	
Independent reflections	4198 [R(int) = 0.0514]	
Coverage of independent reflections	99.6%	
Absorption correction	Multi-Scan	
Max. and min. transmission	0.9790 and 0.9540	
Structure solution technique	direct methods	
Structure solution program	XT, VERSION 2014/5	
Refinement method	Full-matrix least-squares on F^2	
Refinement program	SHELXL-2017/1 (Sheldrick, 2017)	
Function minimized	$\Sigma\, w(F_o^2 - F_c^2)^2$	
Data / restraints / parameters	4198 / 0 / 235	
Goodness-of-fit on F^2	1.039	
Final R indices	3644 data; I>2σ(I)	R1 = 0.0411, wR2 = 0.0819
	all data	R1 = 0.0524, wR2 = 0.0879
Weighting scheme	$w=1/[\sigma^2(F_o^2)+(0.0297P)^2+0.4894P]$ where $P=(F_o^2+2F_c^2)/3$	

Absolute structure parameter	0.07(5)
Largest diff. peak and hole	0.196 and -0.411 eÅ^{-3}
R.M.S. deviation from mean	0.049 eÅ^{-3}

3.5 References

(1). Karmakar, R.; Pahari, P.; Mal, D. *Chem. Rev.* **2014,** *114*, 6213.

(2). Cragg, G. M.; Newman, D. J.; Snader, K. M. *J Nat Prod* **1997,** *60*, 52.

(3). Lin, G.; Chan, S. S.-K.; Chung, H.-S.; Li, S.-L. *Elsevier: Amsterdam* **2005,** *32*, 611.

(4). Liu, Y.; Chen, Q.; Mou, C.; Pan, L.; Duan, X.; Chen, X.; Chen, H.; Zhao, Y.; Lu, Y.; Jin, Z.; Chi, Y. R. *Nat. Commun.* **2019,** *10*, 1675.

(5). Bundgaard, H.; Buur, A.; Hansen, K. T.; Larsen, J. D.; Møss, J.; Olsen, L. *Int. J. Pharm.* **1988,** *45*, 47.

(6). David T. Smith, M. D. D., Haziq Qureshi, Jón T. Njarðarson *Njardarson Group* **2019**. URL: https://njardarson.lab.arizona.edu/content/top-pharmaceuticals-poster.

(7). Vitaku, E.; Smith, D. T.; Njardarson, J. T. *J. Med. Chem.* **2014,** *57*, 10257.

(8). Kim, J. C.; Dong, E.-S.; Ahn, J.-W.; Kim, S.-H. *Arch. Pharmacal Res.* **1994,** *17*, 135.

(9). Stark, H.; Krause, M.; Rouleau, A.; Garbarg, M.; Schwartz, J.-C.; Schunack, W. *Bioorg. Med. Chem.* **2001,** *9*, 191.

(10). Karimov, A.; Faskhutdinov, M. F.; Abdullaev, N. D.; Levkovich, M. G.; Mil'grom, E. G.; Rashkes, Y. V.; Shakirov, R. *Chem. Nat. Compd.* **1993,** *29*, 774.

(11). Huang, H. J.; Lee, C. C.; Chen, C. Y. *Evid. Based Complement. Alternat. Med.* **2014,** *2014*, 830490.

(12). Leete, E.; Bodem, G. B. *J. Chem. Soc., Chem. Commun.* **1973**, 522.

(13). Sloan, K. B.; Koch, S. A. M. *J. Org. Chem.* **1983,** *48*, 635.

(14). Wheeler, D. D.; Young, D. C.; Erley, D. S. *J. Org. Chem.* **1957,** *22*, 547.

(15). Revol, G.; McCallum, T.; Morin, M.; Gagosz, F.; Barriault, L. *Angew. Chem. Int. Ed.* **2013,** *52*, 13342.